Multi-scale quantification of woody biomass in heterogeneous landscapes: Leveraging traditional field sampling, spectral unmixing, and allometric modeling in Kalahari savanna ecosystems

Thoralf Meyer
Austin, Texas

Dipl. Ingenieur (FH), Anhalt University of Applied Sciences, Bernburg, Germany, 1999

Staatlich gepruefter Umweltschutztechniker, Technical College, Weissenfels, Germany, 1994

A Dissertation presented to the Graduate Faculty
of the University of Virginia in Candidacy for the Degree of
Doctor of Philosophy

Department of Environmental Sciences

University of Virginia,
May 2014

_____
Paolo D'Odorico

_____
Herman H. Shugart

_____
Howard E. Epstein

_____
Teresa B. Culver

_____
Gregory S. Okin

Abstract

Savannas are complex arid or semi-arid biomes, covering approximately 20 % of the terrestrial surface of the earth and providing substantial ecosystem services, such as carbon storage, firewood, rangeland and protection against soil erosion. They are systems best described as prone to constant change in productivity, diversity and abundance of species and structure. Due to this complexity, savannas are extremely heterogeneous ecosystems where, despite past and current research, the ongoing processes between the abiotic and biotic environment remain poorly understood. This knowledge gap and its importance are only amplified by increasing anthropogenic influences, increasing human population, and increasingly varying climate change.

This dissertation contributes to the ongoing scientific debate regarding the role of savannas as a carbon sink or source. A key factor in understanding carbon cycling is the role of woody vegetation. Multiple drivers of shrub encroachment were assessed as to their impacts on diversity and abundance of woody vegetation across the rainfall gradient of the Kalahari Transect, located in western Botswana. This study underscores the importance to study the combination of multiple drivers and their effects on species with similar functional and structural traits. Further, allometric relationships were developed to estimate biomass using different morphological parameters, therefore providing a useful tool to estimate biomass on multiple scales. These relationships are useful for informing decisions and management ranging from the plot (management) scale to the local scale (where active remote sensing systems may be deployed). Regional and global carbon

monitoring efforts are in the most need of properly calibrated, reliable information derived from regional-scale satellite imagery but to date there remains skepticism on the reliability of those data.

To overcome the challenges associated with the quantification of biomass across large tracts of land, this work took on the challenge to extract biomass using a two-dimensional passive remote sensing system. Extensive field-derived measurements, including fractional cover of green vegetation (GV), non-photosynthetic vegetation (NPV), soil, vegetation structure and species for all woody plants, were collected in both wet and dry seasons over 15 sites along a 950km transect. These *in situ* data were used to develop, test, and validate a new method, the Spectral Line Point Intercept Transect – SLPT, to obtain spectral information efficiently across long distances. Multiple validation methods were leveraged to test the performance of various spectral unmixing techniques in heterogeneous savanna environments to derive fractional cover of GV, NPV, soil and shade at structurally different sites and in different phenological conditions (wet vs. dry season). The fractional cover of shade derived using Multiple Endmember Spectral Mixture Analysis (MESMA) and the Moderate Imaging Spectroradiometer (MODIS) Enhanced Vegetation Index (EVI) products were used to derive a relationship (φ) that identifies fractional cover of woody vegetation for a given MODIS pixel. By combining the MESMA, φ, and the allometric relationships described above, this research was able to develop a modelling approach that successfully quantifies biomass and woody vegetation cover across the Kalahari region.

Acknowledgments

I would like to take the opportunity to thank my committee members for years of guidance and support. Special thanks to Dr. Herman H. Shugart for the encouragement to start graduate school in Virginia and for the financial support to do so. Dr. Paolo D'odorico and Dr. Gregory S. Okin for saving my scientific career in multiple ways, firstly for supporting me financially and secondly for their scientific advice and high levels of tolerance and patience. I would also like to thank my committee members Dr. Howard Epstein for his advice and Dr. Teresa Culver for agreeing to be my external committee member.

The government of Botswana needs mentioning for granting me a research permit to conduct my studies across the Kalahari region.

My field crew, Thomas, Val and Gully did an amazing job in helping to implement the field work, thanks for the hard work and the fun.

My family in Germany supported the idea from day one, thanks for moral and financial support.

Special thanks goes to my friends in Maun, Collin, Daryl, Colm & Cherry, uncle Toni and aunty Di, Marie and Derek, Tiaan, Dr. Sven Bourquin and Elmar who continued supporting the ideas and helped with their encouragement, logistics and multiple rescue

missions. Neil, thanks for the encouragements, looking after my stuff and for a great friendship. Cheers bud.

Thanks to Matthew for almost literally throwing his weight behind me and pushing me over the finish line.

I would like to apologize to my staff for abandoning the office and leaving you guys by yourself.

My ‘spare’ family, the McAllisters, need to be thanked for being there for me for the last 16 years, without you guys, this would not have been possible.

The University of Texas at Austin for providing me a lab space. I am especially thankful to my office colleagues, Molly, Paul and Niti.

Last but not least, I would like to thank Karl Heinz Gimpel, for his hospitality, years of friendship and the overseeing of my company while I was in the States.

Finally, my wife showed a high level of support and even more tolerance, in the field, in the office, at home. It’s one thing off the plate.

Table of Contents

Chapter 1

Introduction to savanna ecosystems, Dissertation structure and scientific approach

Unpublished

Author: Meyer, T.

1.1 Ecology of savanna ecosystems

Savanna ecosystems are mixed communities of woody plants (trees or shrubs) and grasses that can be found in all continents (except Antarctica). They cover approximately 20% of the Earth's land surface, including about 40% of Australia, South America, and Africa (Scholes and Walker 1993). Savannas provide important services such as rangeland for livestock production, firewood, carbon sequestration, and protection against soil erosion. Though savannas can be found in temperate and sub-humid environments, they represent a major biome of arid and semiarid regions, where their dynamics have often been investigated with respect to conditions of water limitation and interspecies competition for water (e.g.,Sankaran et al. 2004). Thus, changes in rainfall patterns and abundance are expected to play a major role in the dynamics of these ecosystems, with important impacts on vegetation structure, ecosystem productivity, and carbon sequestration in plant biomass.

Arid and semiarid regions (which include but are not limited to savannas) cover approximately 40% of the Earth's land surface and are home to about one third of the world's human population (MEA 2005). Apart from the arid lands of the United States, Spain, and Australia, most of these regions are situated in developing countries or countries whose economy strongly depends, directly or indirectly, on rangeland and agricultural production. Arid and semi-arid ecosystems are ecologically and economically important regions worldwide and are highly vulnerable to drought, climate change and changes in land use patterns (Archer et al. 1995). Multiple models predicting changes in mean annual precipitation (MAP) and temperature indicate a decrease in rainfall and an

increase in temperature for most savanna regions on a global scale (Christensen 2007). These changes directly affect the availability of natural resources that are the basis for subsistence and micro-economy. For instance, tropical savannas are often used as rangelands for livestock production. Shifts in rainfall regimes and land use patterns may result in important changes in plant community composition, with severe implications for the ability of the land to provide these functions and ecosystem services.

Research in savanna ecology historically concentrated on the coexistence of woody plants and grasses (Sarmiento 1984; Walter and Mueller-Dombois 1971), the underlying dynamics (e.g.,Sankaran et al. 2004), and their susceptibility to the effects of land management and climate change (Anderies et al. 2002; Noy-Meir 1975; Scholes and Archer 1997; Scholes and Walker 1993; Walker et al. 1981). In particular, research has tried to investigate how plant community composition and tree/grass fractional covers change as a function of the mean and interannual variability of precipitation (Caylor et al. 2003; Scanlon et al. 2002).

An often overlooked aspect of savanna ecosystems is the role they play in the global carbon cycle, particularly with respect to their ability to store carbon. It has been estimated that savannas contribute about 15% (Taylor and Lloyd 1992) to 29% (Mohamed et al. 2004) of the global terrestrial net primary productivity. Despite their important role in the global carbon balance, the contribution of savannas to the global stocks of organic carbon remains poorly quantified. It is unclear (i) how much biomass exists in savannas; (ii) how it is partitioned between above- and belowground stocks; and

(iii) how these stocks are expected to change under different land use and climate change scenarios. This lack of a quantitative assessment of biomass (and carbon stocks) in savanna vegetation is a major limitation to the understanding of whether changes in climate, land management, or disturbance regime might turn savannas into important sources or sinks of atmospheric CO_2 (Wang et al. 2009; Williams et al. 2007).

This dissertation concentrates on the above three points and uses data from intensive field campaigns and advanced remote sensing techniques to quantify how carbon storage in savannas varies as a function of mean annual rainfall. Changes in vegetation structure and composition induced by shifts in rainfall regime will be inferred through a "space-for-time" substitution along a rainfall gradient. This approach is effective if other major environmental conditions (most notably, land use, soils and geomorphic features of the landscapes) do not vary along the spatial rainfall gradient. Savanna ecosystems located along the Kalahari Transect (KT) offer a unique opportunity to investigate the effect of rainfall regime on vegetation composition, structure, and carbon stocks because in this region a rainfall gradient exists on the relatively uniform soil substrate of the Kalahari's sand sheet (Wang et al. 2007); moreover, the region exhibits an overall uniform topography with no relief and a poor dissection of the landscape by rivers and streams. The consistent soils of the Kalahari combined with a documented rainfall gradient provide an excellent "open air laboratory" to study the effects of climate change on vegetation patterns, the distribution and production of biomass, and the region's carbon storage capacity (Scholes et al. 2004).

Studies of arid and semi-arid systems with water-limited vegetation have often focused on aboveground vegetation. Yet understanding root structure and dynamics is key to a proper assessment of vegetation dynamics (Breshears and Barnes 1999; Sankaran et al. 2004), particularly given the dependence on water and nutrient uptake, belowground resource competition, and plant-soil feedbacks on root distribution and dynamics (Casper et al. 2003; Schenk 2005). Much research has supported the importance of root-related processes for understanding the dynamics of water-limited vegetation (Breshears and Barnes 1999; Sala et al. 1997), but has not yet explicitly and adequately investigated these dynamics across suitable spatial extents (Casper et al. 2003; Caylor et al. 2006; Couteron and Lejeune 2001; Laio 2006; Ringrose et al. 1998; Sala et al. 1997; Schlesinger et al. 1990). The potentially confounding effects of soil differences (across study sites) and differences in method of investigation have often precluded conclusive verification of belowground controls on either total biomass and carbon storage capacity or vegetation structure.

Vegetation composition and structure, in turn, determine both total ecosystem carbon storage and short- and long-term response of ecosystems to climate variability. Despite the fundamental nature of these issues and the vast areas to which they apply, the way that plants allocate carbon to structural and fine roots as well as the degree to which fine root turnover couples with soil organic carbon dynamics in water-limited ecosystems remains poorly understood. Recent fieldwork in the southern Kalahari quantified the root:shoot ratio at various sites along the transect. These studies are necessarily conducted at the plot-to-field scale but alone are unable to scale to a reliable regional

assessment of vegetation biomass, carbon storage capacity, or species composition in the Kalahari. In order to obtain accurate estimates of carbon distribution within the Kalahari, small scale variations in vegetation composition and structure resulting from variations in soil, landuse patterns, and disturbance regimes need to be accounted for and incorporated into the assessment. Remote sensing methods can then be used to "connect the dots" between field site observations and provide an integrated regional scale assessment of changes in carbon stored in plant biomass along the rainfall gradient.

A variety of remotely sensed indices (e.g., Normalized Difference Vegetation Index or NDVI, Soil Adjusted Vegetation Index or SAVI, and Enhanced Vegetation Index or EVI) have been applied to upscale locally observed patterns to the landscape/ ecosystem level of the Kalahari (Ringrose et al. 2003; Ringrose et al. 1996; Scanlon et al. 2002). These indices, however, are mainly indicators of photosynthetic activity and do not provide direct correlates of actual biomass, fractional cover of green vegetation (GV) and non-photosynthetic vegetation (NPV), or reliable data on vegetation structure. Recently developed remote sensing approaches, such as Relative Spectral Mixture Analysis (RSMA) and Multiple Endmember Relative Spectral Mixture Analysis (MESMA), provide excellent tools to upscale field measurements (RSMA) across an entire region and to quantify and qualify these changes in fractional cover of GV, NPV and soils (the main factors determining carbon storage capacity) by including spectral field measurements (MESMA).

1.2 Research Objectives

This dissertation evaluates how woody plant biomass is distributed from south to north along the Kalahari rainfall gradient and provides a quantitative assessment of woody biomass in the Kalahari. To address this central goal, this research requires (a) detailed field measurements at the plot, landscape, and regional scales, including species identification, plant distribution, size (height, basal area, canopy diameter), (shoot and root) biomass, and spectral attributes; (b) development of reliable allometric relationships relating biomass to size for different sites, species and plant functional groups, and the development of an "aggregated" allometric relationship that can be used to calculate tree biomass as a function of morphological attributes that can be determined from air photography or remote sensing; (c) the development and testing of new remote sensing methods that can be used to upscale field observations to the regional scale; and (d) the use of all of these methods to evaluate the dependence of woody plant biomass (and the associated carbon stock) on rainfall and disturbance regimes.

Therefore, the dissertation developed a number of research activities with the following main objectives:

Objective 1 – to quantify total woody biomass and investigate/explain changes in plant community composition across the Kalahari, particularly with respect to rainfall and disturbance regimes. There is in general no consensus as to how ecosystem composition and species diversity are expected to change across the Kalahari rainfall gradient. While the intermediate disturbance hypothesis formulated by Grime (1973), Horn et al. (1975)

and Connel (1978) suggests the existence of higher diversity in moderately disturbed areas, Ringrose et al. (2003) and Trollope and Trollope (2004) indicated that in the Kalahari a more homogeneous vegetation composition is found in areas with higher disturbance intensity (herbivory, land use, and fire). Savanna vegetation is often nutrient limited in the more mesic regions and water limited in the drier environments (Sankaran et al. 2005; Scholes and Walker 1993; Wang et al. 2010). Thus Kalahari vegetation is expected to be nutrient-limited in the north and water-limited in the south, while, based on ecological theories (e.g.,Tilman 1982, 1988), the highest species diversity is expected in areas where species from both the water and the nutrient limited regimes overlap (in this case, the Ghanzi area). I hypothesize that either end of the transect (i.e., the dry or the wet extremes) exhibits a more homogeneous vegetation composition, expressed in lower species richness and diversity, while higher species richness and diversity exist in the middle of the transect (in the Ghanzi area).

Objective 2 – to develop allometric biomass-size relationships for woody vegetation in the region. This part of the project entailed surveys of vegetation composition and structure at 15 sites across the southern Kalahari and capitalized on existing measurements of plant biomass at 4 core sites (a total of 342 trees/shrubs and 240 soil pit excavations). The repeated vegetation sampling at the same sites during dry and wet seasons allowed for the quantification of the fractional cover of green vegetation (GV) and non-photosynthetic vegetation (NPV) and bare soil. These data were used for the subsequent validation of remote sensing observations.

Objective 3 – to test the performance of unmixing procedures in the heterogeneous environment of savannas in general and the Kalahari in particular. This approach uses spectral datasets of various end-members such as different plant species, NPV cover fractions and variations in soils, which were validated against field-derived measurements and observations.

Objective 4 – to develop and test a model, allowing for the quantification of woody biomass, structure and cover, by combining field-derived measurements and passively sensed remote sensing products at a regional scale.

Objective 5 – to produce a map quantifying the woody vegetation cover and biomass across the entire Kalahari region by combining allometric relationships, unmixing techniques and additional remotely sensed datasets on photosynthetic activity.

1.3 Study Region

The Kalahari Sand Deposit covers approximately 2.5 million km^2 of the interior of southern and central Africa (Scholes et al. 2004; Van Rooyen et al. 2001). It stretches over nine countries from the Oranje River (S. Africa) in the south, almost to the equator in the north. The main geomorphological feature throughout the Kalahari's extent is the reportedly relatively uniform sand deposited in the so-called Kalahari Basin (FAO 1995). The Kalahari Beds are the result of aeolian processes, with sands likely derived from the weathering of Stromberg Sandstones and water-borne deposition (King 1978; Wellington 1955). The older Kalahari deposits were formed in the northwest during the Eocene to

Pliocene period, 2 – 7 Million years ago and then transported by the wind in easterly to south-easterly directions (DuToit 1966).

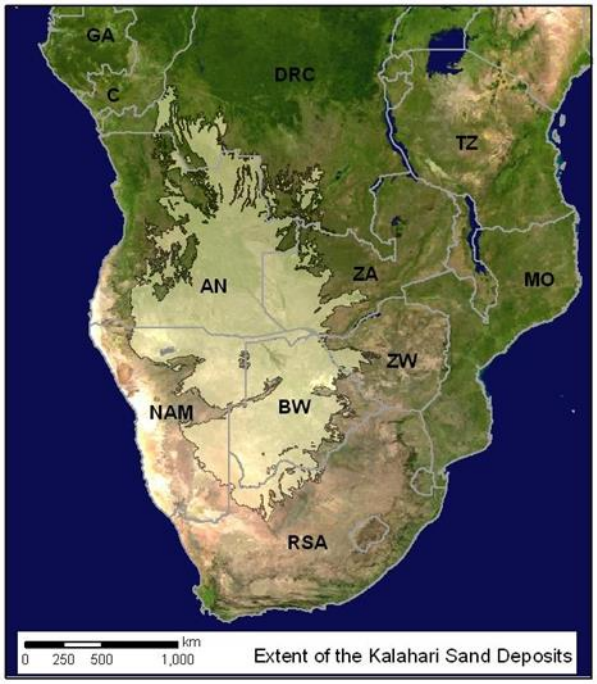

Figure 1: Extent of the Kalahari sand deposits (DSM 2003; ESRI 2000), map design by author)

The rainfall gradient across the Kalahari ranges from 200 mm in the extreme south to more than 1000 mm annually in the northern parts (Shugart et al. 2004). Therefore the so-called "Kalahari Desert" is relatively humid and should be classified as a semi-arid region in its southern central parts and as a dry sub-humid area in the north (Mainguet 1994). The research presented in this dissertation covers the drier southern part of the region, within a rainfall gradient of approximately 200-600 mm/y. The northern part of southern Africa (e.g., northern Botswana) is situated at the interface between two climate systems: the Inter Tropical Convergence Zone (ITCZ) and the High Pressure Zone (HPZ) (Aspel 1995). The southern part of the region, which includes the extreme south of

Botswana, lies at the interface between the HPZ and the Temperate Zone (Van Regenmortel 1995). Both the ITCZ and the Temperate Zone are areas of relatively high rainfall, whereas the high pressure belt (HPZ) between them is generally an area of little rainfall. The seasonal movement of these zones determines the alternation of dry and wet seasons. Slight inconsistencies in the extent or timing of the movement of these zones can cause considerable inter-annual variability in climate conditions and seasonal rainfall. There is a general increase in mean annual precipitation from south to the north and from west to east (e.g., Ringrose et al. 2002).

As noted above, the reportedly consistent soils combined with the rainfall gradient provide an excellent "open air laboratory" to study the effects of climate change on vegetation patterns and the distribution and production of biomass and the region's carbon storage capacity. Until recently, however, the interactions among climate, soil and vegetation in the Kalahari region have remained poorly investigated and understood in comparison to studies focusing on the distribution of plants and animals. A good deal of research and information is available on the vegetation of the Kalahari, starting with the early explorers of the region in the late 19th century (Andersson 1875; Livingstone 1857; Passarge 1904). A number of field guides published in the past focused on the characterization of woody vegetation and the geographic distribution and abundance of tree species in the region. More recently, several studies assessed the vegetation cover and structure along the Kalahari Transect (KT) and established important links between the vegetation structure and non-biotic factors such as nutrient and water availability. While research has been undertaken to assess fractional cover and vegetation structure

(Caylor et al. 2003; Scanlon et al. 2005; Scholes et al. 2004; Wang et al. 2009), regional scale studies on vegetation in this region have yet to quantify the total biomass, species composition or diversity.

1.4 Study Sites

This dissertation concentrates on the portion of the Kalahari stretching over 950 km from the South Africa/ Botswana border (the village of Bokspits) to the northern border of Botswana with Namibia (the village of Shakawe). This transect covers the western part of the Botswana Kalahari (Figure 2).

Figure 2: General transect layout, background image by (ESRI 2000), map design by author

The soils are consistent Kalahari sand deposits with local alluvial deposits found in depressions and ancient river beds, such as the Okwa and Nxamasere Valleys, and along the Ghanzi Ridge. Within these areas calcrete formations, deriving from groundwater aquifers or open water bodies such as pans and prehistoric lake deposits, are sometimes present (Gobagoba 2005), especially across the Mabuasehube and Tshane areas. The sand deposits are deep across the entire transect, sometimes reaching 200 m. The southern part of the transect is characterised by red sand, often forming relatively high sand dunes. The area flattens out in the northern part of the Kgalagadi Transfrontier Park. The whitish – grey colour of the sand in these areas suggests that these sediments have been exposed to longer periods of various forms of weathering processes. These whitish – greyish sands stretch north for 250 km. The most obvious topographical features along this line are the Okwa River, the Hannahai Valleys and the Ghanzi Ridge. Here, calcrete formations can be found relatively close to the surface. Further north the topography is characterised by a large vegetated dune field running in the north-west to south-east direction.

The rainfall gradient along the transect ranges from 250 mm in the south to 600 mm in Shakawe, though extreme high and low values have been observed in the past. As an example, Maun (located in the top third of Botswana) has experienced rainfall highs of 1195 mm in 1973/74 and lows of 192.6 mm in 1922/23, while the average is 450 mm (Meyer 1998). The area is characterised by a distinct rainy season starting in October and ending in March. Rain usually falls in strong, locally restricted showers, associated with convective thunderstorms following a continuous build-up of clouds during the day (Mendelsohn and El Obeid 2004).

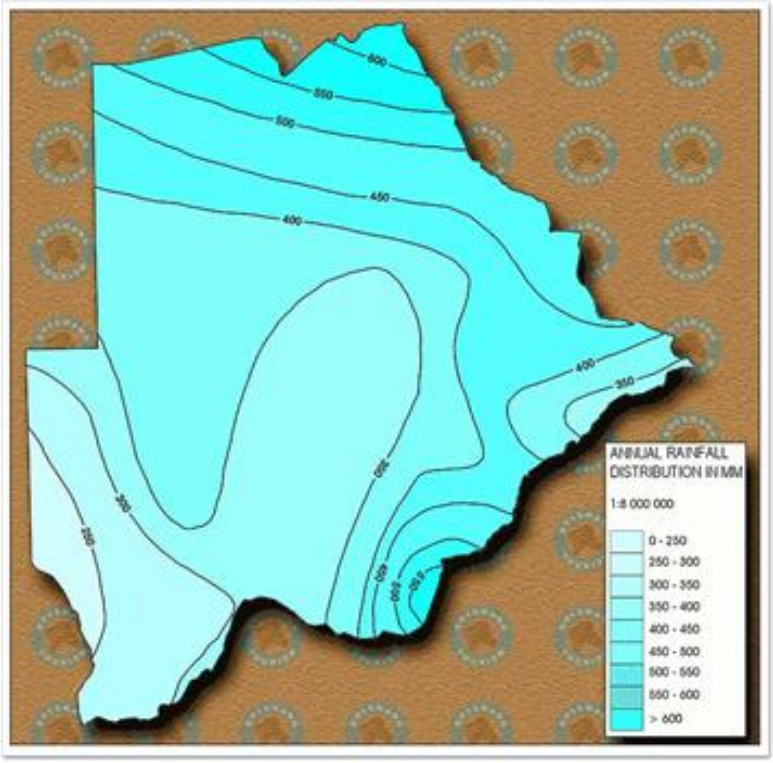

Figure 3: Annual distribution of precipitation across the study area (BTO 2005)

Vegetation along the KT was investigated and is characterized in detail in chapters 2-5. Here I provide a summary of the main characteristics of vegetation at four core sites: Bokspits, Thsane, Kuke and Shakawe. In the Bokspits area, at the southernmost part of the transect (mean annual precipitation of 250 mm), the woody vegetation is dominated by *Acacia erioloba* and *Acacia mellifera* followed by *Rhigozum trichotomum, Lycium hirsutm* and *Pheoptilium spinosum*. In the area *Acacia hemataxylon, Parkinsonia africana, Boscia albitrunca,* and *Cadaba aphylla* are also present but their occurrence is more unusual.

Woody vegetation in the Tshane area (150 km north of the previous site; mean annual precipitation of 350 mm (Scholes et al. 2004)) is dominated by *Acacia leuderitzii* and

Acacia mellifera; other species found include *Lycium hirsutum, Boscia albitrunca, Terminalia sericea, Rhus tenuiveris, Pheoptilium spinosa, Grewia flava, Zizyphus mucronata, Cadaba aphylla, Rhigozum brewispinosum* and *Acacia erioloba*.

At the Kuke site, (200 km north of Tshane, in an area receiving a mean annual precipitation of 424 mm) woody species dominance seems to depend on small scale site factors, likely associated with differences in soils and water/ nutrient availability between dunes and interdunes. In total, 32 woody species were observed at this site.

The northern-most part of the transect can be described as an open woodland with shrub-grass understory. Dominant tree species at the site in Shakawe are *Pterocarpus angolensis, Terminalia sericea, Terminalia prunoides,* various *Combretum spp., Lonchocarpus cappasa, Lonchocarpus nelsii, Boscia albitrunca* and *Grewia spp*. There is an increase in woody canopy cover from south to north and a change in woody vegetation morphology where the south is dominated by relatively short bipinnate species with open canopies while the north becomes a woodland savanna dominated by tall broadleaf species and a distinct sub-canopy layer consisting of broadleaf shrub species.

1.5 Research Components

To achieve the research objectives outlined in section 1.2 this dissertation develops the following research components:

Component A - Vegetation sampling and analysis

Component B – Development of allometric models to determine biomass-size relationships

Component C - Collection of spectral data and remote sensing analysis

Component D – Model development and application

Component E – Synthesis of results

1.6 General research approach and thesis structure

Vegetation sampling forms the basis of the dissertation research, providing necessary background information on vegetation composition, coverage and morphological structure. The experimental design aims to capture small scale changes of these variables across a regional transect of about 1000 km. Apart from general information on vegetation, the transects also provide the baseline information for spectral analyses including derivation of the fractional cover of photosynthetically active vegetation or green vegetation (GV), non-photosynthetic vegetation (NPV) and bare soil. Allometric models are then applied to satellite-derived fractions of GV, NPV and bare soil. The use of field-derived vegetation measurements, field-derived spectral measurements and fractional cover derived from remote sensing allowed for the models to be validated across multiple sites and growing seasons.

1.6.1 Component A - Vegetation sampling (represented in chapters 2-5)

The regional transect stretches from Bokspits in the far southwestern corner of Botswana over 950 km to Shakawe in the northwestern corner of Botswana (Figure 2). Fifteen field sites (roughly 75 km apart) were selected along the regional transect. At each site vegetation was surveyed along three 100 m long landscape-scale transects. These transects intersect in their midpoints and radiate at 120 degree angles. All measurements

were repeated on wet and dry seasons (figure 4) resulting in a total of six transects per site.

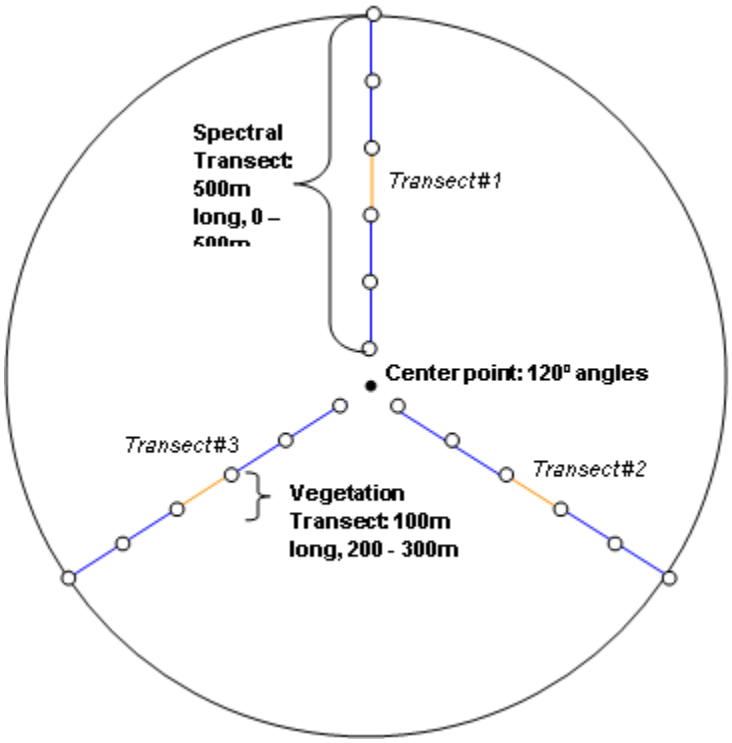

Figure 4: general transect layout including 100m breakpoints (circles), vegetation transect (yellow), spectral transect (blue + yellow)

Data collection followed the procedures and methods described for a line interception method by Krebs (1998). For each transect line, all woody vegetation taller than 25cm was identified. Average height, distance covered over the line, and distance and direction of the stem(s) were recorded to calculate total crown diameter. In order to calculate the total vegetative cover, herbaceous and grass layers were recorded along the same line. Due to the lack of adequate field guides, species levels could only be identified for woody species. The field-derived information on plant composition and abundance were used to statistically explore the effect of disturbance regimes such as fire and grazing with observed land use patterns on vegetation.

1.6.2 Component B - Development of allometric models to determine biomass (chapter 3 & 5)

Field data on woody vegetation were derived from 4 core sites described above: Shakawe, Kuke, Tshane and Bokspits. At each site, three 20 m x 20 m plots were cleared and all vegetation was identified following the nomenclature of Palgrave (1977). Before clearing, structural parameters such as height, crown diameter and basal diameter of each individual were determined. While harvesting the woody vegetation, the above ground biomass of all trees and shrubs in the 20m x 20m plots was weighed. Using a regression approach the relationship between structural parameters and biomass was assessed extensively, on a per site, per species, and all species basis. Species were also grouped into five established morphological groups and allometric relationships were determined for each group.

1.6.3 Component C - Spectral collection and remote sensing analysis (chapter 4 & 5)

Spectral measurements were taken along the transect using an ASD (Analytical Spectral Devices Inc.) field spectrometer. The spectrometer measures in the visible light (400nm – 700nm), the near infrared (700 nm – 1000 nm) and the middle infrared section of the spectrum (1000 nm – 2500 nm). Using the bare fibre of the instrument's optic sensor, canopy spectra were collected at each site and season along the entire transect at every 5 meters. End-members were collected using a leaf clip unit with an artificial light source. End-members of fractional cover were collected for each site and season and formed the basis for various spectral end-member libraries. These libraries were leveraged to test the

performance of different unmixing approaches, such as Relative Spectral Mixture Analysis (RMSA), Spectral Mixture Analysis (SMA) and Multiple Endmember Spectral Mixture Analysis (MESMA). All unmixing procedures were applied to all sites and seasons at the scale of Moderate Resolution Imaging Spectroradiometer (MODIS) satellite imagery (463.3 m pixel size). Results were validated leveraging the field-derived measurements of fractional cover and the field-derived spectral canopy samples.

1.6.4 Component D – Model development and application (chapter 5)

Measured vegetation parameters (such as fractional cover of woody vegetation and crown diameter), together with mean annual precipitation (MAP), Enhanced Vegetation Index (EVI), Normalized Vegetation Index (NDVI), MESMA calculations from canopy spectra, and the developed allometric relationships were together used to develop a model to extract biomass across large extents of the Kalahari. Model performance was tested against field data measurements derived from spectral transects and field-measured amounts of biomass. The model was applied across the entire area to produce a biomass distribution map of the region and to analyze change in plant biomass over the past decade.

1.6.5 Component E – Synthesis of results (chapter 6)

The last component synthesizes the results of the various other components and discusses the effects and factors at play and the limits of applications. The results were interpreted in light of the functioning of savanna ecosystems in general and the effect on the Kalahari region in particular.

Chapter 2

Fire, rainfall, land use, grazing: An assessment of multiple drivers determining species composition and structure across the Kalahari

Submitted to: Journal of Rangeland Ecology and Management

Authors: T. Meyer, P. Holloway, T. Christiansen, J. Miller, P. D'Odorico, G.S. Okin

2.1 Introduction

Savannas are mixed plant communities comprised of grasses and woody vegetation that cover a large fraction of the Earth's land surface, including roughly half of the African continent (Scholes and Archer 1997). Savannas are an important socio-economic landscape in Africa, with as much as 84% of savanna land used to raise livestock in southern Africa (Grossman and Gandar 1989). Southern African savannas (as well as many other savannas worldwide) are susceptible to changes, especially to shifts in plant community composition associated with bush encroachment (Moleele et al. 2002; Ringrose et al. 2003). Studies attempting to explain the ecological processes underlying these changes in vegetation have often found conflicting results, thus limiting the use of this knowledge as the basis for decision-making. Bush encroachment and its negative impacts have been observed worldwide (Archer 1989; Eldridge et al. 2011; Van Auken 2000), with a particularly concerning aspect involving the reduction of palatable grasses and herbs by encroaching woody species, often thorny and unpalatable for the livestock that are raised in the savannas (Ward 2005). With ranching an integral aspect of current economic stability in African savannas (Acemoglu et al. 2001; Robinson and Parsons 2006), the threat of bush encroachment needs to be better understood in order to be better managed.

Grazing pressure was initially believed to be the main driver of bush encroachment (Walter 1954). Walter's two-layer hypothesis suggested that in savannas, grass roots dominate the top-most soil layers while tree roots dominate lower layers. When grass is removed by grazing, tree roots are allowed to dominate in the upper layers and prevent

the grasses from re-establishing. Studies have proven inconclusive for the two layer hypothesis, finding evidence both in support (Perkins and Thomas 1993; Skarpe 1990) and opposition (Brown and Archer 1999). Bush encroachment has also been observed in geological settings where soils are too shallow to allow for root separation (Wiegand et al. 2005). Moreover Angassa and Oba (2008) found that many encroaching bush species did not differ significantly in terms of percentage of composition and density when the differences were studied between enclosed and open grazed areas. As a result, several other hypotheses have been suggested as potential main drivers of bush encroachment, including fire suppression, climate warming, and the increase in atmospheric CO_2 concentrations (Ravi et al. 2011; Van Auken 2000).

Because spatially distributed data of grazing rates are seldom available, the effect of grazing on bush encroachment is often evaluated by looking at changes in vegetation cover and composition as a function of the distance from boreholes (e.g.,Lange 1969). Boreholes are narrow shafts drilled into the ground in order to extract water; in most of Botswana, farmers rely on boreholes to provide groundwater for their livestock. The animals rarely stray more than 13 – 18 km from this water source (Stringer and Reed 2007), with the total amount of woody vegetation found to increase beyond 400 m of a borehole up to where the cattle stop regularly using the land (Moleele et al. 2002). Moleele et al. (2002) interpreted this trend as an effect of cattle's impact on the soil and vegetation due to trampling. Savannas are characterized by low soil nutrient content (Dougill and Thomas 2004; O'Halloran et al. 2010; Wang et al. 2009), although many areas have biological soil crusts that increase soil surface stability thereby reducing

nutrient loss by erosion and increasing soil nitrogen availability through atmospheric nitrogen fixation (Thomas 2012). Trampling caused by the high frequency and density of pastoral farming causes significant declines in cyanobacterial soil crust (Eldridge 1998; Thomas 2012) and studies have found that the soil crust is greatly influenced by this pastoral trampling within 2 to 8km of a borehole (Dougill et al. 1999; Moleele et al. 2002). Therefore, species such as *Acacia mellifera* that show tolerance to trampling are often found within areas close to boreholes (Berkeley et al. 2005a; Berkeley et al. 2005b).

Fire plays an important role in equilibrium of savanna ecosystems and, although fire frequency in African savannas varies, since the 1950s the number of fires in Botswana has decreased because of fire prevention strategies (Mouillot and Field 2005). Fire is often considered as the dominant process that prevents savanna trees from forming full canopies (Higgins et al. 2000; Sankaran et al. 2004; van Wilgen et al. 2003) by removing tree seedlings, preventing establishment of new trees, and thus hindering bush encroachment (Trollope 1980). This effect of fire on vegetation composition has replaced earlier views that fire removes grass and in turn competition for space, allowing bush encroachment (Schultz et al. 1955). In fact, in unmanaged areas, the role of fire in reducing woody cover is well documented, as the build-up of large quantities of grass biomass in the understory results in high-intensity fires which are capable of destroying trees (Bond et al. 2003). Thus, fire can be observed to reduce established woody cover (Sankaran et al. 2008). In many managed areas, fires are not frequent or intense enough to have such an impact on mature trees (Higgins et al. 2000).

Recent studies have moved away from a singular cause of bush encroachment (Kraaij and Ward 2006; Ward 2005; Wiegand et al. 2005). By advancing on Tilman's (1982, 1988) resource allocation framework, Ward (2005) developed a mechanistic model which could explain the balance between savanna grasses and woody vegetation based on the availability of resources. In a pot experiment (simulated grass/tree growth in plant pots) where rainfall, nitrogen, fire and grazing were controlled, Ward found that rainfall frequency was the most important factor affecting germination and the survival of *Acacia* seedlings. Nitrogen addition was also important for suppressing tree germination, but fire and grazing were not significant variables in the process. Likewise, Kraaij and Ward (2006) undertook a similar experiment, by investigating rainfall, nitrogen and grazing in both garden experiments and three sites in the Northern Cape. Their results were similar to Ward's (2005) findings that above average precipitation and frequent rain events are required for mass tree recruitment. While Ward's (2005) study controlled for grazing and fire by clipping the grasses, many of the side effects to these processes such as fire-induced tree mortality, trampling, and associated change in nutrient concentrations were excluded from the experiment. Therefore, it is difficult to state with certainty that precipitation amount and frequency are the most important factors affecting bush encroachment because other factors may also play a role. Thus, multiple drivers need to be considered in the study of bush encroachment.

Variation in species characteristics is fundamental to understanding biogeographic patterns (Lomolino 2000). One reason for the possible lack of conclusive evidence explaining the main drivers of bush encroachment in previous research could be the level

of specificity of studies to focus either on one species or to study all the species found. Assessing diversity as total species richness does not always adequately characterize the way in which species differ from each other, and it is these differences in traits which oftentimes indicate that species respond in different ways to changes in the environment (Marquet et al. 2004). Alternatively, studying only one species in isolation could lead to species-specific results that are not generalizable to the larger system or to other species.

This study investigates the vegetation composition of the Botswana Kalahari, with the aim to establish if any drivers of bush encroachment can be identified at a national scale. By categorizing species into morphological groups based on physiological traits, the drivers of woody vegetation richness and abundance (number of individuals) can be interpreted more meaningfully than by considering either only one vegetation class, or all the different woody plant species separately.

2.2 Methodology

2.2.1 Study Area and in situ data collection

Research was conducted at 15 sites (Table 1) across the western part of Botswana (Figure 1). Sites are spaced along a 950 km transect from Shakawe in the northwest to Bokspits in the far south-western corner of the country. Data collection at each site was conducted during both the dry and wet seasons between late 2009 to early 2011. The location of each site was determined by accessibility and a distance to the previous site of approximately 75 kilometer. At each site six 100 meter transects were laid out radially from a center point, where the direction of the first transect was determined by a random

number. Each other transect was offset by 120 degrees for a total of three transects for the first seasonal field campaign. Transects of the second site visit were spaced exactly between the transects of the previous season, resulting in an offset of 60 degrees from the very first transect chosen. Transects were started 200 meters away from the center point to avoid over-sampling a small area and were laid out using a measuring tape. Data capture and interpretation followed the procedures and methods described for line interception transects (LIT) by Krebs (1999) and all woody vegetation taller than 25cm was identified, following the nomenclature provided by Palgrave (1977).

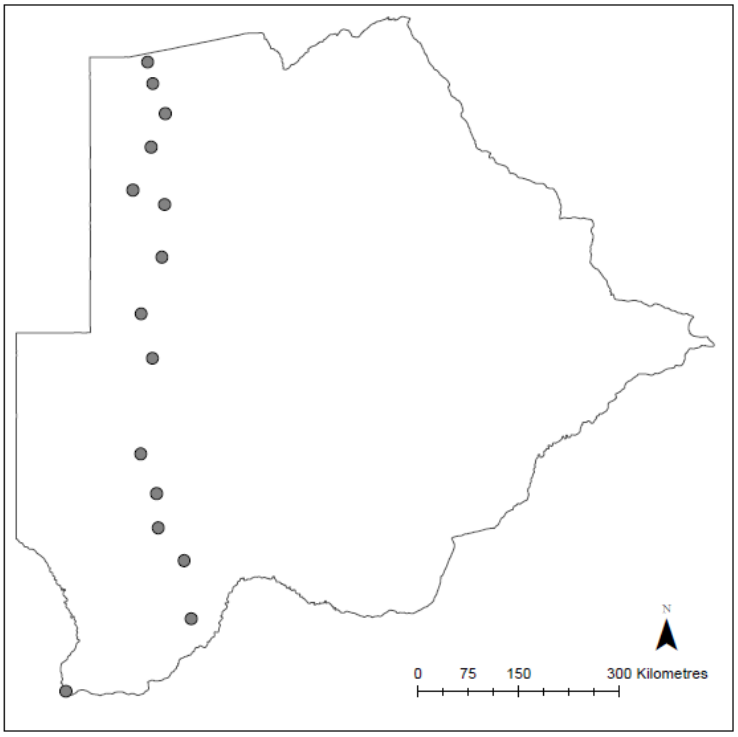

Figure 1: The 15 sites studied along the Kalahari Transect of Botswana. From north to south the sites are: Shakawe, Tsodilo, Gumare, Quangwa, Drotsky's Caves, Ng 5, Kuke, Ghanzi, Ghanzi S., Bere, Tshane, Tshane S, Mabuasehube, Tsabong, and Bokspits. Map by author.

The recorded species were then clustered into five morphological groups (see appendix in section 2.8) following the classifications established by Meyer et al. (2013). The categorization considers differences in species distribution and morphological adaptions to environmental conditions occurring across the rather large spatial extent of the western Kalahari, as suggested by Marquet et al. (2004).

Table 1: site characteristics indicating land use categories (1 – wilderness, 2 - wilderness/ communal grazing, 3 – community grazing, 4 – livestock farm, 5- game farm), grazing intensity (1 – non/ low, 2 – medium, 3 high), number of fires, annual rainfall and number of boreholes within 8 km radius.

	Land use category	Grazing intensity	# fire 2000 - 2011	Annual rainfall mm/ yr	# BH within vicinity of 8 km
Shakawe	3	1	3	550	4
Tsodilo Hills	2	1	3	550	1
Gumare	3	1	3	500	0
Quangwa	3	1	1	500	0
Drotsky's Caves	2	1	1	500	0
NG 5	2	1	3	500	0
Kuke	1	1	0	450	0
Ghanzi	5	1	0	450	20
Ghanzi S	3	3	0	400	4
Bere	4	2	1	350	1
Tshane	3	2	0	350	0
Tshane S	2	1	0	300	0
Mabua	2	2	0	300	1
Tsabong	3	3	0	300	5
Bokspits	3	2	0	300	18

2.2.2 Ex situ data collection and processing

Land use and intensity of cattle grazing was noted during vegetation data collection (Table 1). Land use categories included; community grazing, wilderness areas, livestock

farms (non-cattle), buffer zones and game farms. Cattle grazing intensity was categorized into low, medium and high intensity based on field notes and the Department of Wildlife and National Parks game and livestock counts in 2005 (Table 1). Borehole data consisting of the location of known boreholes was obtained from Department of Water Affairs, Maun. Eight kilometers was taken as the distance within cattle have the most impact on soil through trampling (Dougill et al. 1999; Moleele et al. 2002) and so the number of boreholes within this 8 kilometer radius of the borehole was identified. Annual precipitation data were obtained from the Digital Atlas of Botswana, Department of Survey and Mapping (DSM 2003), with the values ranging from 300 – 550mm.

We used the Moderate Imaging Spectroradiometer (MODIS) MCD12Q1 (land cover product) to determine land cover change for the time period 2000 to 2013, where the number of pixels in each image classified as a certain land cover type has been extracted and compared to the previous year. The MODIS classifications of land cover have a spatial resolution of 500 m per pixel and the temporal resolution of one input image per year. The criteria for each class are mainly dependent on the amount of herbaceous or woody cover for a certain area. Detailed criteria are indicated in Table 2.

Table 2: Land cover criteria for MODIS MCD12Q1 product.

Land cover type	Criteria
Closed shrubland	Woody vegetation with height < 2m, canopy cover > 60%
Open shrubland	Woody vegetation with height < 2m, canopy cover > 60%
Woody savanna	Woody vegetation with height > 2 m, canopy cover 30 – 60 %

Savanna	Woody vegetation with height > 2 m, canopy cover 10 – 30 %
Grassland	Tree and shrub cover < 10 %

Since over that timeframe change is possible from one habitat transitioning to (theoretically) any other habitat type defined and return, we both tracked change in each class over time (see Figure 2 for temporal trends) and also mapped where the primary changes were occurring by starting (year 2000) class (see Figure 3).

The MODIS MCD45A1 burned area product was use to reconstruct the fire history of the area as a sum of the fire events occurring at each pixel on a daily basis. Fire history was calculated as the sum of fire events per pixel across the entire time period.

2.2.3 Data Analysis

The *in situ* and *ex situ* datasets formed the basis of various statistical analyses. Regression analyses were performed to relate the abundance and species richness of the five morphological groups to several environmental variables. All regression analyses were performed in R, version 2.15.3. The regression method used for these analyses was selected based on a preliminary evaluation of the data and their distribution. Histogram exploration identified a mixture of Poisson and censored Gaussian distributions. For data that had a Poisson distribution, a Generalized Linear Model procedure, with Poisson error distribution and a log link function was used:

$$\log(y) = \beta_0 + \beta_1 X_1 + \ldots + \beta_n X_n \quad (1)$$

where y is the abundance, X_n is the nth predictor and β_n is the Poisson regression coefficient.

A censored Gaussian distribution represents a dataset that has normal error distribution, but has some limit, either from below or above. Species richness of woody vegetation is censored at zero (i.e. there cannot be a species richness of -1), and so any parameter estimates obtained by conventional ordinary least squares would be biased. Developed by Tobin (1958), the Tobit regression model can be used to fit a set of parameters to where the dependent variable is left-censored at zero:

$$y_i^* = x_i\beta + \varepsilon_i \quad (2)$$

$$y_i = \begin{cases} 0 \text{ if } y_i^* \leq 0 \\ y_i^* \text{ if } y_i^* > 0 \end{cases} \quad (3)$$

where the subscript $i = 1, 2, 3 \ldots N$ indicates the observation, y_i^* is an unobserved variable, x_i is a vector of explanatory variables, β is a vector of unknown parameters, and ε_i is the error term.

To estimate the censored regression models, we used the censReg package in the R software program. Within Tobit regression there is no measure of goodness of fit analogous to the R^2 in linear regression; however McFadden's pseudo R^2 (1973) can be calculated for anything estimated by maximum likelihood:

$$1 - (L_1 - L_0) \quad (4)$$

where L_1 is the log-likelihood value for the fitted model, and L_0 is the log-likelihood value for the null model excluding all the explanatory variables.

This calculation produces a statistic on a [0,1] scale, with 0 indicating that the explanatory variables failed to increase likelihood, and 1 indicating that the model perfectly predicts each observation. Terms were retained in the minimal adequate model if they were significant at $\alpha = 0.05$.

2.3 Results

The land cover change assessment reveals that the area has undergone dramatic changes in land cover. Five habitat types have been identified in the area and all of them show a significant shift in habitat type based on a definition of woody cover components. According to the MODIS MCD12Q1, the two dominant land cover types of the area are open shrubland and savanna. While savannas, defined as woody cover between 10 – 30 %, covered most of the area in 2000, their extent indicates a decline from above 60 % of the total cover in 2006 to 48 % cover in 2010. The curve presented in Figure 2 shows that the decline is almost entirely offset by a gain in open shrublands for the same time period.

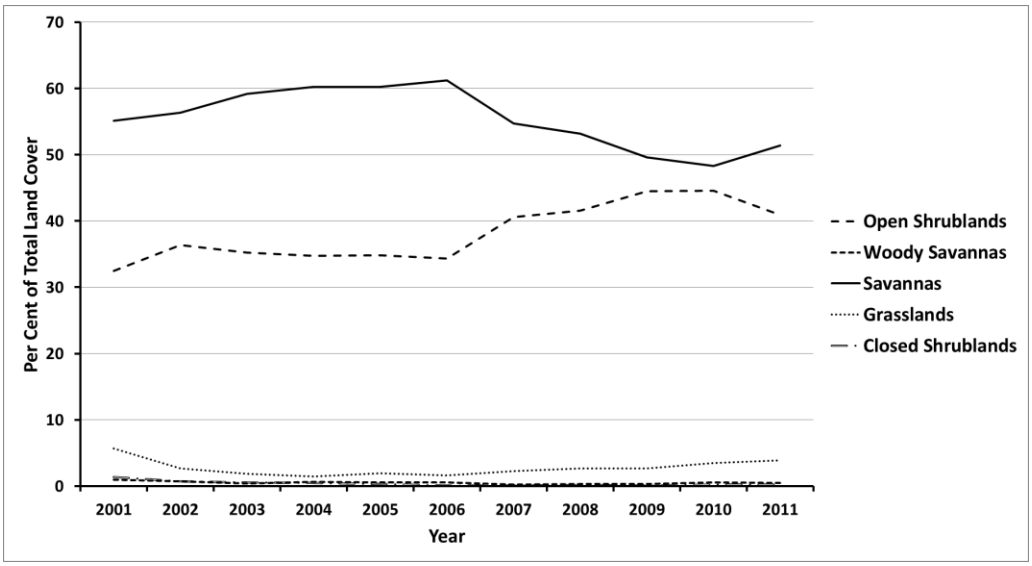

Figure 2: Land cover change 2000 – 2011

The changes from one land cover type to another are presented in Table 3 while the total gain or loss per land cover type is presented in Table 4. Most of the transitions took place by savanna transitioning into open shrubland and grassland converting to open shrubland. This results in a gain for open shrubland over a time period of 11 years of approximately 43270 km^2. All other changes in cover types can be attributed to a total gain in open shrublands, reducing the total area covered by any other cover type (Tables 2, 3 and Figure 3).

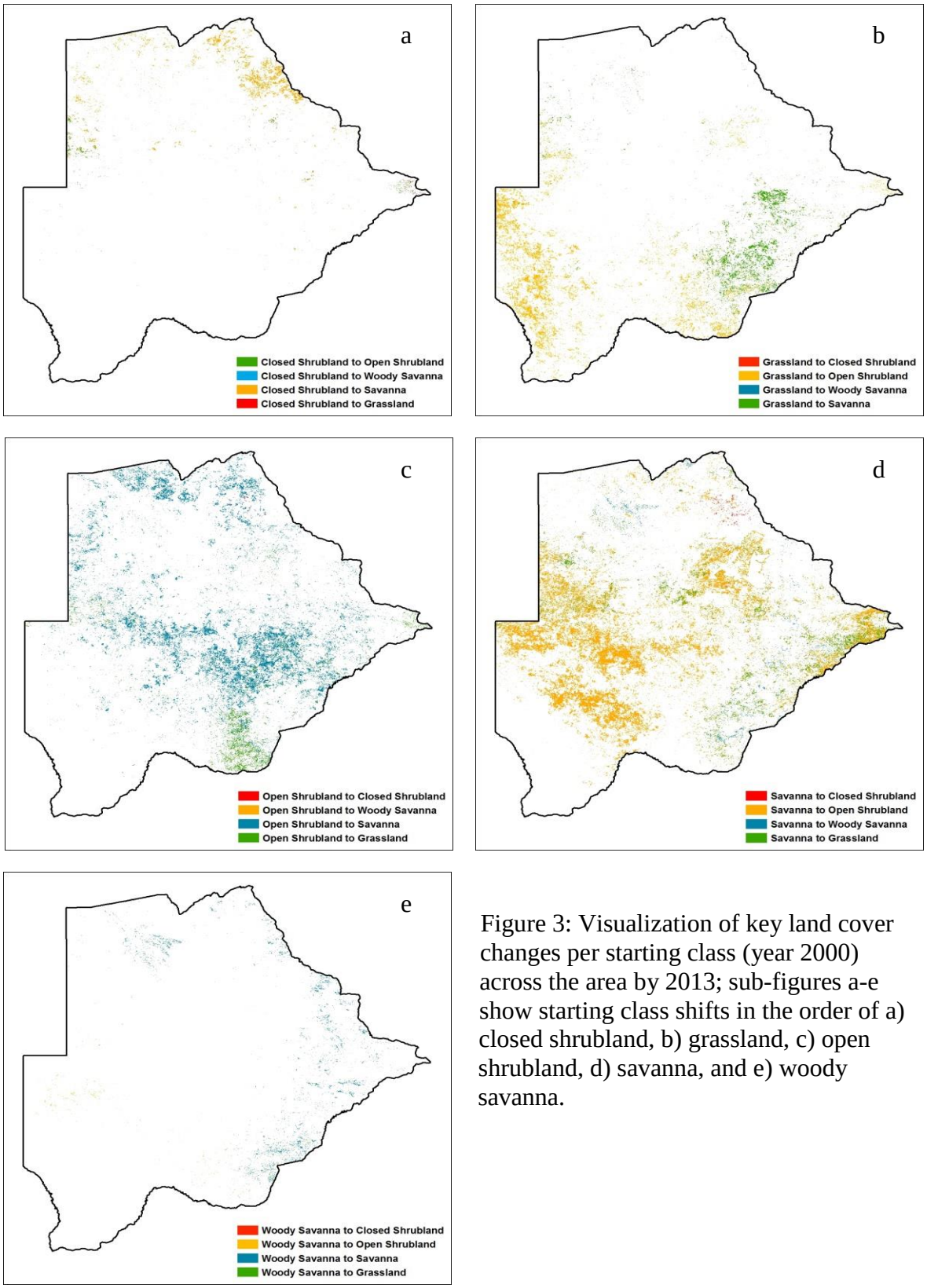

Figure 3: Visualization of key land cover changes per starting class (year 2000) across the area by 2013; sub-figures a-e show starting class shifts in the order of a) closed shrubland, b) grassland, c) open shrubland, d) savanna, and e) woody savanna.

Table 3: Land cover change per change scenario with net gain (in bold)

Land Cover Transition	**Quantified Change (km^2)**	**Land Cover Transition**	**Quantified Change (km^2)**
Closed Shrubland ↔ **Open Shrubland**	786.26	Woody Savanna ↔ **Open Shrubland**	351.81
Closed Shrubland ↔ Woody Savanna	1.72	Closed Shrubland ↔ **Grasslands**	140.81
Grassland ↔ **Savanna**	4056.39	Grassland ↔ **Open Shrubland**	13238.13
Closed Shrubland ↔ **Savanna**	5619.03	Grassland ↔ **Woody Savanna**	88.65
Savanna ↔ **Open Shrubland**	28894.05	Woody Savanna ↔ **Savanna**	1803.47

Table 4: Total change

Habitat type	**Change 2000 - 2013**
Closed shrubland	- 6544.38
Open shrubland	43270.25
Woody savanna	-2068.35
Savanna	-17415.16
Grassland	-17242.36

The visualization in Figure 3 shows that most of the savanna and grassland to open shrubland transitioning took place in the western part of the Kalahari with a strong change indicated in the Ghanzi area.

Fire frequencies across the area range from no fire to a maximum of eleven fires recorded for the northern part of the country along the border with Namibia's Caprivi Strip. Most pixels indicate a frequency of one fire during the observed time period (Figure 4). Figure 4 also shows that most areas that burned have a fire frequency between 1 fire and 3 fires

for the observed time frame. Most of these areas are indicated in the north-western and central parts of the region.

# of fires	Area Burned (km^2)
1	2661.41
2	1832.88
3	1037.61
4	617.76
5	399.89
6	246.21
7	108.61
8	42.72
9	7.08
10	1.72
11	0.43

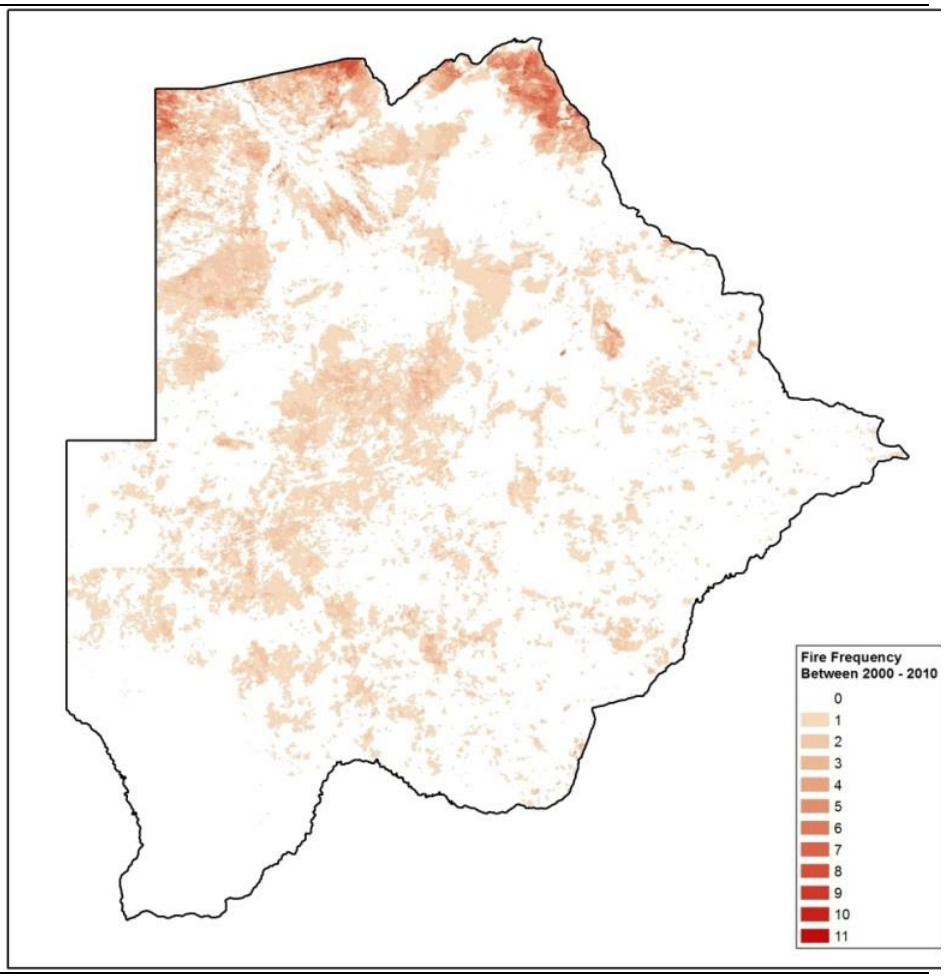

Figure 4: Burned area and fire frequency across the Kalahari region.

Across the field sites, fire frequency ranged from 0-3, with a total of seven sites having been affected at least once during the time period. Fire frequency shows that most fires occurred at the northern-most sites of the transect. Return intervals for fire occurrences seem to be higher at the northern site locations while all southern sites with the exception of Tsabong were unaffected by fire.

At the site level, a total of 44 woody plant species were identified across all field sites. The highest abundances (number of individuals) were found in the data from the wet season collection at transect # 3 of Kuke and lowest abundance (n=2) identified at four transects located in Bokspits (2), Tsabong (1) and Tshane (1). The dry season collection of transect # 2 at Kuke also indicated the highest species richness of all transects with a recorded number of woody plants of 13 species. Figure 5 identifies the total abundance found across the 15 sites. The highest site abundance is at Quangwa, with the lowest found at Bokspits. Eight species were identified as *Acacia* species (morphological group 1), 14 as tall dense canopy species (morphological group 2). The highest numbers of species were categorized as small dense species (morphological group 3) with 15. Five species were identified as tall and open canopies (morphological group 4), while only two species were identified as small open canopy species (morphological group 5).

Table 5: Regression models for total species richness and abundance
** indicates significant at $\alpha = 0.01$ and * indicates significant at $\alpha = 0.05$

	Total Species Richness	**Total Abundance**
	Tobit (Left Censored at 0)	Tobit (Left Censored at 0)
	Pseudo-R^2 20.173	Pseudo-R^2 0.144
	Log Likelihood -147.879	Log Likelihood -270.772
	Likelihood Ratio 61.840	Likelihood Ration 91.210
Intercept	4.065 ±1.184**	-37.323 ±4.737**
Land Use (Wilderness Area)	-2.967 ±0.651**	
Land Use (Community Grazing)	-2.386 ±0.584**	-4.901 ±1.987 *
Land Use (Livestock Farm)	-2.691 ±0.872**	
Land Use (Game Farm)		-12.556 ±3.705**
Grazing (Mid)		
Grazing (High)		

Boreholes	-0.193 ±0.036**	
Annual Precipitation	0.0108 ±0.002**	0.160 ±0.012**
Number of Fires		-10.414 ±1.390**

Table 5 lists the regression outputs for total species richness and abundance. All land use categories included in the final model had significantly lower coefficient values than the buffer zone, serving as the reference for both richness and abundance. Boreholes and fire frequency showed negative relationships with richness and abundance respectively, while annual precipitation indicated a positive relationship with both richness and abundance.

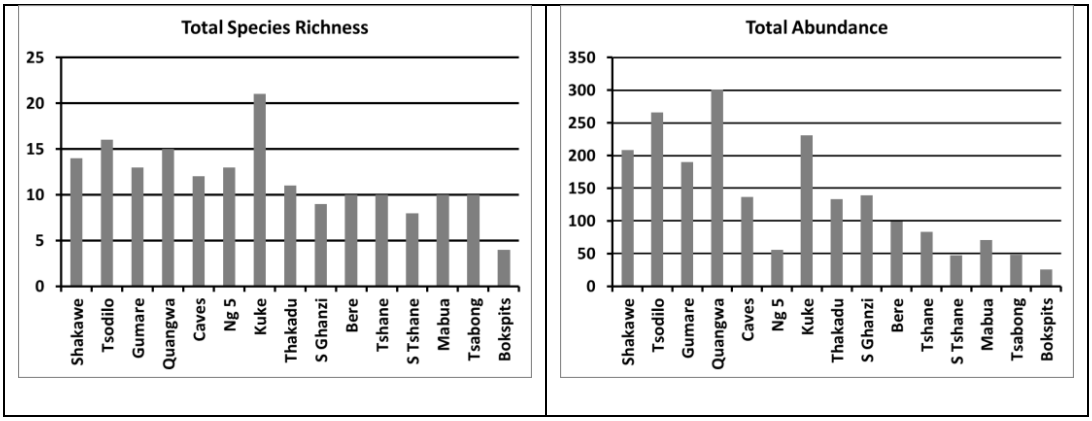

Figure 5: Total species richness and abundance at each of the 15 sites across western Botswana

There was a variety of significant positive and negative relationships with all of the drivers for species richness (Table 6) and abundance (Table 7) for the identified morphological groups. Buffer zones have higher richness and abundances than any land use included in the final model, except for abundance of *Acacia* in game farms. Higher grazing intensities [game or livestock] led to higher likelihoods of abundances of *Acacia* and small dense canopy species. Borehole numbers had a negative relationship with *Acacias*, small dense canopy species and open canopy species for both richness and abundances. Fire frequency had a positive relationship with *Acacias* richness and tall

open canopy species richness and abundance, but a negative relationship with both tall dense canopy species richness and small dense canopy abundance. Finally, annual precipitation had a positive relationship with both small and tall dense species richness and abundance, but a negative relationship with *Acacia* richness and small open canopy species richness and abundance.

Table 6: Regression models for species richness of the five morphological groups
Regression type T refers to a Tobit model, and P refers to a Poisson distribution
** is significant at $\alpha = 0.01$ and * is significant at $\alpha = 0.05$

Dependent Variable	Morph Group 1	Morph Group 2	Morph Group 3	Morph Group 4	Morph Group 5
Regression Type	T	T	T	P	P
Pseudo-R2	0.052	0.223	0.249	-	-
Residual Dev.	-	-	-	76.690	17.130
Intercept	3.135 ±0.609**	-6.372 ±0.935**	1.480 ±0.735 *	-1.163 ±0.240**	6.328 ±1.807**
LU (Wilderness Area)			-1.956 ±0.410**		
LU (Community Grazing)		-0.775 ±0.365 *	-1.573 ±0.407**		
LU (Livestock Farm)			-2.036 ±0.535**		
LU (Game Farm)					
Grazing (Mid)					
Grazing (High)			1.154 ±0.391**		
Boreholes			-0.168 ±0.026**		-0.722 ±0.138**
Annual Precipitation	-0.005 ±0.002**	0.021 ±0.002**	0.006 ±0.001**		-0.020 ±0.006**
Fire Frequency	0.342 ±0.162 *	-1.147 ±0.242**		0.480 ±0.158**	

Table 7: Regression models for abundance of the five morphological groups.

Dependent Variable	Morph Group 1	Morph Group 2	Morph Group 3	Morph Group 4	Morph Group 5
Regression Type	P	P	P	P	P
Pseudo-R2	-	-	-	-	-
Residual Dev.	198.728	379.980	121.550	412.780	71.104
Intercept	0.564 ±0.182**	-1.432 ±0.729 *	-2.812 ±0.588**	1.626 ±0.551**	4.737 ±1.200**
LU (Wilderness Area)		-1.118 ±0.269**		-1.685 ±0.679 *	
LU (Comm Grazing)			-0.861 ±0.157**	-1.716 ±0.706**	
LU (Livestock Farm)			-0.716 ±0.321 *	-2.085 ±0.743**	
LU (Game Farm)	2.020 ±0.551**				
Grazing (Mid)	1.387 ±0.248**	-11.020±3.070**	0.727 ±0.292 *		
Grazing (High)	0.748 ±0.326 *		1.672 ±0.239**		
Boreholes	-0.054 ±0.018**		-0.098 ±0.017**		
Annual Precipitation		0.009 ±0.002**	0.012 ±0.001**		-0.016 ±0.004**
Fire Frequency			-0.559 ±0.079**	0.4587 ±0.163**	

2.4 Discussion

Bush encroachment is a serious problem in nations that rely on savanna landscapes for ranching (game and/or livestock). Botswana is one of these nations, with ranching interwoven with their current economic stability (Acemoglu et al. 2001; Robinson and Parsons 2006). Figure 3 shows the changing percentage of land cover classified as

savannas and shrublands by MODIS product MCD12Q1 and confirms the trend of the conversion of savanna landscapes to shrublands on a national level in Botswana as described in the literature (Perkins and Thomas 1993; Ringrose et al. 2003; Ringrose et al. 1996). Most of the savanna to shrubland transition takes place in the western parts of the Kalahari with particular concentrations in the Ghanzi area itself and the areas to the south. As far as fire return intervals are concerned, highest fire frequencies were observed in the north, with most other parts of the region still affected by fire but with lower return intervals. Apart from the northern sites, areas most affected by fires were located in the central part of the region. Research conducted in this area and elsewhere has identified several possible drivers of bush encroachment but consensus on the overall underlying mechanism remains a source of continued investigation. The analyses presented in this study shed light on the relative influence of a variety of drivers across various savanna landscapes in Botswana, and in particular, the importance of studying the drivers for specific morphological groups.

The rainfall gradient of the Kalahari has been associated with an increase in canopy density (Caylor et al. 2003; Caylor and Shugart 2006) and our results are in agreement with this trend (Figure 5) by showing an overall increase in the total abundance of woody species with mean annual precipitation across 15 sites. However, some deviations from this trend can be observed, particularly at the Drotsky's Caves site as well as at the NG 5 site. While the regression results point to land use category and fire occurrence as the potential main drivers controlling the abundance of woody plants (Table 5), in the cases of the sites mentioned above, fire and grazing pressure cannot explain the low species

abundance at these sites that are located in a low grazing intensity and fire occurrence area (Table 1). The general trend also holds in the most part for species richness, however, the highest species richness was recorded at Kuke, where the annual precipitation is 450mm, approximately in the middle of the rainfall gradient. The substantially higher species richness at this particular site can be explained by an increased heterogeneity, since the Kuke site is located in an area buffering the Ghanzi farm-block to the south and the wildlife areas to the north. No anthropogenic land usage takes place in the Kuke / buffer zone area, so both livestock and wildlife numbers are low. Further, fires have not occurred in this area due to both fire prevention strategies in the farms to the south of the buffer zone and the existence of the veterinary cordon fences to the north of the buffer zone acting as a fire break.

Midgely and Bond (2001) state the importance of not studying *Acacia* species in isolation of each other, and this idea can be extended to all woody vegetation species that could constitute part of the encroaching bush. It was decided that this research would investigate the impact of these drivers on morphological groupings of woody vegetation. This focus would allow for interpretation of the results to relate to the structure and physiological properties of the species, while not being so specific that one could not develop general trends, and not being so general that any patterns were confounded by different traits.

Precipitation had a positive relationship with total species richness and abundance for morphological groups 2 and 3. This relationship was expected since these groups are

characterized by dense canopy broad leaf species resulting in higher Leaf Area Index (LAI) and hence higher water requirements (White et al. 2000). Surprisingly, a negative relationship for *Acacia* richness as well as small open canopy species richness and abundance was found. This finding apparently contradicts Ward (2005) and Kraaj and Ward (2006), who found precipitation frequency is important for *A. mellifera* recruitment. *Acacia* trees are known for being versatile plants, well adapted to drought conditions typically found in more xeric environments (Sankaran et al. 2005). Therefore, their species richness is expected to be higher in lower precipitation areas where their general morphological characteristics and ecological traits outcompete the majority of broad leaved vegetation. The negative relationship with the small open canopy species, such as *Lycium hirsutum* (Table 7), had been expected considering the range of the species included in the group as indicated by Palgrave (1977).

The correlations of fire and morphological group suggest that fire also has differing effects on richness and abundance. It is found that fire is generally negatively correlated to the overall abundance of woody species in agreement with observations from other dryland ecosystems (Van Auken 2000; van Wilgen et al. 2003) and a mechanistic understanding of the effect of fires in mixed tree-grass plant communities (Dublin et al., 1990; Higgins et al., 2000; Anderies, et al., 2002; D'Odorico et al., 2011). Our data analysis, however, indicates that fire has a positive effect on *Acacia* and species characterized by tall open canopies, such as *Dichostachys cinera, Catophractes alexandri,* and *Rhigozum* species, with regard to both abundance and species richness. Fire negatively influences small dense canopy species, because they are prone to intense

canopy fires that remove more biomass. It has been confirmed that fire is an important driver within savanna ecosystems, but its impacts seem to vary by morphological group.

The number of boreholes within 8 km of the site did not have a positive relationship with any morphological groups, but did have significant negative relationships with total species richness, *Acacia* abundance, and small dense species richness and abundance. The negative relationship with small dense species is intuitive, as trampling loosens the soil and prevents these species from rooting. Our finding of a negative association of *Acacia* abundance and boreholes is not supported by other studies that identified *Acacia* species as thriving in areas close to boreholes (Berkeley et al. 2005a) but could be caused by overbrowsing by goats. However, the highest concentration of boreholes at our study site can be observed in fenced farm areas where movement of livestock is managed to reduce the effects of soil trampling. Therefore, the rotation of boreholes for use by cattle by farmers could negate the impact of trampling on the soil and subsequently reduce the rate of bush encroachment.

Both medium and high grazing intensity areas have higher *Acacia* abundances than low grazing intensity areas. This result agrees with the research that has stated competition with grasses is reduced in overgrazed areas (Ward 2005).Thus, once established, thorny *Acacias* are not disturbed by cattle. Higher grazing intensities also have a positive relationship with small dense canopy species richness and abundance. Small dense canopy species such as *Grewia* species, *Rhus tenuiveris, Ziziphus mucronata* notably have relatively low palatable values (Le Houérou and Corra 1980). Thus, if these species

were already established when the grazing intensities increased in the area, they would not be affected by livestock. Finally, land use is a significant variable for several relationships, with a higher species richness and abundance found in the buffer zones. This trend highlights again that the absence of any disturbance results in higher abundance of woody vegetation.

2.5 Conclusion

This study shows how the phenomenon of bush encroachment is potentially affected by multiple factors. While our analysis cannot evaluate the causality of the relationship between woody species abundance and richness, and environmental drivers such as precipitation, fire, or grazing, it does indicate the importance of not studying woody species in isolation from each other. Deconstruction of species richness into the five morphological groups provided better insights into the differences in the ways that woody vegetation species respond to environmental factors. This deconstruction could reconcile the divergent hypotheses surrounding bush encroachment, as all environmental variables had a significant relationship with species richness and abundance for at least one morphological group. If the results from total species richness and abundance were only considered, then grazing intensities would not have been found to be significant, despite being significant for *Acacias* and dense canopy species. Fire was a significant variable for *Acacias*, tall dense and tall open canopy species richness, while boreholes were a significant variable for small dense canopy species richness. All land uses had a significantly lower richness and abundance (except *Acacia* abundance on game farms) than buffer zones, regions where many of the anthropogenic influences of bush

encroachment (grazing and trampling) are removed, but where fire is suppressed. The observed decrease in total species richness, and specifically for *Acacias* and small dense canopy species, with the proximity of boreholes indicates that livestock in general have a negative impact on species richness in the area, regardless of the type of land use. The importance of the rainfall gradient was also identified in this research, in agreement with the results from previous research (e.g. Caylor et al. 2003). Nevertheless the highest species richness was found at an intermediate site (Kuke) along the Kalahari's rainfall gradient, an area that can be considered as isolated from human land use and not affected by natural fires or grazing. Stakeholders involved with the issue of bush encroachment should analyze the species affected based on morphological traits to make informed decisions.

2.6 Appendix

Species	Morphological Group	Morphological Group Number
Acacia ataxacantha	*Acacias*	1
Acacia erioloba	*Acacias*	1
Acacia erubescence	*Acacias*	1
Acacia fleckii	*Acacias*	1
Acacia hebeclada	*Acacias*	1
Acacia luederitzii	*Acacias*	1
Acacia mellifera	*Acacias*	1
Albizia anthelmintica	*Acacias*	1
Baikea plurijuga	Tall Dense Canopy	2
Baphia mosambicensis	Small Dense Canopy	3
Bauhinia petersiana	Small Dense Canopy	3
Boscia albitrunca	Tall Dense Canopy	2
Burkea africana	Tall Dense Canopy	2
Cadaba aphylla	Small Open	5
Catophractes alexandri	Tall Open	4
Combretum apiculatum	Tall Dense Canopy	2
Combretum collinum	Tall Dense Canopy	2
Combretum hereroense	Tall Dense Canopy	2
Combretum molle	Tall Dense Canopy	2
Combretum psidioides	Tall Dense Canopy	2
Combretum zeyeri	Small Dense Canopy	3
Commiphora africana	Small Dense Canopy	3
Commiphora angolensis	Small Dense Canopy	3
Commiphora glandulosa	Small Dense Canopy	3
Dialium englerianum	Tall Dense Canopy	2
Dichostachys cinera	Tall Open	4
Grewia bicolor	Small Dense Canopy	3
Grewia flava	Small Dense Canopy	3
Grewia flavescense	Small Dense Canopy	3
Guibourtia coleosperma	Small Dense Canopy	3
Gymnosporia senegalensis	Small Dense Canopy	3
Lonchocarpus nelsii	Small Dense Canopy	3
Lycium hirsutum	Small Open	5
Mundulea sericea	Small Dense Canopy	3
Pterocarpus angolensis	Tall Dense Canopy	2
Rhigozum brevispinosum	Tall Open	4

Rhigozum obovatum	Tall Open	4
Rhigozum trichotomum	Tall Open	4
Rhus tenuiveris	Small Dense Canopy	3
Strychnos pungens	Tall Dense Canopy	2
Terminalia prunoides	Tall Dense Canopy	2
Terminalia sericea	Tall Dense Canopy	2
Vangueria infausta	Tall Dense Canopy	2
Ziziphus mucronata	Small Dense Canopy	3

Chapter 3

An analysis of structure: Biomass structure relationships for characteristic species of the western Kalahari, Botswana

Published in: Journal of African Ecology, March 2013

Authors: Meyer, T., D'Odorico, P., Okin, G.S., Shugart, H.H., Caylor, K.K., O'Donnell, F.C., Bhattachan, A., Dintwe, K.

3.1 Introduction

Savanna ecosystems cover about 20% of the Earth's land surface, including about 40% of Australia, South America, and Africa (Scholes and Walker 1993). They provide important services such as rangeland for livestock production, firewood, carbon sequestration, and protection against soil erosion. It has been estimated that savannas contribute about 15% (Taylor and Lloyd 1992) to 29% (Mohamed et al. 2004) of the global terrestrial net primary productivity. Despite their important role in the global carbon balance, the contribution of savannas to the global stocks of organic carbon remains poorly quantified. It is unclear (i) how much biomass is stored in savannas; (ii) how it is partitioned between above- and belowground stocks; and (iii) how these stocks are expected to change under different land use and climate change scenarios. This lack of a quantitative assessment of carbon stocks in savanna vegetation is a major limitation to the understanding of whether changes in climate, land management, or disturbance regime might turn savannas into important sources or sinks of atmospheric CO_2 (Wang et al. 2009; Williams et al. 2007).

Possible changes in vegetation structure and composition induced by shifts in rainfall regime can be inferred through a "space-for-time" substitution along a rainfall gradient. Thus, we focus on savanna ecosystems located along the Kalahari Transect (KT), where a rainfall gradient exists on the relatively uniform soil substrate of the Kalahari's sand sheet. The consistent soils of the Kalahari combined with a documented rainfall gradient provide an excellent "open air laboratory" to study the effects of climate change on vegetation patterns, the distribution and production of biomass, and the region's carbon

storage capacity (Scholes et al. 2004). Previous research has assessed changes in vegetation cover, composition and structure along the KT and elucidated the relations existing between vegetation structure and abiotic factors such as nutrient (Wang et al. 2010) and water availability (Caylor et al. 2006). Empirical relations to determine the above ground biomass of woody species in the Kalahari have been established by Tietema (1993), who provided allometric relationships for fuel-wood relevant hardwood species but did not consider other woody species. In this study we aim to determine a set of allometric relations for woody plants in the Kalahari, which has been limited by an inadequate set of empirical allometric relations capable of providing a relatively accurate estimate of plant biomass based on some easy-to-measure quantities such as basal diameter, plant height or the size of the canopy footprint.

Although basal diameter is commonly used as the independent variable in allometric relationships, this approach is difficult to implement for smaller multistem shrubs that often characterise entire landscapes throughout the western and central parts of the Kalahari and savannas in general. In these landscapes it is impractical to determine woody biomass using allometric relationships with basal area because each shrub may have numerous and hard-to-reach stems. The basal area approach is more suitable for defined stands where DBH (diameter at breast height) or the basal diameter can be accurately measured. To this end, this paper also investigates the suitability of crown area as a predictor for above ground woody biomass. Unlike stems, which can only be measured in the field, woody crowns have the potential to be remotely sensed through a

variety of methods and the empirical relations determined in this paper could pave the road to remote methods for the estimation of woody biomass.

3.2 Materials and Methods

3.2.1 Research sites

We focus on the Botswana segment of Kalahari Transect, which stretches 950 km in the south-north direction across the western part of the country along a rainfall gradient ranging from 170mm/yr in the south to 550 mm/yr in the north (Figure 1). Along this transect, four sites were selected in areas with different average annual rainfalls. The transect stretches from Bokspits (driest) in the far south to Shakawe (wettest) in the far northwestern corner of the country. Site information is reported in Table 1.

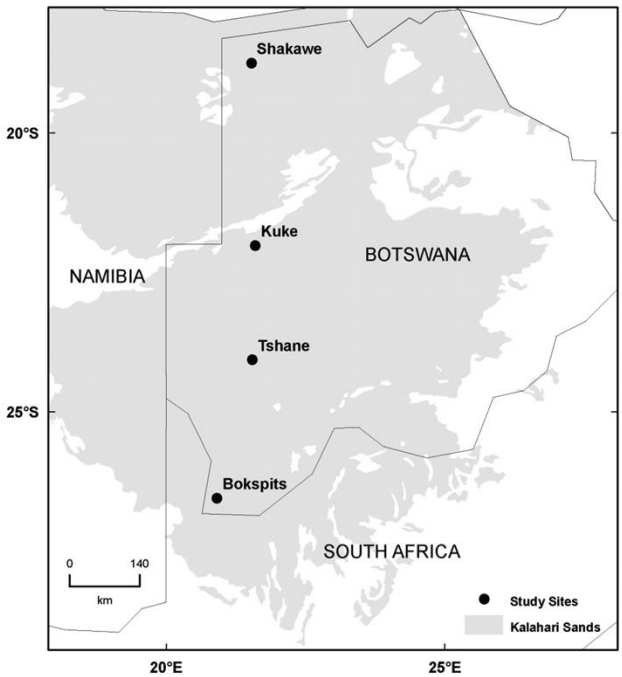

Figure 1: Site locations (source DSM (2003), map by author)

Table 1: Climate, soil, and vegetation characteristics at the four field sites. Rainfall values refer to mean annual precipitation (MAP) in 1971-2006 measured by the Botswana Department of Meteorology.

Site	**MAP** (mm)	**Soil Type**	**Vegetation Type**	**Canopy structure**	**Dominant species**
Shakawe	539	Aeolian sand	Kalahari Thornveld – Miombo Transition	Tree (>15 m),	*Pterocarpus angolensis, Burkea africana, Baikiaea plurijuga*
				Multi stemmed Tree/Shrub (8m), Multi stemmed Shrub (2m)	*Terminalia sericea, Ochna pulchra, Burkea africana, Grewia flavescense*
Kuke	439	Aeolian sand	Kalahari Thornveld	Multi stemmed Shrub (2 m),	Croton gratissimus, *Philenopteranelsii, Grewia flavescense, Boscia albitrunca, Bauhinia petersiana*
Tshane	358	Aeolian sand	Kalahari Thornveld	Tree (< 7 m)	*Acacia luederitzii var. Luederitzii*
				Multi stemmed Shrub (3 m),	*Grewia flava, Lycium hirsutum, Boscia albitrunca, Rhus tenuivervis, Rhigozumbrevispinosum*
Bokspits	177	Aeolian sand (dune field)		Widely spaced Tree (15 m)	*Acacia haematoxylon, Acacia erioloba, Boscia albitrunca*
				Multi stemmed Shrub (4m)	*Acacia mellifera*
				Multi stemmed Shrub (1.5 m),	*Lycium bosciifolium, Rhigozum trichotomum.*

3.2.2 Sampling protocol

At each site, three 20 m x 20 m plots were cleared and all vegetation was identified following the nomenclature of Palgrave (1977). Before clearing, structural parameters

such as height (H), crown diameter (CD) and basal (stem) diameter (BD) of each individual were determined.

While harvesting the woody vegetation, the above ground biomass of all trees and shrubs in the 20m x 20m plots was weighed using spring scales. Height (H) was measured as maximum height of the top of the canopy using a measuring tape if maximum height could be reached and using a clinometer in the case of taller trees.

In order to avoid bias and to account for structural variety, the crown diameter was measured twice, along the east-west and north-south directions. The average was recorded as crown diameter (CD) and formed the basis for canopy area (CA) calculations ($CA=\pi/4\ CD^2$). The BD was measured just above the basal swell at roughly ankle height, because most woody vegetation grows in multi-stemmed forms at all sites (Dayton 1978). For multi-stemmed individuals the total basal area (BA) was calculated as the sum of the basal areas of all stems:

$$BA = \pi/4 \sum_i BD_i^2 . \qquad (1)$$

3.2.3 Calculation of regression curves

Regression curves were determined to relate aboveground wet biomass to the three structural parameters. Power-law relationships of biomass versus height, crown diameter and basal area were plotted using a logarithmic scale in order to account for changes in magnitude. The bias introduced by compressing values of different magnitudes onto a

logarithmic scale (i.e. by giving them less weight in comparison to small values) was corrected using the approach described by Beauchamp and Olson (1973) and Sprugel (1983).

The power-law relationships between biomass and the three structural parameters height, crown diameter and basal area were derived for four cases: 1) all individuals at all sites, 2) all individuals at each site, 3) each species of which more than 15 individuals were sampled, and 4) all species in each of five distinct morphological classes: *Acacia* spp, tall (> 2 m) dense canopy species, small (≤ 2 m) dense canopy species, tall (> 2 m) open canopy species, small (≤2 m) open canopy species). The coefficient of determination (R^2) values were calculated as well as the root mean squared error (RMSE) of log-transformed values. The regressions derived for all woody species across the entire transect indicate that height, basal diameter, or canopy size can all be used in allometric relationships with plant biomass.

3.3 Results

The total number of individuals included in the assessment across the four sites was 342 with 55 individuals at Shakawe, 125 at Kuke, 122 at Tshane and 40 at Bokspits (Table 3). A total of 23 different woody species were measured during the study. Table 2 lists all the species sampled along the transect.

Table 2: Species, number of individuals sampled, site (B=Bokspits, T=Tshane, K=Kuke, S=Shakawe) and morphological category (1 Acacias, 2 tall dense canopy spp, 3 small dense canopy spp, 4 tall open canopy spp, 5 small open canopy spp).

Scientific name	Total number	Site ID	Morphological Category
Acacia erioloba	4	B	1
Acacia luederitzii	12	T	1
Acacia mellifera	42	T,B	1
Acacia tortillis	2	K	1
Bauhinia petersiana	3	K	4
Boscia albitrunca	16	K,T	2
Burkea africana	17	S	2
Cadaba aphylla	2	T	5
Combretum colinum	1	S	2
Combretum molle	5	K	2
Combretum zeyeri	15	K	2
Croton gratissimus	65	K	3
Grewia flava	15	T	3
Grewia flavescense	17	K	3
Lycium bosciifolium	5	B	5
Lycium cinerum	56	T	5
Ochna pulchra	20	S	2
Philenoptera nelsii	1	K	3
Rhigozum brevispinosum	1	T	4
Rhigozum trichotomum	4	B	4
Rhus tenuiveris	10	T	4
Spirostachys africana	9	K	2
Terminalia sericea	20	S,K	2
Total	342		

3.3.1 All individuals at all sites

Plant biomass was related to the three structural parameters, basal area (BA), crown area (CA) and height (H) (Figure 2). This analysis included all the 342 trees and shrubs sampled regardless of species, site, or growth form. The R^2 values (Table 3) indicate that the regression of biomass vs. basal area performs better than the regressions using the other parameters (H and CA), with R^2 values of 0.82 for BA, 0.73 H and 0.75 for CA.

However, the calculated RMSE indicates only minor differences between the three regressions with values of 0.87 for BA, 1.05 for H and 1.01 for CA (Table 3).

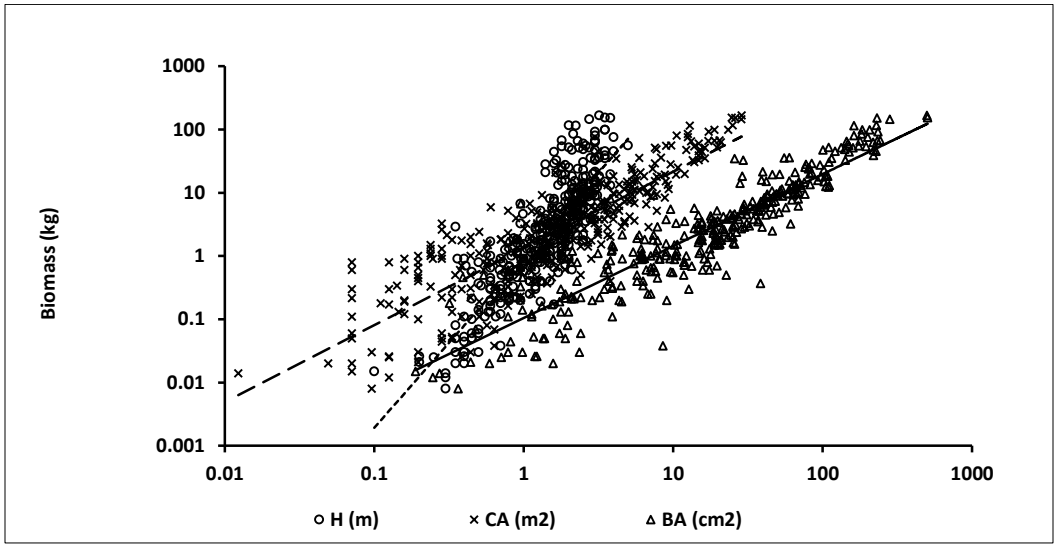

Figure 2: Regression for all species and sizes (BA – solid line, CA – dashed line, H – dotted line)

3.3.2 All individuals at each site

The results of an analysis of all individuals at each site are shown in Figure 3, which provides the power law fitting parameters for the relationships between plant biomass and the three structural parameters BA, H and CA for the four different field sites. The corresponding R^2 values (i.e., R^2_H, R^2_{BA}, and R^2_{CA}, respectively) and the RMSE values are reported in Table 3. These results indicate that basal area is a good predictor of biomass at all sites, with R^2 ranging from 0.82 at Shakawe, Tshane and Bokspits and 0.79 at Kuke. Height is overall the worst predictor with R^2 values dropping to 0.51 at Kuke. The canopy area performs well at all sites, and at Kuke even better than the basal area, reaching an R^2 value of 0.89.

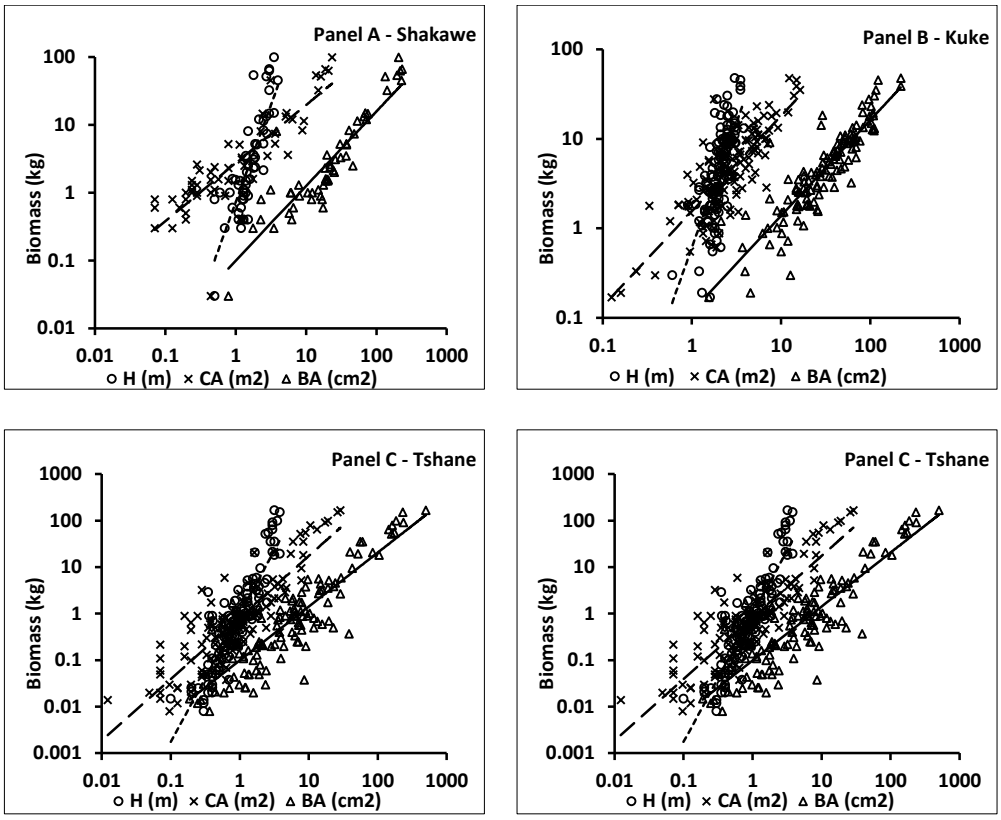

Figure 3: Site-specific regression of all species and sizes (BA – solid line, CA – dashed line, H – dotted line)

3.3.3 All individuals of each species

Species-specific analysis was conducted only on species with more than 15 sampled individuals. Due to morphological similarity *A. luedertizii, A. tortillis* and *A. erioloba* have been combined in one group representing species characterised by bipinnate leaf structures.

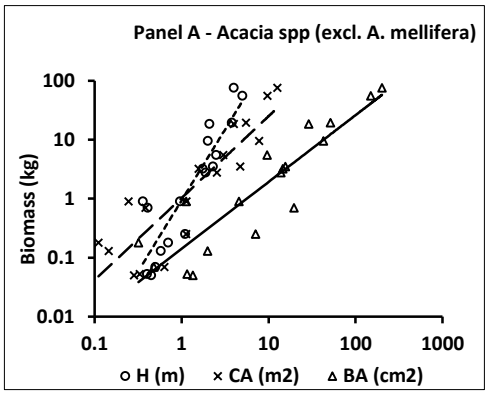
Panel A - Acacia spp (excl. A. mellifera)
Biomass (kg)
100
10
1
0.1
0.01
0.1
1
10
100
1000
H (m)
CA (m2)
BA (cm2)

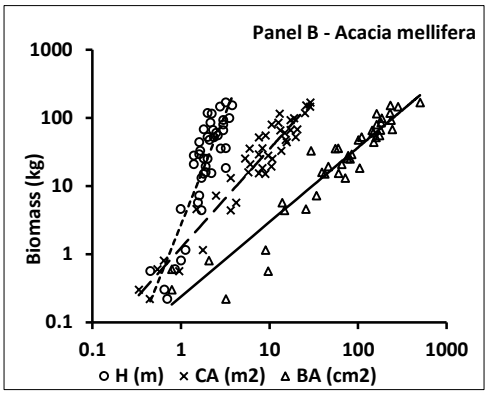
Panel B - Acacia mellifera
Biomass (kg)
1000
100
10
1
0.1
0.1
1
10
100
1000
H (m)
CA (m2)
BA (cm2)

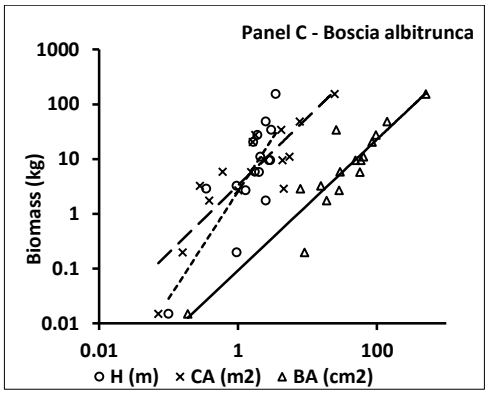
Panel C - Boscia albitrunca
Biomass (kg)
1000
100
10
1
0.1
0.01
0.01
1
100
H (m)
CA (m2)
BA (cm2)

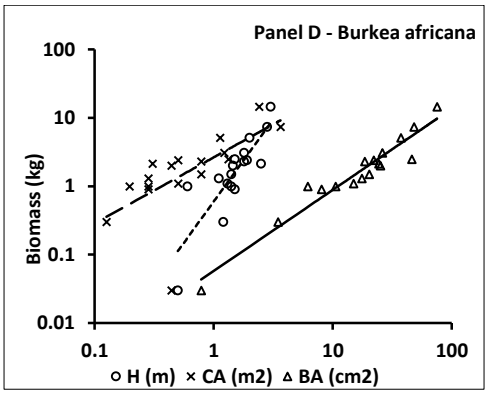
Panel D - Burkea africana
Biomass (kg)
100
10
1
0.1
0.01
0.1
1
10
100
H (m)
CA (m2)
BA (cm2)

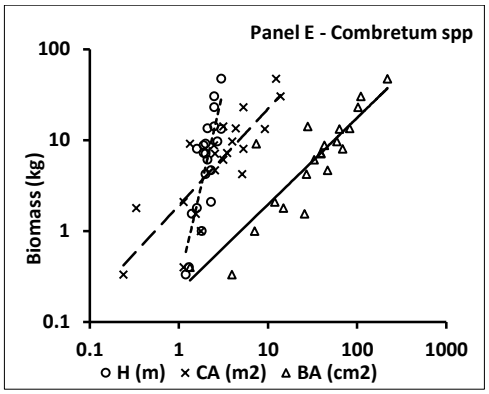
Panel E - Combretum spp
Biomass (kg)
100
10
1
0.1
0.1
1
10
100
1000
H (m)
CA (m2)
BA (cm2)

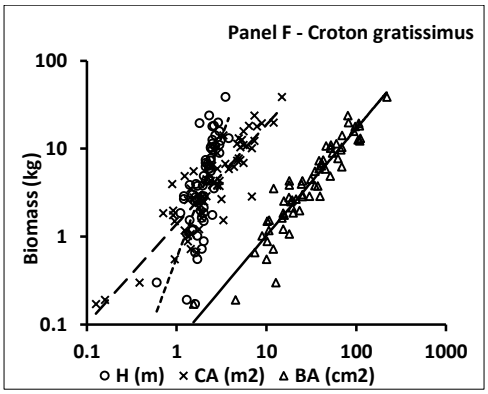
Panel F - Croton gratissimus
Biomass (kg)
100
10
1
0.1
0.1
1
10
100
1000
H (m)
CA (m2)
BA (cm2)

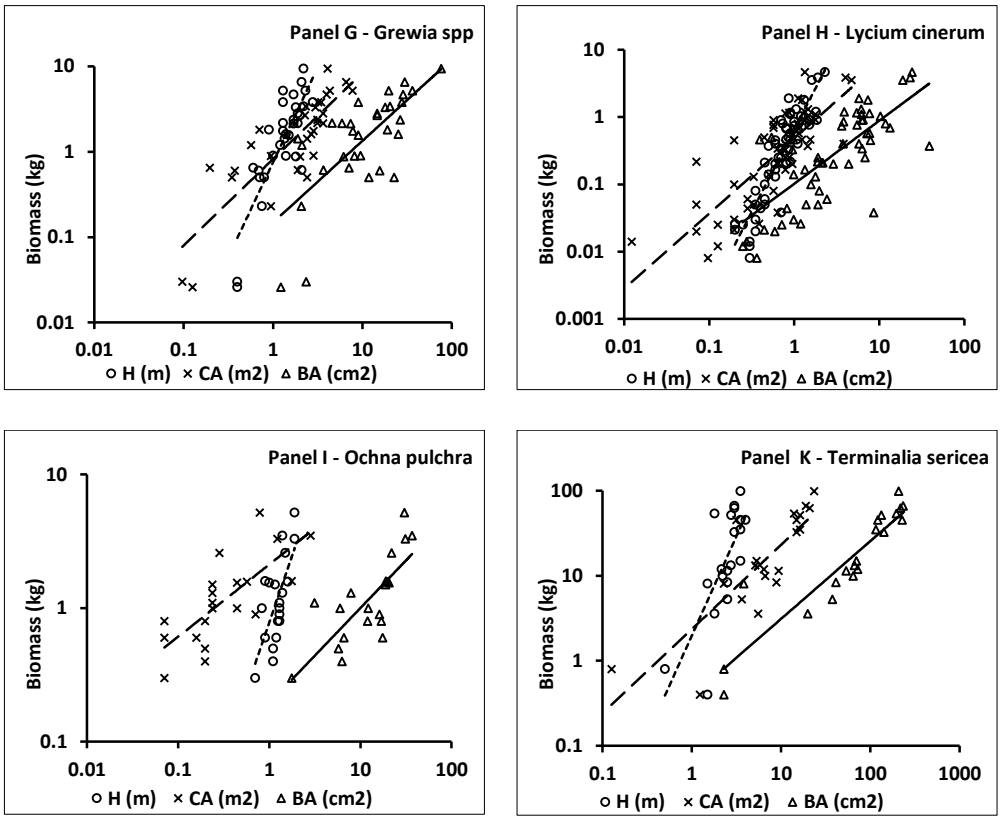

Figure 4: Species-specific regression (BA – solid line, CA – dashed line, H – dotted line)

Results from this analysis are presented in Figure 4 and the corresponding R^2 values are summarized in Table 3. These results present a mixed picture: while the regression using basal area provides best results for large woody species, the biomass of small shrubs such as *Lycium* and *Grewia spp* is better estimated using height or crown diameter. Crown area performs overall well as a predictor of plant biomass throughout the entire range of species. The best R^2 value of 0.97 was observed for *Burkea africana* while R^2 values for *Ochna pulchra* are the lowest among all species for all three structural parameters used. The RMSE (ln) values represent the same outcome and support the crown area to be a useful indicator. Overall best results have been achieved for *A. mellifera* with high R^2 values for all parameters (CA =0.90, H=0.76, CA=0.92).

3.3.4 All individuals of each morphological class

All species were grouped into five categories, representing different growth forms and patterns. The categories are based on wood density, leaf form and growth patterns. The category associated with each plant species is presented in Table 2. The allometric relations for these grouped species with similar morphological characteristics indicate that crown area is an overall good predictor of biomass, with R^2 values ranging from 0.9 for morphological group I to 0.62 for morphological group V. While in some cases other parameters might perform better than crown diameter, the R^2 values suggest that the differences are relatively small (less than 11 per cent) and that canopy area consistently performs well for all of these morphological groups. While for tall trees and shrubs basal area is a good predictor of plant biomass, it shows weak allometric relationships when applied to small, open and mainly multi stemmed vegetation represented in category 4 and 5 with R^2 values as low as 0.45 for category IV (Table 3, Figure 5).

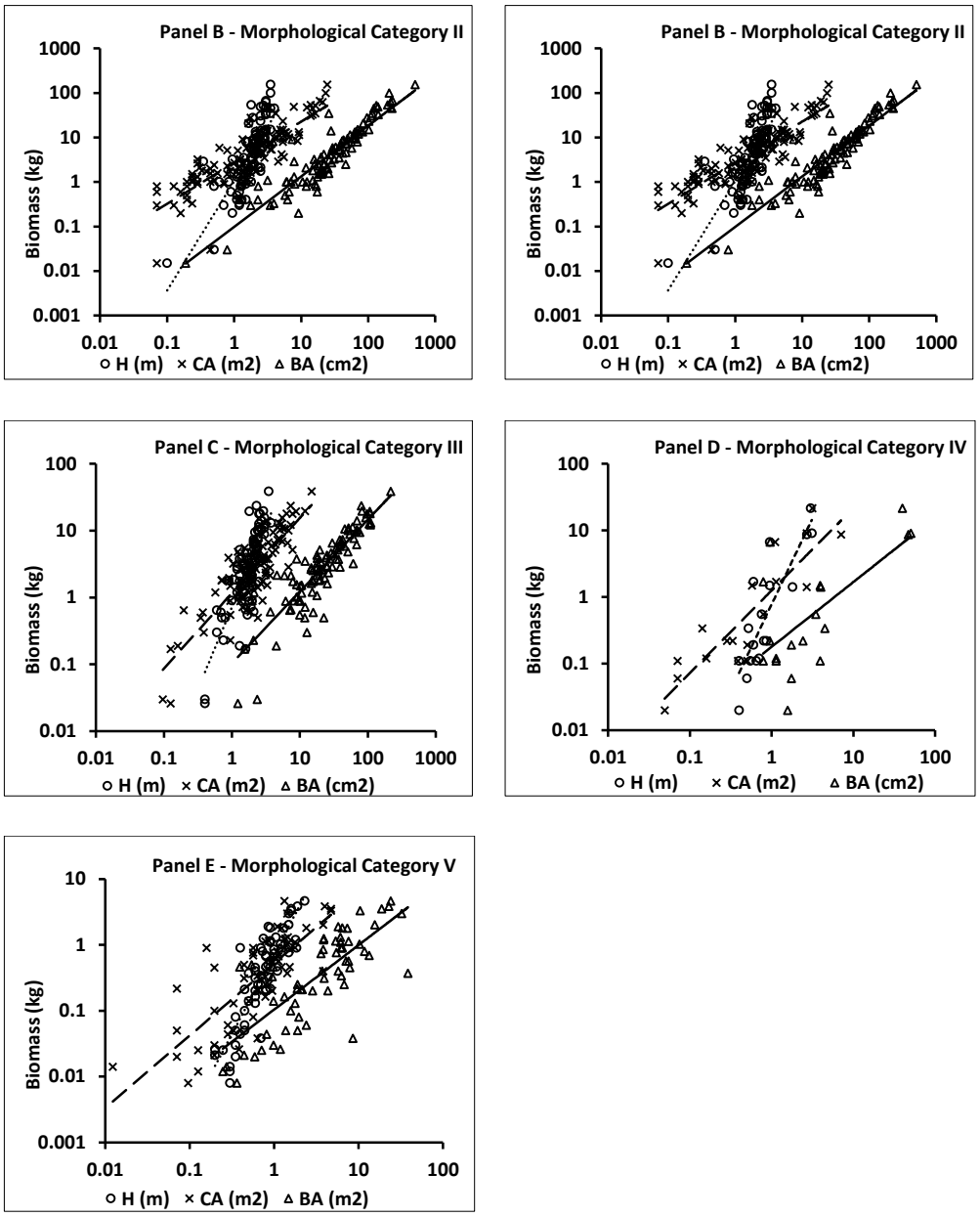

Figure 5: Categorized regression (BA – solid line, CA – dashed line, H – dotted line)

Table 3: Regression analysis results

Grouping	**# of samples (n)**	**Slope**	**R2**	**RMSE (ln)**
All individuals	**342**			
Basal Area (BA)		$0.1046 \times BA^{1.1400}$	0.82	0.87
Height (H)		$0.9399 \times H^{2.7454}$	0.73	1.05
Crown Area (CA)		$1.3175 \times CA^{1.2183}$	0.75	1.01
Site Shakawe	**55**			
Basal Area (BA)		$0.1000 \times BA^{1.1141}$	0.82	0.69
Height (H)		$0.7189 \times H^{3.4273}$	0.69	1.00
Crown Area (CA)		$2.7414 \times CA^{0.8678}$	0.72	0.87
Site Kuke	**125**			
Basal Area (BA)		$0.1179 \times BA^{1.0765}$	0.79	0.51
Height (H)		$0.6104 \times H^{3.2868}$	0.51	0.84
Crown Area (CA)		$1.5535 \times CA^{1.0782}$	0.67	0.64
Site Tshane	**122**			
Basal Area (BA)		$0.1046 \times BA^{1.1488}$	0.82	1.11
Height (H)		$0.9643 \times H^{2.8118}$	0.73	1.02
Crown Area (CA)		$1.3175 \times CA^{1.2299}$	0.75	1.12
Site Bokspits	**40**			
Basal Area (BA)		$0.2835 \times BA^{1.0559}$	0.82	0.83
Height (H)		$2.7809 \times H^{4.0156}$	0.75	0.99
Crown Area (CA)		$1.8323 \times CA^{1.2688}$	0.89	0.77
Acacias	**18**			
Basal Area (BA)		$0.1415 \times BA^{1.1801}$	0.81	1.00
Height (H)		$0.9321 \times H^{3.0604}$	0.80	1.18
Crown Area (CA)		$1.0251 \times CA^{1.5185}$	0.78	1.10
Acacia mellifera	**42**			
Basal Area (BA)		$0.2382 \times BA^{1.1040}$	0.90	0.55
Height (H)		$2.7115 \times H^{4.0373}$	0.76	1.05
Crown Area (CA)		$1.2369 \times CA^{1.4668}$	0.92	0.48
Boscia albitrunca	**16**			
Basal Area (BA)		$0.0931 \times BA^{1.2492}$	0.75	0.82
Height (H)		$2.5703 \times H^{2.8129}$	0.67	1.49
Crown Area (CA)		$3.3214 \times CA^{1.3621}$	0.86	1.08
Burkea africana	**17**			

Basal Area (BA)		$0.0574 \times BA^{1.2101}$	0.93	0.35
Height (H)		$0.5967 \times H^{3.6868}$	0.71	1.05
Crown Area (CA)		$2.6452 \times CA^{1.2218}$	0.97	1.04
Combretum spp	**21**			
Basal Area (BA)		$0.2182 \times BA^{0.9897}$	0.77	0.64
Height (H)		$0.2713 \times H^{14.2216}$	0.68	7.41
Crown Area (CA)		$1.9200 \times CA^{1.1421}$	0.68	0.74
Croton gratissimus	**65**			
Basal Area (BA)		$0.0625 \times BA^{1.2259}$	0.88	0.40
Height (H)		$0.5722 \times H^{3.6455}$	0.53	1.04
Crown Area (CA)		$1.3862 \times CA^{1.1490}$	0.77	0.55
Grewia spp	**32**			
Basal Area (BA)		$0.1486 \times BA^{1.0335}$	0.50	0.94
Height (H)		$0.7526 \times H^{2.6886}$	0.70	0.77
Crown Area (CA)		$0.8205 \times CA^{1.0487}$	0.71	0.71
Lycium cinerum	**56**			
Basal Area (BA)		$0.1019 \times BA^{0.9761}$	0.52	1.08
Height (H)		$0.6525 \times H^{2.6421}$	0.79	0.71
Crown Area (CA)		$0.4834 \times CA^{1.1581}$	0.63	0.95
Ochna pulchra	**20**			
Basal Area (BA)		$0.1939 \times BA^{0.7515}$	0.59	0.48
Height (H)		$0.7831 \times H^{3.7578}$	0.48	0.77
Crown Area (CA) Area		$2.1224 \times CA^{0.5601}$	0.55	0.48
Terminalia sericea	**20**			
Basal Area (BA)		$0.3790 \times BA^{0.9348}$	0.84	0.57
Height (H)		$1.9731 \times H^{4.4869}$	0.55	2.30
Crown Area (CA)		$2.3588 \times CA^{1.0577}$	0.69	0.81
Morphological Group 1				
Basal Area (BA)		$0.1672 \times BA^{1.1672}$	0.90	0.73
Height (H)		$2.0518 \times H^{3.5310}$	0.75	1.19
Crown Area (CA)		$1.1403 \times CA^{1.4806}$	0.90	0.72
Morphological Group 2				
Basal Area (BA)		$0.0978 \times BA^{1.1447}$	0.83	0.68
Height (H)		$1.0429 \times H^{2.6806}$	0.64	1.00
Crown Area (CA)		$2.7155 \times CA^{0.9304}$	0.72	0.86
Morphological Group 3				

Basal Area (BA)		$0.1034 \times BA^{1.0860}$	0.75	0.64
Height (H)		$0.7124 \times H^{2.6730}$	0.64	0.79
Crown Area (CA)		$1.1580 \times CA^{1.1415}$	0.73	0.68
Morphological Group 4				
Basal Area (BA)		$0.1780 \times BA^{1.1825}$	0.45	1.48
Height (H)		$0.7722 \times H^{3.8619}$	0.73	1.30
Crown Area (CA)		$1.2509 \times CA^{1.3333}$	0.78	0.93
Morphological Group 5				
Basal Area (BA)		$0.1042 \times BA^{1.0128}$	0.56	1.05
Height (H)		$0.7230 \times H^{2.6370}$	0.76	0.79
Crown Area (CA)		$0.5242 \times CA^{1.1328}$	0.62	0.97

3.4 Discussion

The regressions derived for all woody species across the entire transect indicate that height, basal diameter, or canopy size can all be used in allometric relationships to determine plant biomass. Basal area measurements are often considered the best indicators of woody biomass in allometric relations for shrubs (Brown 1976) and trees (Ter-Mikaelian and Korzukhin 1997). Basal area has also been found to perform better than height measurements in multiple stem growth forms in the Kalahari (Tietema 1993). Tietema (1993) found that several woody species in Botswana exhibit great similarity in allometric relations between above ground biomass and basal area, especially *Acacia* and *Combretum* spp. In addition to providing allometric relationships for each species, Tietema (1993) also developed a combined regression for important fuel wood species (e.g. *Acacia, Combretum, Terminalia spp*. and others) that dominate the upper canopy. Other species, such as *Grewia, Rhigozum,* and *Lyzium*, have not been considered in his

study, since these have very little to no relevance with regard to fuel wood. However, these species should be considered when determining the ecosystem's above ground biomass and carbon storage. In our study we have included multiple small shrub, low wood density species to see if findings presented by Tietema (1993) are still valid.

Our application of power-law regression analysis, combined for all species and sites, indicates that the relationship between biomass and basal area generally becomes weaker compared to Tietema (1993) when shrubs are included. This is represented as an R^2 drop of 13% when shrubs are included. Yet for the combined curve, basal area proves to be the better predictor of plant biomass than the other structural parameters. The lower performance of height and crown area might be the result of difficulties in measuring height or crown diameter (as the determining factor of CA) of shrubs accurately, while stem diameter is measurable with higher accuracy.

The regression analyses performed in this study indicate a slightly weaker relationship for all species and sizes combined, with an R^2 value of 0.81 for basal area. This decline in explained variance can be ascribed to the addition of smaller shrub species that generally perform worse than trees, as indicated by the per species analysis. However, the regression presented in Figure 2 is still acceptable to determine biomass using a regression based on basal area for all species and sizes.

Looking at site-specific differences, basal area performs better than height and canopy area at the two northernmost sites, Shakawe and Kuke. Best performance was reached

using height at Tshane and crown diameter at the Bokspits site. It should be noted, however, that the differences in R^2 values observed between basal area and crown diameter are minimal. The results also reflect the great variety in structural patterns generally observed in savanna areas (Caylor and Shugart 2006). A change in slope of all regressions is noticeable comparing the two northern to the two southern sites, indicating stronger increase in biomass accumulation with increasing plant size (expressed by either one of these three structural parameters) in the north. This difference might be attributed to differences in plant community composition.

The growth form of woody species in the Kalahari is variable, ranging from single stemmed trees to multi-stemmed large shrubs of the same species (e.g. *Terminalia sericea*), to dense canopy shrubs (e.g. *Combretum spp.*), dense bipinnate leaved (e.g. *Acacia leuderitzii*) to small shrubs with dense or open canopies seldom exceeding heights of 2 m (e.g. *Grewia spp. and Lycium spp.*). In order to determine aboveground biomass across the Kalahari ecosystem, these morphological characteristics should be taken into consideration. Our species analysis reveals that species exhibiting multi-stemmed and low (under 2m) growth forms (categories 4 and 5) show low R^2 values of 0.45 and 0.56 for relationships between basal area and biomass. Basal area is therefore not well predicted. As a result of the multi-stemmed characteristics of these species, basal area is obtained as the sum for all stems (often more than 50); thus, measurement inaccuracies are squared for each diameter while converting to basal area, and errors can be amplified when this is repeated for each stem and all basal areas. For smaller, multi-stemmed shrub species height and crown area are better indicators of plant biomass in allometric

relationships. Our study indicates that depending on the morphological characteristics of a species, the best parameter to determine biomass may vary between basal area, crown diameter and height (Table 3). The strongest relationships were observed using BA for category I, II, III, using CA for category IV and H for category V.

Allometric relations are commonly developed in ecology and forestry to provide an empirical framework for the quantification of biomass based on non-destructive measurements of suitable structural or morphological parameters. To simplify the use of these relations for the quantification of biomass, easily measurable parameters should be preferably selected. A number of species in the Kalahari occur in multi-stem shrub life-form. Therefore, the measurement of the basal area of each stem can be a challenging task, particularly in thorny species such as *A. mellifera*, which typically exhibits numerous and hard-to-reach stems. While basal area is the accepted standard independent variable for univariate regression-based allometric studies, the measurement of basal area and height in the field, especially in remote regions and across large areas remains a challenge with regard to logistics, manpower and costs. This limits their usefulness in the determination of woody biomass in the Kalahari.

This study shows that crown diameter is a good indicator that can be used to determine biomass. In fact the differences between biomass estimates based on crown diameter and basal area are minimal for large species that dominate the upper canopy levels, while canopy area performs better than basal area for small dense shrubs (category 4) and small brush-like species with open canopy and lower stem density. The view emerging from

this study is that crown diameter provides an acceptable alternative to basal area in plant allometric relationships for the woody species in these savannas particularly in the case of multi-stemmed individuals. Because ground measurements of basal area and height are impractical or impossible to perform for landscapes covered by multi-stem shrubs, canopy area should be considered as a reasonable and easy-to-measure alternative to basal areas that provides robust estimates of aboveground plant biomass. The crown diameter or crown area of savanna vegetation can be extracted across entire landscapes by leveraging high resolution optical remote sensing products. In particular space and airborne LIDAR systems seem to be promising for the determination of woody biomass.

Chapter 4

Evaluation of spectral unmixing techniques in a structurally complex savanna environment for retrieval of green vegetation, nonphotosynthetic vegetation, and soil fractional cover

Under review: Journal of Remote Sensing of the Environment, November 2013

Authors: Meyer, T., Okin, G.S.

4.1 Introduction

Spectral unmixing procedures such as spectral mixture analysis (SMA) and multiple endmember spectral mixture analysis (MESMA) are techniques applied to multispectral remote sensing or imaging spectroscopy data. These techniques are based on the assumption that the apparent surface reflectance can be modeled as a combination of the spectra of separable ground components, and that the coefficients of that mixture are equal to the actual fractional cover of those components on the ground. Spectral unmixing is widely used to determine the fractional cover of green vegetation (GV), non-photosynthetic vegetation (NPV), soil and/or snow. Various studies of these techniques indicated varying performances for different fractions and landscapes (Ballantine et al. 2005; Eckmann et al. 2008; Guerschman et al. 2009; Okin et al. 2013; Shreve et al. 2009). While separating NPV and soil in all environments remains difficult due to their spectral similarity, this problem is likely to be exacerbated in structurally complex landscapes where multiple scattering and mutual shadowing complicate the signal and where spatial heterogeneity makes it difficult to connect remote measurements with validation sites on the ground. The ground-truthing aspect of any unmixing study of GV, NPV, and soil is also complicated by the necessity in the field of classifying vegetation as either GV or NPV when in truth tissue can appear as a mixture of both.

In this study we test the performance of SMA and MESMA in the heterogeneous, semi-arid environment of the Kalahari at the MODIS scale (500 m). Two methods for the collection of ground fractions were used: a traditional line-intercept transect (LIT) and a new spectral line point intercept transect method (SLPT).

The ability to determine fractional cover of GV, NPV and soil in savanna environments using coarse resolution satellite imagery could provide valuable information regarding general conditions of an ecosystem threatened by desertification and bush encroachment, information on fuel load, carbon storage, climate modeling, wildlife potential, and livestock stocking capacities. Over large areas, e.g. on regional and national scales, the determination of these factors remains a challenge for land use managers due to the associated spatial extent. Previous studies conducted in the area, and others tried to determine vegetative cover using Normalized Difference Vegetation Index (NDVI) and other vegetation indices (Grist et al. 1997; Palmer and van Rooyen 1998; Ringrose et al. 2003; Scanlon et al. 2007). These indices are known to underperform in areas with vegetative cover less than 30 percent (Huete et al. 2002; Qi et al. 1994) and only provide information on one ground cover component, GV. Study and management of dryland ecosystems using remote sensing requires knowledge of surface dynamics that go beyond just the green fraction (e.g. Okin, 2010). At present spectral unmixing is the most promising approach for determination of these other ground cover components, and yet, to be useful, these methods need to be tested in heterogeneous dryland environments.

4.2 Methods

4.2.1 Field Sites

The Botswana part of the Kalahari Transect stretches 950 km from Shakawe in the northwest to Bokspits in the far south western corner of the country (Figure 1). The transect follows a rainfall gradient, where precipitation ranges from 550 mm in the North

in Shakawe to <250 mm in the south (Hijmans et al. 2005). The rainfall pattern of the area is characterized by a distinct rain season starting in October and ending in March the following year.

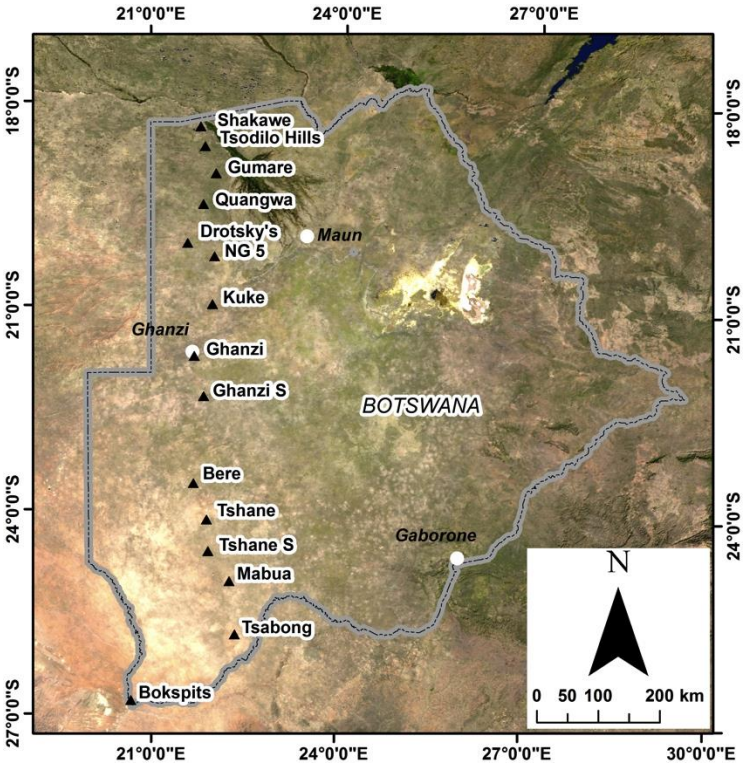

Figure 1: Research Site Locations (source (DSM 2003; ESRI 2000); map by author)

However, rainfall events across the entire area and increasingly towards the southern end are characterized by sporadic, locally restricted convective thunderstorms events. On a large scale, the soils of the Kalahari are mainly of aeolian origin (Thomas 1991). However, local differences can be observed in the form of active (Site 15), inactive (Site 1,2,3,4,5,7) or over washed (site 7) dune fields, riverbeds, or surfacing bedrock formations (site 8). Vegetation across the area can be best described as Kalahari thornveld (Thomas 1991) with increasing canopy density and height from south to north

(Caylor et al. 2003; Sankaran et al. 2005). On a local scale vegetative composition varies with regard to species composition and structure.

Fifteen, roughly evenly spaced sites were chosen along the 950-km of the transect. At each site, three 500-meter transects were laid out using measuring tapes. Each site was visited once in the wet season and once in the dry season. Table 1 indicates the center point at each site and the dates when the site was visited. A random number generator was used to establish the direction of the first transect and each of the following transects were rotated clockwise at a spacing of 120°. The transect starts were located 20 m from the center point. During the second visit, transects were offset from those on the first visit by 60°.

Table 1: Research Sites, names, dates and coordinates

Site #	Name	Date I	Date II	Lat	Long
1	Shakawe	5/22/10	8/5/09	-18.3886	21.7716
2	Tsodilo	5/21/10	5/4/11	-18.6798	21.8418
3	Gumare	8/22/09	5/13/11	-19.0776	22.0099
4	Quangwa	8/19/09	5/7/11	-19.5293	21.8174
5	Drotsky's	8/15/09	5/15/11	-20.1019	21.5742
6	NG 5	12/12/09	5/2/11	-20.2981	21.9933
7	Kuke	12/14/09	10/2/10	-21.0012	21.9648
8	Ghanzi	2/8/10	12/17/09	-21.7621	21.6833
9	Ghanzi S	2/11/10	9/21/10	-22.3542	21.8327
10	Bere	9/30/10	2/19/10	-23.6335	21.6773
11	Tshane	9/23/10	2/19/10	-24.1679	21.8899
12	Tshane S	9/24/10	2/17/10	-24.6304	21.9163
13	Mabua	8/5/10	2/16/10	-25.0681	22.2607
14	Tsabong	9/26/10	2/15/10	-25.8497	22.3547
15	Bokspits	9/27/10	2/13/10	-26.8199	20.6729

4.2.2 MODIS Imagery and Analysis

The availability of the nadir, bidirectional reflectance function adjusted reflectance (NBAR) product (MCD43) derived from MODIS provides a valuable product to observe changes in the environment at moderate spatial resolution and temporal compositing of 16 days (Schaaf et al. 2002). The product is corrected for the effects of atmospheric disturbances and bidirectional reflectance distribution function (BDRF). Here, we used the 500-m product (MCD43A4). 3x3 pixel areas were clipped from the MCD43A4 images, centered on the pixel that contains the latitude and longitude of the center point of the field sites. The 16-day composite of which the middle date falls closest to the date of field data collection was used in all instances (Table 1 & 2).

In SMA, the apparent surface reflectance is assumed to be a linear combination of the reflectance of the spectra of the ground components "endmember", weighted by their fractional cover in each pixel.

The SMA equation for *n* endmembers at time t_i is:

$$\rho_{pixel}^{t_i} = \sum_{k=1}^{n} f_k^{t_i} \rho_k + \varepsilon, \qquad (1)$$

where $\rho_{pixel}^{t_i}$ is the reflectance of the pixel at time t_i, ρ_k is the reflectance of the *k-th* endmember, and $f_k^{t_i}$ is the fractional area covered by the *k*-th endmember at time t_i (Shimabukuro and Smith 1991).

When derived from laboratory or field spectra, ρ_k are sometimes called "reference endmembers" (Roberts et al. 1998b). The final term, ε, is the residual spectrum remaining after best-fit coefficients, $f_k^{t_i}$, have been determined.

Equation (1) is sometimes subject to the constraints that f_k must belong to the interval [0,1] and

$$\sum_{k=1}^{n} f_k^{t_i} = 1. \tag{2}$$

SMA assumes that the reference endmembers are spatially invariant. Use of SMA in the context here, where the same endmembers are used to unmix images from different times, further requires the assumption that the endmembers are temporally invariant.

Two sets of endmembers were used for SMA. $SMA_{standard}$ used the same set of endmembers ("standard endmembers") for all sites. $SMA_{specific}$ used endmembers collected at a specific site and season ("site-specific endmembers") to unmix data from that site and season. Multiple site and season specific endmembers were used for MESMA. MESMA is a version of SMA in which the best-fit coefficients of many different SMA models (a model is a unique combination of endmember spectra) are calculated and the best model is picked among these (Roberts et al. 1998a). One criterion often used in MESMA to pick the best model is *RMSE*:

$$RMSE = \left(\frac{1}{m} \sum_{b=1}^{m} (\varepsilon_b)^2 \right)^{1/2}, \tag{3}$$

where *m* is the number of bands in the remote sensing imagery (MCD43A4 has seven bands); the model with the lowest RMSE is chosen (Roberts et al. 1998b).

For applications with a large number of bands, such as those using imaging spectroscopy data, other criteria can be used (e.g., Dennison et al. 2004; Roberts et al. 1997). The number of endmembers used for each site for MESMA is shown in Table 2.

Table 2: number of MESMA endmembers per season (dry/wet) and ground component (GV, NPV, soil)

Site	# of endmembers	Site	# of endmembers	Site	# of endmembers
01	dry: 23,13,7 wet: 19,14, 5	06	Dry: 20,7,12 Wet: 20,12,15	11	Dry: 10,14,19 Wet: 49,10,32
02	Dry: 9,7,8 Wet: 16,1,7	07	Dry: 13,13,19 Wet: 20,10,9	12	Dry: 10,15,18 Wet: 30,3,16
03	Dry: 3,13,7 Wet: 10,6,7	08	Dry: 15,11,22 Wet: 17,10,9	13	Dry: 8,15,11 Wet: 23,2,14
04	Dry: 4,11,15 Wet: 8,3,4	09	Dry:11,10,5 Wet: 21,5,6	14	Dry: 17,15,5 Wet: 17,2,8
05	Dry: 17,6,14 Wet: 17,4,10	10	Dry: 4,5,22 Wet: 23,10,24	15	Dry: 3,4,10 Wet: 20,2,9

Collection of field spectra used as endmembers for MESMA is discussed below. Models were constructed by using all possible combinations among applicable GV, NPV, and soil spectra.

For both SMA and MESMA, unmixing was conducted using the "constrained_min" routine in IDL (Excelis Visual Information Solutions, inc., Boulder, Colorado; Lasdon and Waren 1986) to minimize RMSE while forcing coefficients to exist in the interval [0,1]. The advantage to this approach compared to another linear unmixing method using

linear algebraic least-squares analysis (including a QR decomposition using the Gram-Schmidt process or the use of singular value decomposition (SVD)) is that constraints can be strictly enforced; values outside [0,1] can be avoided if desired. Roberts et al. (1998a) using a least-squares mixing approach based on a QR decomposition using Gram-Schmidt orthogonalization, for instance, allowed endmembers to be slightly outside the [0,1] constraints. In cases where there exists a solution for the endmembers that falls within the constraints, both the method used here and linear algebraic least-squares will provide the same solution.

No constraint on the sum of non-shade endmembers was imposed for the unmixing and shade was set to one minus the sum of the non-shade endmembers. This method is equivalent to that used in Roberts et al. (1998a) where the constraint that all endmembers sum to one is imposed by inferring an additional photometric shade endmember (zero reflectance in all bands) that is not used in the actual unmixing. This approach is required because photometric shade cannot be used directly as an endmember in a spectral mixture model (see Okin et al. 2013 for more discussion). After calculation of endmembers, normalization of the non-shade endmembers was done by dividing each non-shade endmember fraction by the sum of non-shade fractions to force the non-shade endmember to sum to one. Okin et al. (2013) showed that this normalization improved GV and NPV endmember fractional cover retrieval while eliminating the bias in the GV cover estimate. Although it also led to an increase in soil fractional cover error estimates, the total error was nonetheless lower for the normalized fractions.

For comparison with GV fractional cover, MODIS Enhanced Vegetation Index data from the 16-day, 500-m MOD13A1 product were extracted from the same tiles and dates as the MCD43A4 data (Table 3).

Table 3: MODIS image parameters

Site	Wet Image	Dry Image
01	MCD43A4.A2010145.h20v10	MCD43A4.A2009217.h20v10
02	MCD43A4.A2011145.h20v11	MCD43A4.A2009225.h20v11
03	MCD43A4.A2011129.h20v10	MCD43A4.A2009233.h20v10
04	MCD43A4.A2011129.h20v10	MCD43A4.A2009233.h20v10
05	MCD43A4.A2010145.h20v10	MCD43A4.A2009289.h20v10
06	MCD43A4.A2010121.h20v11	MCD43A4.A2010345.h20v11
07	MCD43A4.A2010353.h20v11	MCD43A4.A2010273.h20v11
08	MCD43A4.A2010041.h20v11	MCD43A4.A2010353.h20v11
09	MCD43A4.A2010041.h20v11	MCD43A4.A2010265.h20v11
10	MCD43A4.A2010041.h19v11	MCD43A4.A2010273.h19v11
11	MCD43A4.A2010049.h20v11	MCD43A4.A2010273.h20v11
12	MCD43A4.A2010049.h20v11	MCD43A4.A2010217.h20v11
13	MCD43A4.A2010049.h19v11	MCD43A4.A2010265.h19v11
14	MCD43A4.A2010049.h19v11	MCD43A4.A2010265.h19v11
15	MCD43A4.A2010049.h19v11	MCD43A4.A2010273.h19v11

4.2.3 Endmember collection, processing, and selection

Spectral endmembers for GV, NPV and soil were collected in close proximity or directly on the vegetation transects utilizing an ASD Fieldspec Pro with leaf-clip attachment (Panalytical, Inc., Boulder, CO). In addition, spectra taken with the bare fiber and solar illumination above the canopy ("canopy scale" spectra) were taken for a variety of species, using a ladder when necessary. Reflectance spectra were obtained by division of endmembers' radiance spectra by the measured radiance of a Spectralon™ panel. Each endmember was visually inspected before its integration into a mixture model. All

resulting reflectance spectra were convolved to MODIS wavebands (see example in Figure 2).

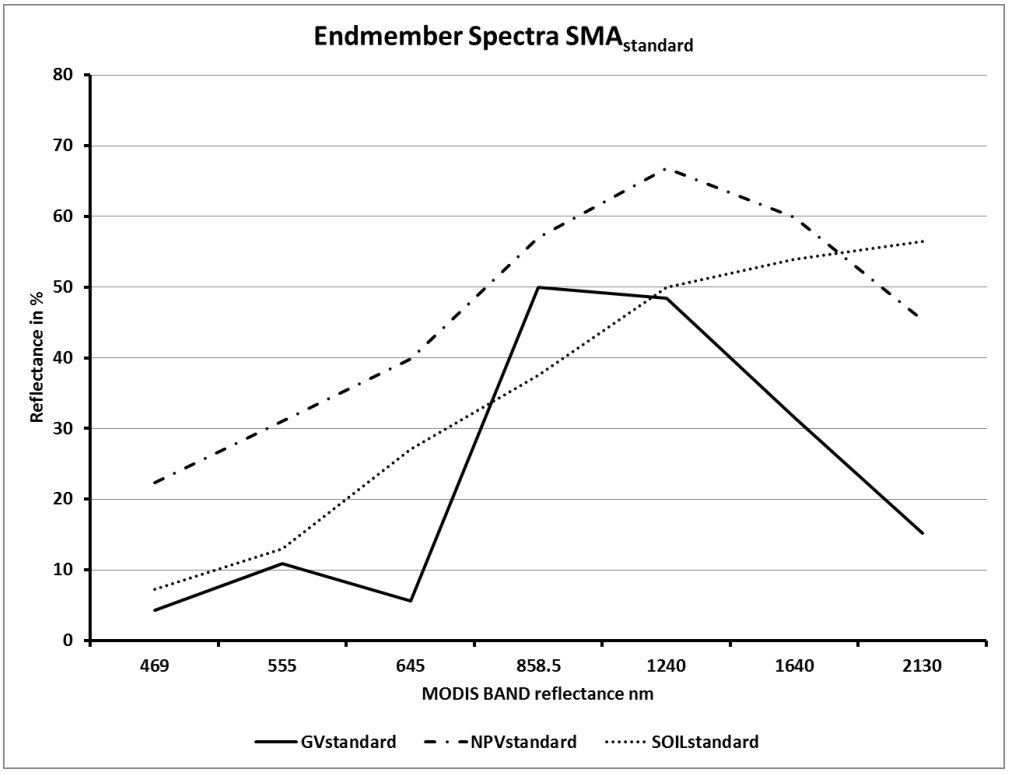

Figure 2: $SMA_{standard}$ endmembers convolved to MODIS wavebands

4.2.4 Collection of in situ cover data

Line intercept transect (LIT)

Measurement of *in situ* fractional cover was conducted at the center of each SLPT transect, ranging from the 200 to the 300 meters mark. Data capture and interpretation follows the procedures and methods described for line intercept transect (LIT) by Krebs (1999). For each line, all woody vegetation taller than 25 cm was identified following the nomenclature provided by Palgrave (1977). Average height, distance covered over the line, and distance and direction of the stem(s) were recorded to calculate total transect

woody canopy cover exceeding 25 cm in height. In order to calculate the total vegetative cover, herbaceous and litter layers were also recorded along the same line. Cover for each clump was categorized by visual inspection based on the 'greenness', with each clump classified as either GV or NPV based on the preponderance of green or nonphotosynthetic tissue. Trees (woody vegetation > 2 m) were classed as GV in the wet season (due to a preponderance of green tissue) or NPV during the dry season (due to the lack of green leaves during this time). Total lengths of GV, NPV, and soil readings along the transects were divided by 100 m to yield fractional cover estimates.

Spectral line point intercept transect (SLPT)

The LIT method uses a binary GV/NPV categorization to produce endmember fractions. The SLPT method is designed to produce spectral data that can be unmixed to give estimates of endmember fractions without resorting to binary categorizations in the field. This binary characterization is a source of error and user bias in any method that requires visual separation of green and nonphotosynthetic tissue. At the clump scale, GV and NPV can be intermingled and much tissue also appears somewhere between the GV and NPV endmembers to the human eye.

The SLPTs span the total length of 500 meters of the vegetation transects. Reflectance spectra (using the ASD field spectrometer) were acquired every 5 meters from 1 m height above the canopy with the bare fiber (~20° field of view). Re-optimizing and re-collection of Spectralon™ spectra were done whenever spectra showed evidence of

saturation or contamination in water vapor bands due to changing atmospheric conditions.

SLPT spectra were unmixed using MESMA endmembers for each site and fractions were averaged for each transect to yield transect-wide estimates of fractional cover. This unmixing was done at full ASD spectral resolution, with water vapor bands and wavelengths > 2350 nm omitted due to the dominance of noise in these bands.

4.2.5 Statistical Analysis

Three metrics of comparison were used in this study: the coefficient of determination (R^2), root-mean squared difference (RMSD), and mean difference (MD). RMSD was calculated as:

$$RMSD = \left(\frac{1}{n} \sum_{i=1}^{n} \left(f_{j,1} - f_{j,2} \right)^2 \right)^{1/2}, \quad (4)$$

where *n* is the number of measurements/estimates of fractional cover and '1' and '2' represent two different methods of estimation. MD was calculated as:

$$MD = \frac{1}{n} \sum_{i=1}^{n} \left(f_{j,1} - f_{j,2} \right). \quad (5)$$

4.3 Results

In general, remotely derived estimates of GV cover (including EVI) show better correlation amongst themselves than they do with ground-based measurements and also better correlation than between the two different ground-based methods (Table 4).

Table 4. R^2 (above the diagonal) and RMSD, MD (below the diagonal) for GV, all 15 sites and 2 seasons

	LIT	SLPT	EVI	$SMA_{standard}$	$SMA_{specific}$	MESMA
LIT		0.51	0.50	0.43	0.45	0.61
SLPT	0.17,0.13		0.40	0.64	0.60	0.62
EVI	n/a	n/a		0.71	0.60	0.62
$SMA_{standard}$	0.18,0.13	0.10,0.00	n/a		0.75	0.70
$SMA_{specific}$	0.17,0.13	0.10,0.00	n/a	0.08,0.00		0.71
MESMA	0.16,0.13	0.09,0.00	n/a	0.09,0.00	0.08,0.00	

Remotely sensed estimates of GV cover show better correlation (and lower RMSD and MD) with SLPT relative to LIT. Comparisons of GV cover between remotely derived estimates and LIT show positive biases (LIT f_{GV} > SMA/MESMA f_{GV}), whereas SLPT does not show any bias. The use of standard or site-specific endmembers in SMA had little effect on how SMA fractional cover compared to field-based measurements (same RMSD and MD, comparable R^2). MESMA showed similar correlation but slightly lower RMSD with field-based estimates than the SMA methods (RMSD=0.09 vs. RMSD=0.10). When compared to SLPT, EVI showed the weakest correlation among the remotely derived methods (RMSD and MD cannot be calculated for EVI so no comparison here is possible). In general, remote vs. *in situ* comparisons indicate that GV cover is retrieved more accurately than cover of NPV or soil.

For NPV, there is no correlation between SLPT and LIT fractional cover estimates (R^2 = 0) and LIT shows essentially no correlation with the remotely derived estimates of NPV cover ($R^2 < 0.04$; Table 5). When compared with SLPT-derived estimates of NPV cover, MESMA showed the highest correlation, followed by $SMA_{standard}$ and then by $SMA_{specific}$, though the ordering for RMSD and MD was MESMA< $SMA_{specific}$ < $SMA_{standard}$. The values of MD indicate that MESMA tends to estimate higher NPV cover (MD < 0 in Table 5) than the two SMA approaches, but that all three remotely derived estimates underestimate NPV cover relative to SLPT (MD > 0 in Table 5).

Table 5: R^2 (above the diagonal) and below the diagonal RMSD, MD (below the diagonal) for NPV, all 15 sites and 2 seasons

	LIT	SLPT	$SMA_{standard}$	$SMA_{specific}$	MESMA
LIT		0.00	0.01	0.03	0.04
SLPT	0.28,-0.08		0.47	0.36	0.55
$SMA_{standard}$	0.32,0.17	0.29,0.25		0.16	0.25
$SMA_{specific}$	0.28,0.04	0.22,0.12	0.27,-0.13		0.70
MESMA	0.25,0.00	0.16,0.08	0.27,-0.24	0.13,-0.04	

For soil, there was again no correlation between SLPT and LIT fractional cover estimates (R^2 = 0) and LIT shows essentially no correlation with the remotely derived estimates of soil cover ($R^2 < 0.10$; Table 6). When compared with SLPT-derived estimates of soil cover, MESMA showed the highest correlation, followed by $SMA_{standard}$ and then by

$SMA_{specific}$, though ordering for RMSD and MD was MESMA< $SMA_{specific}$ < $SMA_{standard}$. The values of MD indicate that MESMA tends to estimate lower soil cover (MD > 0 in Table 6) than the two SMA approaches, but that all three remotely derived estimates overestimate soil cover relative to SLPT (MD < 0 in Table 6).

Table 6: R^2 (above the diagonal) and below the diagonal RMSD, MD (below the diagonal) for soil, all 15 sites and 2 seasons

	LIT	SLPT	$SMA_{standard}$	$SMA_{specific}$	MESMA
LIT		0.00	0.01	0.04	0.10
SLPT	0.29,-0.05		0.48	0.45	0.57
$SMA_{standard}$	0.39,-0.30	0.29,-0.25		0.42	0.38
$SMA_{specific}$	0.34,-0.17	0.23,-0.12	0.24,0.13		0.64
MESMA	0.28,-0.13	0.17,-0.08	0.25,0.17	0.17,0.04	

4.4 Discussion

An important component of any comparison between *in situ* and remotely derived estimates of surface characteristics is the decision of how to represent the "truth" portion of ground truthing. Issues of scale of field measurement vs. spatial resolution of remote sensing and difficulty in co-locating field measurements with remote sensing pixels (due to field locational error, errors in coregistration, or signal integration in moving remote sensing platforms) plague all efforts at ground truthing. For studies of fractional cover of GV, NPV, and soil, other issues also arise. There is as of yet no standard method for estimation of GV, NPV, and soil cover (but see Muir 2011).

The problem is complex. With the human eye vegetation cover (GV + NPV) can be distinguished from soil easily enough, but determining categorically whether a leaf, plant, or clump should be classed as GV or NPV can be difficult in the intermediate where the vegetative material appears as a mix of the two. In situations where more than one person is doing the classification (not here), the problem is amplified as different people may place the visual boundary between GV and NPV in different places. Spectrally, on the other hand, GV is easily distinguished from NPV and soil. NPV and soil, however, are difficult to distinguish from one another spectrally; both have similar spectral shapes, particularly in data that do not have separate bands in the SWIR beyond 2000 nm (as with MODIS, Okin 2007).

Thus, in any comparison of fractional cover estimates of GV, NPV, and soil collected in the field by visual inspection with estimates produced by analysis of multispectral data, there are two potential sources of discrepancy. The retrieval of NPV cover is afflicted by both; NPV can be confused with GV in the field and it can be confused with soil in multispectral imagery. To investigate one of these (the GV-NPV classification problem), we used both the LIT- and SLPT-based methods for determination of *in situ* fractional cover. SLPT does not require any assumption in the field that measured vegetation belong to either GV or NPV classes, thus sidestepping the binary classification problem. Furthermore, by using the full-reflected solar spectrum at high spectral resolution, the ability to distinguish NPV from soil is improved (Asner and Heidebrecht 2002). Our results confirm the intuition that the two methods can produce radically different

estimates of fractional cover. Indeed, the results also indicate the direction of bias in this case: LIT-derived estimates of GV (NPV) are greater (less) than SLPT-derived estimates. Here, the crew in the field (T. Meyer) tended to classify clumps as green at a rate higher than would be predicted by the SLPT method, resulting in an overestimation of GV cover and an underestimation (relative to SLPT) of NPV cover.

It is impossible to know whether the LIT- or SLPT-based estimates best represent the "truth" in the field, but the fact that, for all cover types, the SLPT-estimated fractions correlate much better with the remotely-derived estimates indicates, at least, that the spectral transect approach better corresponds to what the satellite instrument "sees" than a categorical approach based on traditional line point intercept transect approach. We thus consider comparisons of remotely derived fractional cover estimates with SLPT-derived estimates the better indication of remote sensing error than comparisons with LIT-derived estimates.

The results for this structurally complex landscape are consistent with results from a similar study of a homogenous landscape of a flat agricultural field (Okin et al. 2013). Both studies show that GV cover can be retrieved much more accurately than NPV or soil cover. MESMA also produced estimates of fractional cover with less error than simple SMA in both studies, though the error in the heterogeneous environment studied here is greater than that studied by Okin et al. (2013). In both studies, spectral unmixing underestimates NPV and overestimates soil cover relative to *in situ* estimates. This is consistent with some NPV being interpreted spectrally as soil in the unmixing process.

The much higher absolute values of the MDs in this study compared to Okin et al. (2013) suggest further that this unmixing confusion might be more common in heterogeneous environments, which would be consistent with a greater influence of multiple scattering as soil spectra are "contaminated" by previous scattering by nonphotosynthetic material. There are few other papers aimed at evaluation of GV, NPV, and soil fractional cover estimates. Guerschmann et al. (2009) do not provide a detailed error analysis that can be compared. And, the data of Asner and Heidebrecht (2002) are not suited for error analysis of the type done here, so no direct comparison is possible. However, the significant correlations between SLPT-derived and unmixing-derived endmember fractions argue that results from these approaches can be better than suggested by these authors' work.

The use of site- and season-specific endmembers reduced both error and (absolute) bias in retrieval of NPV and soil using simple SMA. However, the benefit of this approach is not entirely clear – $SMA_{standard}$ results actually showed better correlation with SLPT estimates than $SMA_{specific}$ results. Thus the use of site-specific endmembers brought estimates closer to the 1:1 line, but increased the scatter in the estimates. We can conclude that the use of site-specific endmembers increases the accuracy of the estimates, but reduces their precision. The loss of precision, particularly for NPV, is a natural consequence of the use of different NPV endmembers for different sites. Soil and NPV spectra can "couple" (Okin et al. 2001), such that one combination of a soil and NPV can appear spectrally indistinguishable from a combination of different soils and NPV occurring in different fractions. Thus, it is not surprising that spectral confusion between

the two can lead to unstable retrievals of fractional abundances, and thus lower precision, when different endmembers are used.

4.5 Conclusions

A new method for the *in situ* estimation of GV, NPV, and soil fractional cover is described in this report (SLPT). Other methods are modifications on more traditional line-point intercept and line-intercept methods (used here). SLPT is potentially superior to these methods in that no classification system is required in the field where human error and bias can impact results. Although there is no consensus method for estimation of fractional cover of these ground components, in Australia, a line-point intercept system has been developed but still requires user interpretation of GV-ness or NPV-ness of vegetation.

The SLPT method, instead, uses spectral data, unmixed at high spectral resolution across the entire reflected solar spectrum, to derive estimates of GV, NPV, and soil spectra. Because it uses a similar logic to the unmixing conducted of remote sensing products, and therefore cannot be said to be independent of it, our results show that the SLPT method does correlate better with what is "seen" by the remote sensing instrument, regardless of specific unmixing approach or ground component. We would argue, therefore, that additional research needs to be carried out on the correspondence of the SLPT method with other methods, but it does appear to be a potentially useful method to collect *in situ* cover data. The benefits are not only scientific, however; SLPT data can be

collected much faster – and therefore over larger areas – than traditional transect-based methods.

It is not surprising that error rates for all ground cover components are considerably higher in the heterogeneous savanna environment, where this research was conducted, compared to the flat, homogenous agricultural fields of Australia investigated by Okin et al. (2013). Both studies confirm that the choice of situation-specific endmember sets or the use of multiple endmembers can improve the retrieval accuracy. However, the possibility of spectral coupling continues to be a source of error – here reducing the precision of the site-specific SMA unmixing approach.

Remote sensing of GV, NPV, and soil fractional cover in heterogeneous landscapes at the MODIS scale remains a difficult enterprise. In this study the retrieval of GV is about twice as accurate (has about half the error) than retrieval of NPV and soil fraction. Nonetheless, the data do show that at a coarse scale – and without overinterpreting results – retrieval of the fractions of these ground components nonetheless has the potential to inform our understanding of the ecosystem dynamics in structurally complex environments.

Chapter 5

Title: Leveraging allometric relationships and spectral unmixing: A MESMA approach to estimate biomass across the Kalahari.

Unpublished

Authors: Meyer, T., Okin, G.S., D'Odorico, P.

5.1 Introduction

The vegetation of savanna ecosystems, such as the Kalahari, plays an important role in the global carbon cycle (Grace et al. 2006; Scurlock and Hall 1998). In order to assess ecological functioning and carbon storage potential, numerous studies have been conducted in the area. Most of these have focused on vegetation and its response to changes in abiotic conditions, such as rainfall as well as nutrient and water availability (O'Halloran et al. 2010; Wang et al. 2009; Wang et al. 2010). Research has reported that woody vegetation cover and height generally increase towards the northern end of the transect (Caylor et al. 2003; Scanlon et al. 2002; Scanlon et al. 2007). The general increase in woody vegetation abundance and density towards the northern end of the Kalahari Transect (KT) has generally been attributed to higher mean annual precipitation (MAP), but other research points out localized differences depending on the presence or absence of disturbance regimes (Meyer et al. 2013; Moleele et al. 2002; Perkins and Thomas 1993). Overgrazing has been identified as a major driver of bush encroachment, resulting in an increase in woody cover and biomass on a more regional scale (Skarpe 1990; Walter 1954). The effect of fire, as one of the main drivers in savannas ecosystems, depends on fire frequency and intensity and vegetative responses differ by species and morphological traits (Sankaran et al. 2008; Trollope 1980). In Botswana, the country that contains the majority of the Kalahari, all these factors depend on land use as well. The main land uses found across the western portion of Botswana are community grazing areas, commercial farms, wildlife management areas and National Parks and Reserves.

With the increasing acceptance of climate change, as well as the introduction of carbon offset programs, land use patterns in these remote areas have moved into the focus of local governments as well as conservation-oriented groups. Determining biomass and therefore carbon content across an entire landscape is costly; attempts have been made to upscale locally observed vegetation patterns to the landscape/ecosystem level of the Kalahari (Ringrose et al. 2003; Ringrose et al. 1996; Scanlon et al. 2002) but have not yet successfully done so with biomass.

Remote sensing provides several potential opportunities for the estimation of woody biomass in savannas in a spatially extensive manner, and indeed, for the past decade, several studies have used both active and passive remote sensing to estimate biomass. Active remote sensing allows direct interrogation of the earth's surface in ways that elucidate the three-dimensional structure of the surface, and light detection and radar (LIDAR) and radio detection and ranging (RADAR) have proven especially useful for this purpose. For instance, Koch (2010) assessed the performance of multiple active remote sensing systems as well as hyperspectral systems (passive) in light of current platform developments. Colgan et al. (2012) and (2009) assessed the performance of LIDAR- and RADAR- based systems in various savanna environments and proved their effectiveness in these ecosystems. However, the deployment of these systems (especially LIDAR) across large areas remains expensive, both financially (in terms of airborne systems) and from a data processing perspective (extremely large amounts of data). Passive remote sensing, on the other hand, has been less used, partially due to the difficulty of interrogating the three-dimensional structure of the surface from

fundamentally two-dimensional information (Mutanga and Rugege 2006). The spectral similarity between woody species and herbaceous species further complicates matters. For instance, the Moderate Imaging Spectroradiometer (MODIS) Vegetation Continuous Fields tree-cover product (VCF) uses MODIS to determine tree cover, but shows limitations in savannas with low woody cover in part due to this mixture (Gessner et al. 2008; Hill et al. 2011). While current and future active remote sensing systems might estimate biomass with higher accuracies, passive remote sensing systems, such as MODIS and Landsat, provide better temporal depth due to their availability for decades (Koch 2010) and in most cases are a cheaper alternative to active approaches.

This study proposes a method to use MODIS data combined with field data and allometric relationships to determine aboveground woody biomass in the Kalahari. The developed model is validated using extensive structure measurements from the area and we further upscale our findings across the region.

5.2 Methods

5.2.1 Field site description and general site layout

We chose 13 sites distributed roughly evenly between the most southern site in Bokspits and the most northern site near Shakawe (Table 1). The total distance covered is approximately 950 km, following a distinct rainfall gradient with arid conditions in the south and more mesic conditions in the north. The observed mean annual precipitation (MAP) ranges from 183 mm yr^{-1} in Bokspits to 532 mm yr^{-1} in Shakawe (Porporato et al. 2003). The observed rainfall patterns across the area indicate a distinct dry and wet

Table 1: Research Sites, names, dates and coordinates

Site #	Name	Date wet	Date dry	Lat	Long
1	Shakawe	5/22/10	8/5/09	-18.3886	21.7716
2	Tsodilo	4/5/11	10/14/09	-18.6798	21.8418
3	Gumare	5/13/11	8/22/09	-19.0776	22.0099
4	Quangwa	5/7/11	8/19/09	-19.5293	21.8174
5	Kuke	12/14/09	10/2/10	-21.0012	21.9648
6	Ghanzi	2/8/10	12/17/09	-21.7621	21.6833
7	Ghanzi S	2/11/10	9/21/10	-22.3542	21.8327
8	Bere	2/19/10	9/30/10	-23.6335	21.6773
9	Tshane	2/19/10	9/23/10	-24.1679	21.8899
10	Tshane S	2/17/10	9/24/10	-24.6304	21.9163
11	Mabua	2/16/10	8/5/10	-25.0681	22.2607
12	Tsabong	2/15/10	9/26/10	-25.8497	22.3547
13	Bokspits	2/13/10	9/27/10	-26.8199	20.6729

season and high variation of annual precipitation both spatially and temporally. With increasing latitude, rainfall events become more sporadic and mainly result from convective thunderstorms. Soil types observed across the area are of mainly aeolian origin and on a large scale do not show significant variation (Thomas 1991). On a local scale, variations can be found in the form of differences in vegetative cover, morphology

of the landscape, such as active (site13) vs non-active (sites 1,2,3) or over washed dune fields, riverbeds, surfacing bedrock materials (site 6) and others. Thomas (1991) classified the vegetation of the area as Kalahari thornveld. While this generalization suggests consistency with regards to vegetation cover and structure, woody vegetation responds to increasing MAP with increase in canopy density and height. On a local scale vegetative composition varies with regards to species composition and structure as a result of the *in situ* physical conditions and in response due to disturbance.

5.2.2 In situ methods to estimate woody biomass

5.2.2.1 Line intercept transect (LIT)

Each of the 13 field sites were visited once in the wet season and once in the dry season. Care was taken to space the sites approximately 75 km apart, but the actual position of the site depended on accessibility and was therefore influenced by the presence of roads (dirt tracks). At each site a center point was determined randomly and three transects were laid out radially for the first season's collection. The starting point of each transect was 10 m away from the center point and transects were spaced at 120 degrees where the direction of the first transect was determined randomly (Figure 3). Each transect was 500 m long and was laid out and staked using multiple measuring tapes. Metal, painted spikes were left at the center, start and end of each transect and location taken using a Trimble ProXRS with Omnistar real-time correction to ease finding the sites in the second season.

During the field campaign, structural vegetation measurements were collected using the line intercept transect (LIT) method described by Krebs (1999). Vegetation

measurements and species identification were recorded at the center 100 m of each transect, from 200 – 300 m. For all woody vegetation > 25 cm in height and overlapping the LIT, structural parameters such as crown dimensions, height, stem distance to line, and stem location were recorded. Measurements were taken and recorded for all transects on all sites across two seasons. The general layout approach described above was implemented for wet and dry season. In order to avoid the introduction of bias due to previous physical damage and to increase the spatial coverage to account for the heterogeneity observed in savanna ecosystems, the transect layout for the second field visit was offset to the previous visit by a rotation angle of 60 degrees, resulting in a total of 6 line intercept transects (LIT).

5.2.2.2 Converting LIT data to biomass

We used the average crown radius, *r*, itself calculated as one-half of the average crown diameter along the major and minor axes, of each tree to estimate the crown area, A_{cr}:

$$A_{cr} = \pi r^2 \quad (1)$$

The average tree area for the *n* trees at each site, A_{av}, was then calculated:

$$A_{av} = \frac{1}{n}\sum_{i=1}^{n} A_{cr} \quad (2)$$

Because only woody canopies that intersected the transect were sampled, the effective area of sampling was the length of the transect (l = 100 m x 3 transects = 300 m)

multiplied by the average crown diameter ($2\bar{r}$) along the transect. Meyer (2013) describes an allometric relationship between the biomass of a given tree in the Kalahari region and its crown area. We used A_{av} and the number of trees found at each site to calculate the total biomass per unit area for each site (M_{LIT}):

$$M_{LIT} = 2\bar{r}ln(1.3175 * A_{av}^{1.2136}) \quad (3)$$

5.2.3 Estimating woody biomass using optical remote sensing

5.2.3.1 Conceptualization of the remote sensing approach

Biomass in each pixel, M_{pix}, is estimated as:

$$M_{pix} = cA_{pix}f_{GV}\varphi\frac{M_{tree}}{A_{av}}, \quad (4)$$

where c is a calibration coefficient, A_{pix} is the area of the MODIS pixel in m^2, f_{GV} is the fraction of the pixel that is covered by green vegetation (GV), φ is the fraction of the total vegetation cover that is comprised of woody vegetation as seen from zenith, M_{tree} is the mass of the average woody plant in the pixel, and A_{av} is the crown area of the average woody plant in the pixel.

This approach assumes that all of the vegetation in the pixel is green (i.e., $f_{veg} = f_{GV}$), and therefore is best used during the greenest portion of exceptionally wet years. The value of the calibration coefficient, c, will to some extent reflect and correct for the validity this assumption. The term $f_{GV}\varphi$ represents the fraction of a pixel that comprised of woody vegetation and therefore $A_{pix}f_{GV}\varphi$ is the total area of woody vegetation in the pixel.

$A_{pix} f_{GV} \varphi / A_{av}$ gives the total number of trees in the pixel which, when multiplied by the mass of the average woody plant in the pixel, M_{tree}, gives the total mass of woody plants in the pixel. M_{tree}, in turn, was calculated using the allometric relationship from Meyer et al. (2013):

$$M_{tree} = 1.3175 * A_{av}^{1.2136} \quad (5)$$

Field data were used to determine site-averaged values of A_{av}. No significant relationship was found between MAP and field-derived A_{av}, nor were other trends found, and therefore the average value of A_{av} for all sites, 6.03 m^2, was used throughout the study.

5.2.3.2 Remote estimation of GV with MESMA and Field spectra

MESMA (Multiple Endmember Spectral Mixture Analysis)

The NBAR (Nadir BRDF Adjusted Reflectance) product provided by MODIS (MCD43) is a passive remote sensing product provided at a temporal compilation of 16 days and a spatial resolution of 500 m and 1000 m per pixel, and corrected using a bidirectional reflectance distribution function (BRDF). For this study, the 500 m resolution product was used as the basis for the unmixing of imagery pixels. Images used for the estimation of biomass (section 2.2) are based on the imagery corresponding to the closest date of the wet-season field visit, while the image used for the calibration of the final models has been chosen to match the peak of the wet season (February) 2011. 3 x 3 pixel regions were clipped from the images that included the field sites.

MESMA (Multiple Endmember Spectral Mixture Analysis) is a version of spectral mixture analysis (SMA) where it is assumed that the measured reflectance at each pixel

and each band is a linear combination of the reflectance of all ground components (endmembers) and that the coefficients of this linear combination are equal to their fractional cover on the ground. The reflectance of an endmember at a given time t_i can be expressed as:

$$\rho_{pixel}^{t_i} = \sum_{k=1}^{n} f_k^{t_i} \rho_k + \varepsilon , \qquad (6)$$

where $\rho_{pixel}^{t_i}$ is the reflectance of the pixel at time t_i, ρ_k is the reflectance of the k^{th} endmember, and $f_k^{t_i}$ is the fractional area covered by the k^{th} endmember at time t_i (Shimabukuro and Smith 1991). Endmembers derived from laboratory or field spectra, ρ_k, are referred to as "reference endmembers" (Roberts et al. 1998b). The remaining term, □, is the residual spectrum remaining after the best-fit coefficients, $f_k^{t_i}$, have been determined. Equation (6) is subject to the constraints that f_k must belong to the interval [0,1] and

$$\sum_{k=1}^{n} f_k^{t_i} = 1. \qquad (7)$$

While SMA (Spectral Mixture Analysis) assumes that endmembers are spatially and temporarily invariant, MESMA uses multiple endmembers to account for variations of reflective properties of objects found in a given pixel and accounts for temporal difference, e.g. differences between wet and dry season. In this study, multiple site- and season-specific endmembers were used for MESMA, where the best-fit coefficients of many different endmember models (a model is a unique combination of endmember

spectra) calculated and the best model applied to a pixel (Roberts et al. 1998a). The criteria used to pick the best model is RMSE (Root Mean Square Error):

$$RMSE = \left(\frac{1}{m} \sum_{b=1}^{m} (\varepsilon_b)^2 \right)^{1/2}, \quad (8)$$

where *m* is the number of bands in the remote sensing imagery (MCD43A4 has seven bands); the model with the lowest RMSE is chosen (Roberts et al. 1998b). The criteria for the endmember selection for this particular study are discussed below (section 2.3.2.2). Models were constructed by using all possible combinations among applicable GV, NPV, and soil spectra.

MESMA was conducted using the "constrained_min" routine in IDL (Excelis Visual Information Solutions, inc., Boulder, Colorado; Lasdon and Waren 1986) to minimize RMSE while forcing coefficients to exist in the interval [0,1]. No constraint on the sum of non-shade endmembers was imposed for the unmixing and shade was set to one minus the sum of the non-shade endmembers. This method is equivalent to that used in Roberts et al. (1998a) where the constraint that all endmembers sum to one is imposed by inferring an additional photometric shade endmember (zero reflectance in all bands) that is not used in the actual unmixing. This approach is required because photometric shade cannot be used directly as an endmember in a spectral mixture model (see Okin et al. 2013 for more discussion). After calculation of endmembers, normalization of the non-shade endmembers was completed by dividing each non-shade endmember fraction by the sum of non-shade fractions to force the non-shade endmembers to sum to one. Okin et

al. (2013) showed that this normalization improved GV and NPV endmember fractional cover retrieval while eliminating the bias in the GV cover estimate.

Field spectra

All spectral measurements were conducted using an ASD field spectroradiometer covering the visible (400nm – 700nm), the near infrared (700 nm – 1400 nm) and the shortwave infrared (1500 nm – 2500 nm) portions of the electromagnetic spectrum.

Endmember spectra were collected using the spectroradiometer in combination with a contact probe containing an internal light source and outfitted with a leaf clip resulting in a 'pure spectrum' across the entire spectral range. The probe was warmed up for 10 min to ensure stabilization of the internal light source. The instrument was optimized every 30 min and white references taken every time a different object was sampled. All relevant cover types observed along the transect were recorded. At least 10 measurements per cover type were taken. Plant leaf measurements were taken using the clip attachment, while measurements of stems, soil, litter, exposed rock etc. were taken by applying the probe directly against the object of interest. These spectra were used to compile an endmember library for each site, with representatives in each of GV, NPV and soil. The spectra were corrected for often occurring jumps (splice correction) due to differences in the fiber optics used at 650 nm and 1447 nm. All resulting reflectance spectra were convolved to MODIS wavebands (see examples in Figure 1).

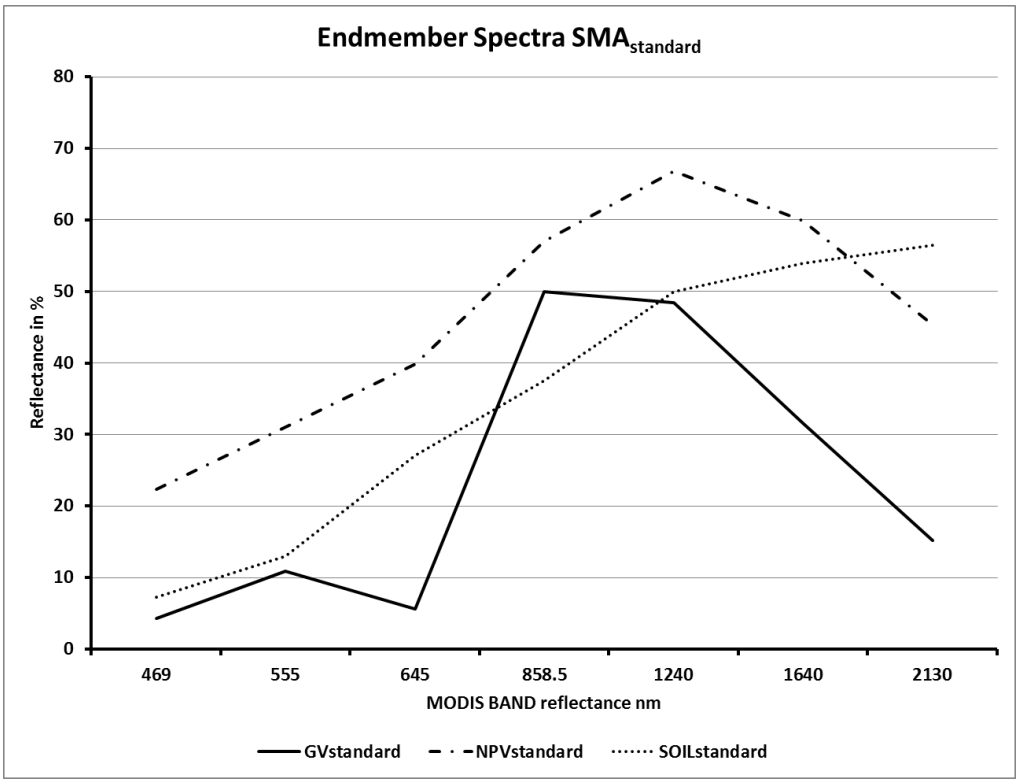

Figure 1: Example of spectral endmembers

5.2.4 Estimation of φ

5.2.4.1 Estimating φ from line-intercept transect (LIT) data

φ is the fraction of all vegetation cover, as seen from zenith, that is composed of woody vegetation. φ_{LIT}, the field-based values of φ, was calculated using the measured LIT data, where tree position and crown coverage along the LIT were used to calculate fractional portion of all vegetation cover that was comprised of woody vegetation.

5.2.4.2 Estimating φ_{LIT} from remote sensing data

Values of φ_{LIT} are only available at the 13 sites where field data were collected. To estimate woody biomass using Equation 4 between these sites, an estimate of φ based on data available outside of the sites was necessary. We tested the relationship between

several gridded parameters from remotely sensed (EVI or Enhanced Vegetation Index, GV, NPV, soil, shade) or ancillary data sets (MAP or Mean Annual Precipitation) to φ_{LIT} to derive a relationship for φ that could be used to interpolate between sites, φ_{interp}. Values of f_{GV}, $f_{NPV,}$, f_{soil}, and $f_{shade,}$ were taken from MESMA analysis. EVI data were taken from the MODIS MYD13A1 product.

5.2.5 Calibration and regression of residuals

The calibration coefficient *c* in equation 4 was chosen as a value that minimized the RMSE of M_{pix} when compared with M_{LIT}. An additional correction was made to these estimates, following the observation of relationships between the model residuals, (that is, $M_{pix} - M_{LIT}$) and other gridded data. Thus a residual correction was made:

$$M_{pix,corr} = cA_{pix}f_{GV}\varphi\frac{M_{tree}}{A_{av}} + C_{residual} \quad (9)$$

where $C_{residual}$ is a linear relationship between the model residual and some gridded dataset.

5.2.6 Model application

The corrected model was applied to a time series using peak wet season MODIS imagery (18th February 2011) and the closest corresponding EVI band from the MODIS MYD13A1 product (Julian day 41; 10th February 2011). In order to account for significant differences in *in situ* conditions, such as topography and soil type, we excluded the Makgadikgadi Salt Pan system, the Okavango Delta and the mountainous

areas to the east, resulting in an area covering approximately 380,000 km^2 or 65 % of the country of Botswana.

5.3 Results

The best relationship between φ_{interp} and φ_{LIT} included EVI and f_{shade}:

$$\varphi_{interp} = 1.23 \cdot EVI + 1.12 \cdot f_{shade} - 0.13 \quad (10)$$

This relationship was highly significant with a multiple-R^2 = 0.73 and p-value = 0.012.Gumare exhibited the highest value of both φ_{interp} and φ_{LIT} (0.85 and 0.51, respectively). The lowest values of φ_{interp} and φ_{LIT} (0.18 and 0.10, respectively) were both observed at Tsabong. Compared across all field sites the relationship between φ_{interp} and φ_{LIT} had an R^2 of 0.53 (Figure 2) with an RMSE of 0.15 t/ha. The largest discrepancies were at Tsodilo in the north and Tshane S.

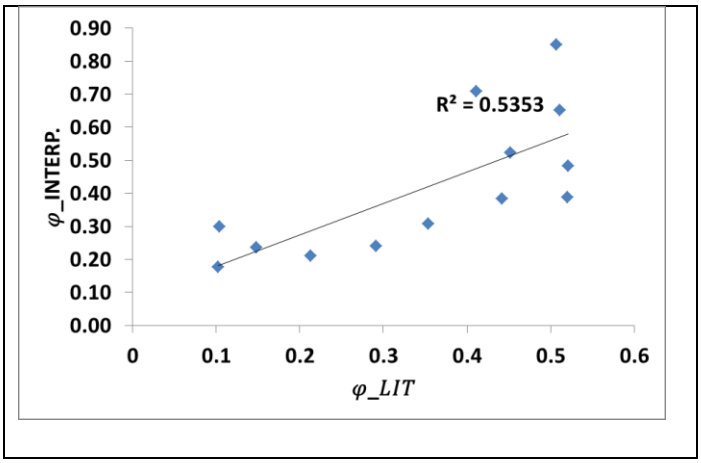

Figure 2: Relationship between φ_{LIT} and $\varphi_{INTERP.}$

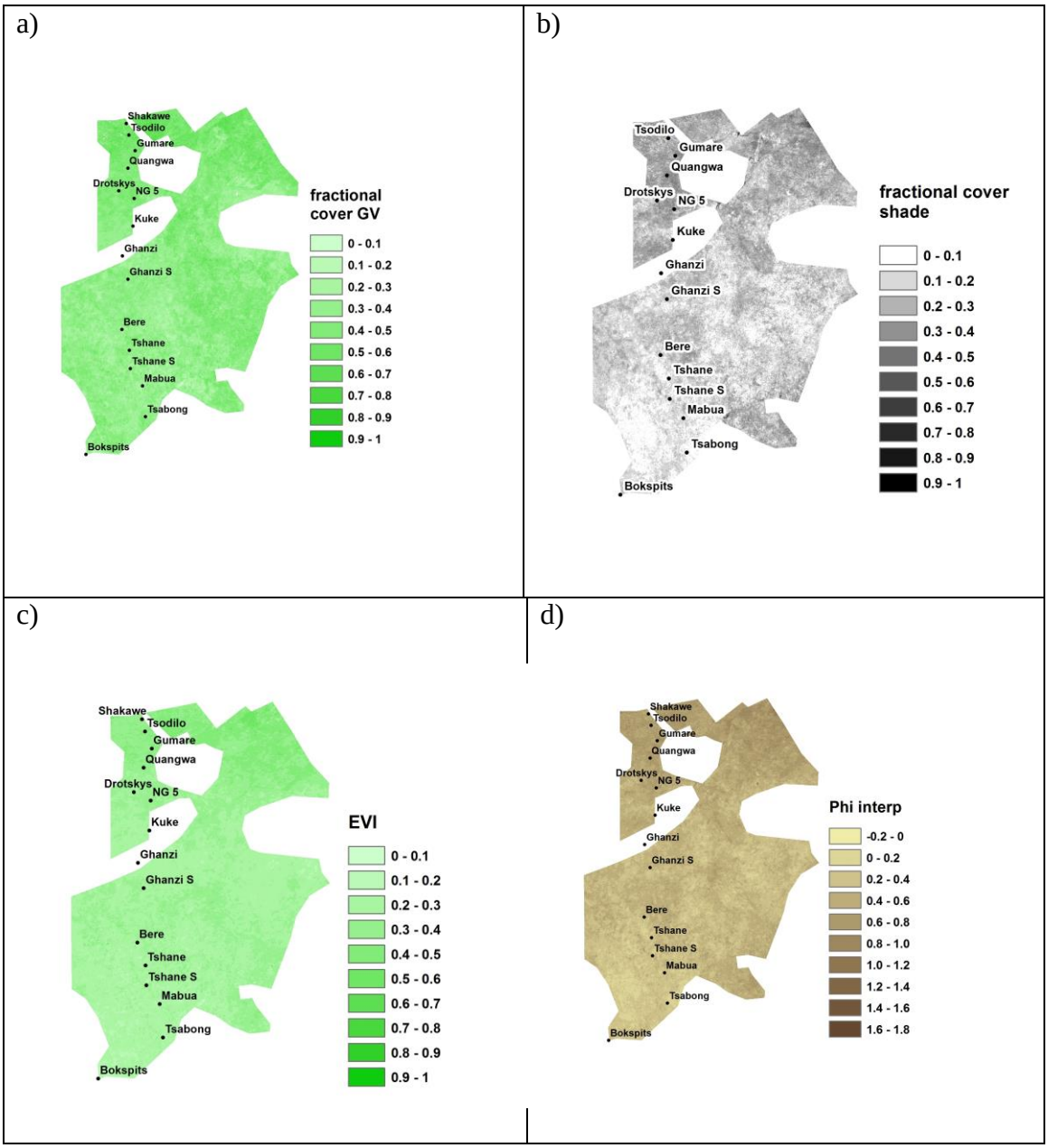

Figure 3: Maps showing a) fractional cover GV, b) fractional cover shade, c) EVI, and d) φ (2011)

Applying MESMA to the wet season (February 10) image in 2011 resulted in high f_{GV} across all sites with a generally increasing trend towards the north. The same trend was observed for the unmixed shade fractions. Exceptionally low shade fractions were found in Tshane and at the southern end of the transect in Bokspits and Tsabong. High shade

fractions occurred in heavily wooded locations such as Gumare, Quangwa and Ghanzi. EVI values for the unmixed dates were high across the entire region. As expected, the lowest value was observed in Bokspits (value of 0.18) while all northern sites showed EVI values around 0.4 (Figure 3). φ as an indication of woodiness varied and ranged from 0.26 in Tshane to 0.79 in Quangwa.

The calibration coefficient *c* in Equation 4 was set to 4.61, which minimized the error of M_{pix}. We also found a strong linear relationship (R^2 = 0.408; p-value = 0.00018) between the residual of M_{pix} and EVI at the peak of greenness (February 10, 2011) such that:

$$C_{residual} = 2.95 \cdot EVI_{peak} - 7.57. \quad (11)$$

Using this relationship, estimates of M_{pix} and $M_{pix.corr}$ were derived using $\varphi_{\mathrm{INTERP}}$ and the f_{shade} and EVI values from February 10, 2011, the peak of the greenness observed during the exceptionally wet year of 2011 (Figure 4). The relationship between M_{LIT} and M_{pix} returned an R^2 value of 0.82 with an RMSE of 4.39 t/ha. Discrepancies were highest in areas with high differences between φ_{LIT} and φ_{INTERP}. This approach seemed to largely overestimate the more woody northern sites, such as Tsodilo, Gumare and Quangwa. Results were improved by residual correction, with the relationship between $M_{pix.corr}$ and M_{LIT} resulting in a R^2 value of 0.81 and an RMSE of 3.18 t/ha.

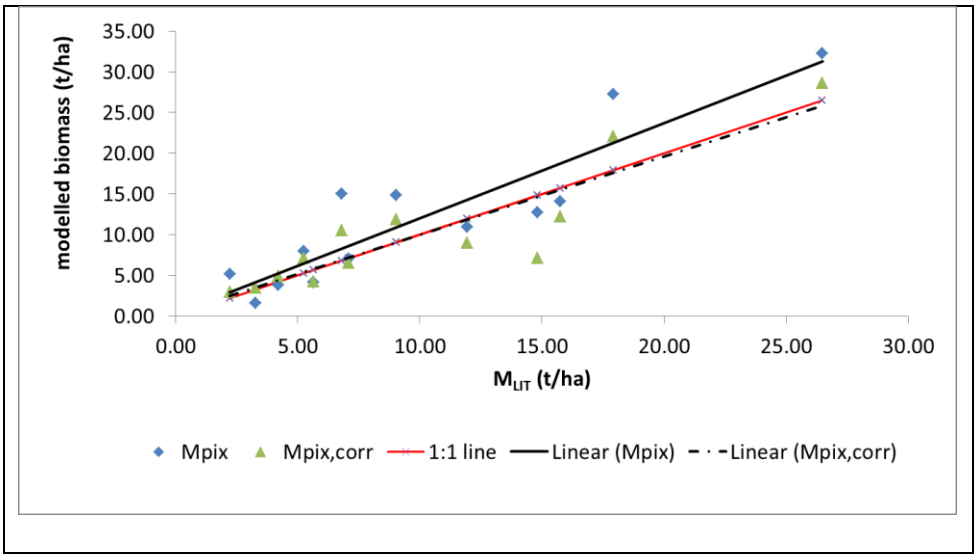

Figure 4: Modeling performance for M_{pix} and $M_{pix,corr}$

Biomass estimated using $M_{pix,corr}$ generally increased towards the north along the Transect. The southern parts were characterized by biomass values typically around 1-5 t/ha. There was also a high variability of biomass in the central part of the study area with peaks reaching 20 t/ha. The northern part of the study area had a biomass value of approximately 50 t/ha; this area is a transition zone between typical Kalahari shrubland vegetation and the Miombo woodland zones, found across southern Angola and Zambia (Figure 5).

The same trends were observed when extracting percent woody cover for the entire region (Figure 6). The southern region was characterized by very low woody cover, seldom exceeding 30%. Cover increases in the central part of the Kalahari to approximately 40 – 50 percent and peaks in the north eastern areas of the Chobe region.

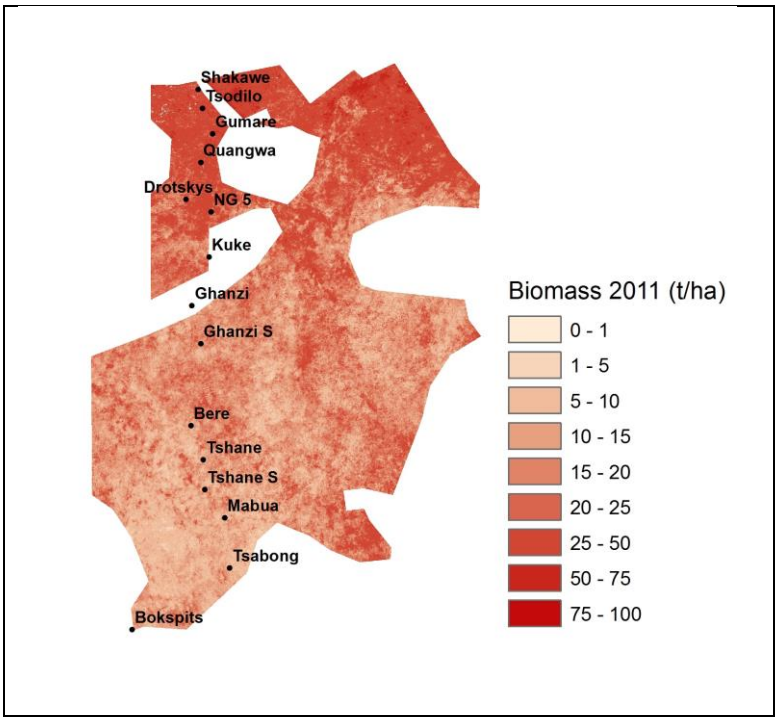

Figure 5: Biomass, 2011

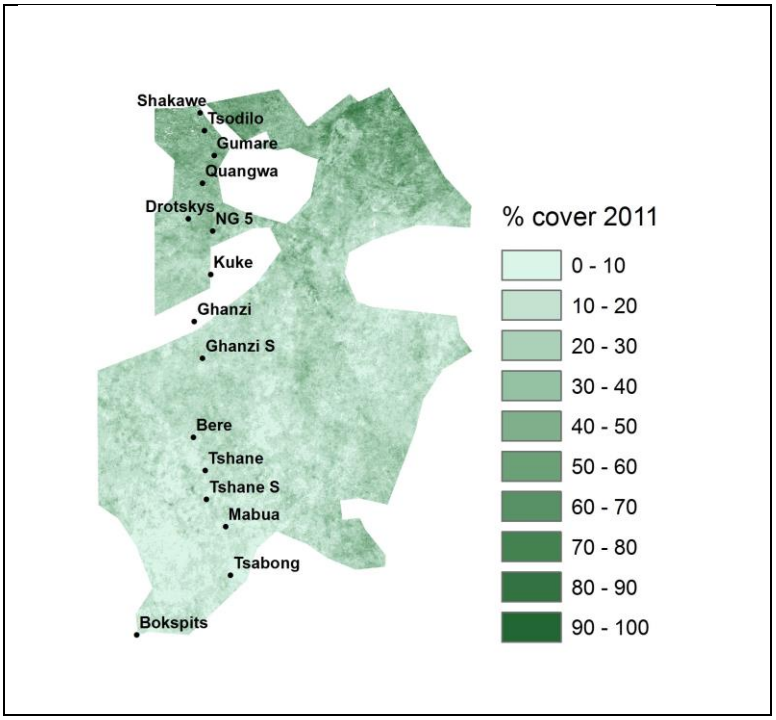

Figure 6: Percent woody vegetation cover (f_{gv}* φ), 2011

5.4 Discussion

Because separation of woody from herbaceous cover is very difficult in remote sensing, especially using the spectrally coarse MODIS data, the modeling approach used here introduced φ as a parameter that represents the fraction of vegetation cover that is woody. In order to obtain estimates of φ in areas where there were no field data, we examined several variates that would correlate with field-based measurements. The best combination we found was a combination of f_{shade} and EVI. EVI outperformed f_{GV}, *with* which it is highly correlated, in these tests for reasons that are not clear. However, the utility of f_{shade} in this relationship makes a great deal of sense. Shade is a common proxy for vertical structure in optical remote sensing (Caetano et al. 1997; Lu et al. 2005; Vohland et al. 2007) and the positive relationship between φ and shade likely represents the increased woodiness resulting in greater shadow casting that is visible with MODIS. EVI was used both in derivation of $\varphi_{INTERP.}$ and $c_{residual}$.

The use of the same dataset in two places risked over-representation of these data in our method for estimating woody biomass. To the extent that this is a place-based calibrated model of woody biomass in the Kalahari, we believe that this use of EVI is acceptable. Furthermore, the approach remains valid even if the correlations are not what one would desire. The fact that EVI proved to be so useful in the estimation of biomass does beg the question, however, if this metric might not be better than f_{GV} in estimating biomass (that is, in place of f_{GV} in equation 4). The correlation using this potential alternate method yielded an R^2 value of 0.68 and therefore we proceeded with the use of f_{GV}. Although they are highly correlated, EVI and f_{GV} do provide slightly different information about the

surface. Our results suggest strongly the utility of MESMA and f_{GV} in deriving useful data from savannas.

Table 4: Field-weighted biomass versus $M_{pix.corr}$

Site	**Source Weighted biomass**	**Weighted biomass (t/ha)**	$\boldsymbol{M_{pix.corr}}$
Shakawe	Kalahari Transect	7.11	7.08
Kuke	Kalahari Transect	7.87	11.89
Ghanzi	Univ. of Texas	13.87	12.19
Tshane	Kalahari Transect	9.61	6.48
Bokspits	Kalahari Transect	5.14	3.45
R^2			**0.49**
RMSE			**2.51**

Our modeled (and corrected) biomass exhibited a strong correlation with the field-derived woody biomass, M_{LIT}, but a better test for the model is its correlation with actual (destructively) measured woody biomass. It becomes challenging to compare the modelled biomass to actual field-measured biomass due to the lack of data. Datasets used by Bhattachan (2012) and Meyer (2013) provide measured aboveground woody biomass for four sites across the region, Shakawe, Kuke, Tshane and Bokspits. One more unpublished dataset for the Ghanzi area was also collected during the course of this study. Using only these five sites, the R^2 value for the relationship between the weighted biomass and $M_{pix.corr}$ was 0.49 with an RMSE of 2.51 t/ha. The largest discrepancy between the modeled and measured sites occurred at the Kuke site and can be attributed

to the difference in geographical location (the Kuke site, where woody biomass was measured is located +/- 50 km east of the site where this estimate of $M_{pix.corr}$ is from). Excluding this site yielded a relationship with R^2 value of 0.89 and an RMSE of 1.97 t/ha.

The field-measured and remotely derived biomass values for Shakawe are in the order of 7 t/ ha. The site is located furthest north and must be seen as a transition zone between the typical Kalahari shrubland to the south and the adjacent Miombo woodland zone to the north. Research conducted in this zone by other investigators suggests much higher woody biomass values for Miombo woodland, on the order of 200 - 36 t/ha (Chidumayo 1990, 1991; Chidumayo and Kwibisa 2003). Considering that Miombo woodland is often characterized by canopy stratification where the top canopy layer consists of large trees, one would expect to identify high woody biomass values for northern Botswana. While our exact field site indicated a relatively low value, the values returned for the northern section of the study area are similar to the biomass derived by Chidumayo (Figure 5) and range from 30 to 50 t/ha. Our values for the central parts of the region as well as the southern part of the region are similar to those described for a savanna ecosystem in Brazil, where woody biomass was measured using field measurements and allometric relationships, indicating a woody biomass of 1.59 – 5.55 t/ha in grassland savannas, 4.23 to 10.96 t/ha in shrub savannas, and 11.35 – 20.57 in savanna woodlands (Santos et al. 2002).

5.5 Conclusion

Across the Botswana Kalahari we tested and applied a model of woody biomass at a spatial resolution of 500 m. Due to both the size of the entire area and size of most common land management units (several hundred to thousands of square kilometers), the approach provides a valuable tool for land managers and decision makers. It is helpful to estimate biomass and / or woody vegetation cover, especially in light of carbon storage but also with regards to stocking densities of livestock and wildlife. Current climate change scenarios for the region predict a decrease in rainfall for most of southern Africa and for the Kalahari region in particular (Christensen 2007; IPCC 2013; Kirtman 2013). The model could be used to monitor expected shifts in vegetation associated with shifts in the current rainfall gradient towards the drier end. Another useful application of these results would be the assessment of vegetation damage after large-scale fire events. The model could be used to quantify the woody vegetation changes associated with these important drivers of savanna ecosystems. Considering that shade provides a proxy for vertical structure, the model could also provide additional information to a much needed structure-incorporated vegetation classification for the Kalahari.

Considering remotely sensed products with higher spatial resolution, the approach has the potential to provide information for smaller land management units such as farms. For areas other than traditional savanna regions, the underlying allometry needs to be modified to fit the observed vegetation on the ground. After this modification, this approach could be tested for use with other systems and regions, e.g. to assess tree

damage caused by elephants, especially in the Chobe area and the woodlands surrounding the Okavango Delta.

Chapter 6

Summary of findings, contributions and future research

Unpublished

Author: Meyer, T.

6.1 Woody plant distribution and plant carbon stocks in savannas as a function of the rainfall regime.

Savannas are complex ecosystems with a high degree of structural heterogeneity. Rainfall regimes as well as disturbances such as grazing and fire greatly determine the ecological state of these ecosystems at the patch, landscape and regional scale. While savanna vegetation at the patch scale by definition constantly undergoes changes in succession, once upscaled across an entire region or ecosystem the successional state remains relatively constant (Chapin III et al. 2011). This balance can be interrupted when the frequency of disturbance events changes, whether naturally or due to anthropogenic influences. The gradient in mean annual precipitation observed in the Kalahari region generally leads to an increase in woody vegetation as one moves farther north (Caylor et al. 2003; Ringrose et al. 2003). While this fact is valid when considering the entire region, on a more localized scale, disturbances and other factors such as nutrient availability determine the abundance and species richness of woody vegetation (Moleele et al. 2002; Wang et al. 2009). Most research has indicated that an increase in livestock density might be one major cause for changes in woody cover not only with regards to abundance but also with respect to species richness (Dougill et al. 1999; Perkins and Thomas 1993). In the Kalahari, livestock densities in combination with fire suppression have led to an increase in woody cover, especially in the central and northern parts of the area (Ringrose et al. 2002). While most studies have been conducted at a local scale and focused on the effect of one particular driver, this research used a statistical approach to test the impact of multiple drivers: fire frequencies, grazing intensities, land use categories, absence and presence of boreholes and mean annual precipitation. This

approach allowed the examination of which driver(s) were correlated with the abundance and richness of woody vegetation at a given site and if there was a correlation with species of similar ecological traits.

Regression models were used to identify drivers associated with impacts on the species richness and abundance of five morphological groups. Results identified that the drivers of high vegetation abundance and richness differed depending on species traits, with all drivers having at least one significant relationship with species richness or abundance for one morphological group. It was also discovered that the presence of boreholes, an indicator of grazing pressure, was negatively related with overall woody species abundance. Relating morphological groups to fire frequency indicated that fire seems to favor the abundance of Acacia species and species characterized by open canopies, such as *D. cinera, C. alexandri* and *Rhigozum spp*. The abundance of Acacias was also positively correlated to areas prone to medium-to-high grazing intensities. Previous research on vegetation densities suggests that an increase in species richness should be observable with an increase in canopy cover towards the north. While this trend was generally confirmed, the overall highest species richness was observed in more centrally located Kuke site.

Woody species abundance in savannas not only determines economic or natural carrying capacities of a certain area, it also largely affects the allocation and cycling of nutrients and carbon within the system (Ringrose et al. 1998; Scanlon et al. 2002; Scanlon et al. 2007). Carbon storage capacities of savanna ecosystems on both global and local scales

remain poorly understood (Giri et al. 2005; Lal 2000). In woody vegetation the amount of assimilated and stored carbon not only changes from species to species, but also with structural characteristics of each individual. Structural characteristics (e.g., height, DBH, number of stems, crown diameters, etc.) vary over time and are greatly influenced by disturbance. Therefore, assessing the structural characteristics of woody vegetation in savannas is an essential stepping stone to quantifying the carbon budget of a given area. Savannas have been recognized as having important carbon stocks on a global scale, and the quantification of these carbon stocks is crucial to understanding the global impact of climate and land use change in savannas. While relationships between structural parameters and the weight of a tree are known for most economically important woody species, little information exists for savanna vegetation, especially in Africa. This dissertation research has related tree structural parameters to the weight of an individual tree or shrub and developed a set of tested allometric relationships that can be used to determine total plant biomass as a function of easily measured parameters. Despite recent advances in savanna ecology, research on allometric relationships in savannas remains confined to a few site-specific studies. In these studies, basal area was typically used as the main morphometric parameter in the allometric scaling with plant biomass. Here, allometric relationships were investigated at four different sites along a 950 km transect in the Kalahari, using data from a total of 342 harvested trees and shrubs to relate basal area, height, and crown diameter to aboveground biomass. These relationships were generally strongest in trees and are weakest in small shrubs. Strong allometric relationships were also determined for morphologically similar groups of woody vegetation. Crown diameter was shown as an effective alternative to basal area in

allometric relationships with plant biomass. While the relationships for basal area and height enhance the ability to determine aboveground biomass at small scales (e.g., a farm or land management unit), the relationships between crown area and aboveground biomass provide an opportunity to estimate woody biomass over large areas using high resolution aerial or satellite imagery and thus without requiring ground-based measurements of basal area.

The performance of a suite of spectral unmixing techniques and two different validation approaches were tested to determine the fractional cover of all green vegetation (GV), non-photosynthetic vegetation (NPV), soil and shade (a separate more technical discussion is provided in section 6.2 below). Multiple Endmember Spectral Mixture Analysis (MESMA) was utilized to derive the fractional cover of GV, NPV, soil and shade at a Moderate Imaging Spectroradiometer (MODIS) scale of 463.3 m spatial resolution for most of the Kalahari environment of southern Africa. Because the fractional cover of GV represents a combination of grass, herbaceous and woody vegetation, the challenge arises to decouple the woody fractional cover. Multiple regression of the Enhanced Vegetation Index (MYD13A1) and the fractional cover of shade (derived using MESMA) had a high correlation with the fractional cover of woody vegetation observed on the ground, allowing for a separation of fractional cover of woody vegetation.

This association together with the identified allometric relationship between crown area and woody biomass forms the basis of a modeling process that has been proven

successful to estimate woody biomass at the regional scale using MODIS imagery. Modeled biomass was validated against field-derived measurements from line intercept transects (calculated biomass) and from field-weighing (actual biomass). Three possible ways to correct the modeled biomass values were created and applied across the entire region at a spatial resolution of 500 m for the peak wet season for the year 2011. As expected, the southern part of the study area exhibited a lower biomass than the wetter central and northern parts of the area. Biomass in the southern part of the study area rarely exceeds 5 t/ha (tons per hectare) while the biomass in the central area shows strong fluctuations between 10 and 40 t/ha. The highest biomass is found in the north where the woody biomass component was estimated to be between 30 and 40 t/ha. Towards both ends (north and south) of the transect, fewer fluctuations in biomass were visible, related to the lower structural heterogeneity as compared to increased heterogeneity in the central areas. Similar trends were observed when leveraging the derived product for woody vegetation cover. The model thus provided an overall effective tool for land managers to determine estimates of woody biomass in a given area.

6.2 Performance of spectral mixture analysis (SMA) techniques in remote sensing of heterogeneous environments

Another important result of this dissertation is the development of a new methodology to quantify photosynthetic and non-photosynthetic vegetation using spectral mixture analysis (SMA) techniques. Savanna ecosystems are functionally diverse and structurally heterogeneous environments where the heterogeneity of the ecosystem results in complex spectral interactions. While previous research has proven the validity for unmixing

procedures in more homogenous environments, the performance of these methods appears to have been less successful in savannas. Field validation of unmixing results is extremely challenging, particularly since the determination of GV, NPV and soil in the field is often influenced by an individual's interpretation of these fractions and thus contains a certain degree of bias (Guerschman et al. 2009; Mishra et al. 2014). For instance, the greenness of a particular blade of grass changes dramatically through time, ranging from hourly differences to the phenological cycle of a given blade of grass. Further, the human eye necessarily can only observe visible light component reflections, introducing further limitations given the much stronger GV response in near and middle infrared regions of light. Therefore in addition to the human-based visual differentiation of GV, NPV and soil, very long spectral transects were introduced as an alternative method to validate image-derived unmixing results. The length of the transect was designed so that the *in situ* derived estimates could be directly compared to those derived from spatially coincident MODIS pixels with spatial resolution of 500 x 500 meters. All these measurements, human visual differentiation as well as field spectral measurements, were collected for two different seasons (wet and dry) and examined for differences between these fractions. This time-intensive collection and assessment allowed for the validation of the unmixing results for different unmixing techniques in time and space. New to the remote sensing community is not only the introduction of MODIS-scale ground spectra collection, but also data and results that are spatially extensive and cover a large variety of savanna types. The results for three different unmixing approaches have been validated against two ground truth data sets using regression, presenting coefficient of determination values as well as root mean square error (RMSE) and root mean square

difference (RMSD) values. Furthermore, the assessment of possible bias in certain unmixing-derived fractional estimates at a given point in time or spatially is an important contribution. The two ground-truth datasets were compared to further a critical discussion of the meaning of ground-truthing of parameters that are in fact demonstrably very difficult to determine in the field.

This dissertation research tested the suitability of spectral mixture analysis (SMA) and multiple endmember spectral mixture analysis (MESMA) for estimation of green vegetation (GV), nonphotosynthetic vegetation (NPV), and soil fractions in the heterogeneous, structurally complex savannas of the western Kalahari using the MODIS nadir-BRDF adjusted reflectance (NBAR) product. Extensive fieldwork took place during the dry and wet seasons of 2009 to 2011 at 15 sites distributed along a 950 km long transect, stretching across western Botswana. Data collection included a traditional line-intercept transect (LIT) and a new spectral line point intercept transect method (SLPT) used to test the performance of a variety of unmixing procedures (MESMA vs. SMA) and endmember models. The results for this structurally complex landscape are consistent with results from similar studies undertaken in more homogeneous areas (Asner and Lobell 2000; Gessner et al. 2013; Guerschman et al. 2009; Mishra et al. 2014; Okin et al. 2013). GV cover was retrieved much more accurately than NPV or soil cover. MESMA also produced estimates of fractional cover with less error than simple SMA in both studies. However, the errors observed were greater than those observed for more homogeneous environments. Unlike the line-point intercept system, which requires user interpretation of vegetation greenness, the new (SLPT) method uses spectral data

collected across the entire reflected solar spectrum to derive estimates of GV, NPV and soil fractional cover through spectral unmixing. Results presented in chapter 4 indicate that that the SLPT fractions generally agree better with remotely derived fractions than the LIT-derived fractions. However, remote sensing of GV, NPV, and soil fractional cover, especially in heterogeneous landscapes and at the MODIS scale, remains challenging. Nonetheless, the data do show that at a coarse scale these unmixing methods have the potential to inform our understanding of ecosystem dynamics in these environments.

6.3 Future Research

In savanna ecosystems generally and in the Kalahari region particularly, the need has been identified to incorporate structural parameters, such as total canopy cover and vegetation height into habitat classifications across the region. In the case of MODIS, this approach provides an option that is capable of adding a third dimension to passive remote sensing products that are freely available. The temporal resolution of MODIS allows for the development of time series that can be used to determine change in woody cover and biomass. While woody biomass can be seen as a proxy for an area's carbon storage and the woody contribution to the total fuel load available, cover can be used to monitor changes with regard to changes in habitat. The latter is especially important in light of tracking shrub encroachment, often associated with overgrazing. An outstanding task is the testing of the model at higher spatial resolution, e.g. Landsat imagery, and in different environments, such as riparian, Acacia and Mopane woodlands. If proven successful, the model could be used to quantify changes that have occurred to these habitats due to

various factors such as logging and damage caused by elephants (Ben-Shahar 1993, 1998). For higher spatial resolution imagery, the model could become a valuable tool to establish carrying capacities for both wildlife and livestock.

While general trends observed along the precipitation gradient were confirmed, the centrally located Kuke area stands out as an exceptional site with regard to species, abundance, richness, cover and biomass. At this point, we can only hypothesize that other factors, such as differences in underlying geology, local geomorphological features such as stabilized sand dunes, or differences in types, frequencies, duration, and intensities of disturbance regimes might be the cause for the observed anomalies. Considering the economic importance of this area, this remains an intriguing anomaly worth exploring.

7 References

Acemoglu, D., Johnson, S., & Robinson, J. (2001). An african success story: Botswana

Anderies, J.M., Janssen, M.A., & Walker, B.H. (2002). Grazing management, resilience, and the dynamics of a fire-driven rangeland system. *Ecosystems, 5*, 23-44

Andersson, C.J. (1875). *Notes of Travel in South-Western Africa*

Angassa, A., & Oba, G. (2008). Herder perceptions on impacts of range enclosures, crop farming, fire ban and bush encroachment on the rangelands of Borana, southern Ethiopia. *Human ecology, 36*, 201-215

Archer, S. (1989). Have southern Texas savannas been converted to woodlands in recent history? *American Naturalist*, 545-561

Archer, S., Schimel, D.S., & Holland, E.A. (1995). Mechanisms of shrubland expansion: land use, climate or CO2? *Climatic Change, 29*, 91-99

Asner, G.P., & Heidebrecht, K.B. (2002). Spectral unmixing of vegetation, soil and dry carbon cover in arid regions: comparing multispectral and hyperspectral observations. *International Journal of Remote Sensing, 23*, 3939-3958

Asner, G.P., & Lobell, D.B. (2000). A biogeophysical approach for automated SWIR unmixing of soils and vegetation. *Remote sensing of environment, 74*, 99-112

Aspel, B. (1995). *Coping with Aridity*: Brandes & Apsel Verlag GmbH, Germany

Ballantine, J.-A.C., Okin, G.S., Prentiss, D.E., & Roberts, D.A. (2005). Mapping North African landforms using continental scale unmixing of MODIS imagery. *Remote sensing of environment, 97*, 470-483

Beauchamp, J.J., & Olson, J.S. (1973). Corrections for bias in regression estimates after logarithmic transformation. *Ecology*, 1403-1407

Ben-Shahar, R. (1993). Patterns of elephant damage to vegetation in northern Botswana. *Biological Conservation, 65*, 249-256

Ben-Shahar, R. (1998). Changes in structure of savanna woodlands in northern Botswana following the impacts of elephants and fire. *Plant Ecology, 136*, 189-189

Berkeley, A., Thomas, A., & Dougill, A. (2005a). Spatial dynamics of biological soil crusts: bush canopies, litter and burial in Kalahari rangelands. *African Journal of Ecology, 43*, 137-145

Berkeley, A., Thomas, A.D., & Dougill, A.J. (2005b). Cyanobacterial soil crusts and woody shrub canopies in Kalahari rangelands. *African Journal of Ecology, 43,* 137-145

Bhattachan, A., Tatlhego, M., Dintwe, K., O'Donnell, F., Caylor, K.K., Okin, G.S., Perrot, D.O., Ringrose, S., & D'Odorico, P. (2012). Evaluating Ecohydrological Theories of Woody Root Distribution in the Kalahari. *PLoS ONE, 7,* e33996

Bond, W., Midgley, G., & Woodward, F. (2003). The importance of low atmospheric CO2 and fire in promoting the spread of grasslands and savannas. *Global Change Biology, 9,* 973-982

Breshears, D.D., & Barnes, F.J. (1999). Interrelationships between plant functional types and soil moisture heterogeneity for semiarid landscapes within the grassland/forest continuum: a unified conceptual model. *Landscape Ecology, 14,* 465-478

Brown, J.K. (1976). Estimating shrub biomass from basal stem diameters. *Canadian Journal of Forest Research, 6,* 153-158

Brown, J.R., & Archer, S. (1999). Shrub invasion of grassland: recruitment is continuous and not regulated by herbaceous biomass or density. *Ecology, 80,* 2385-2396

BTO (2005). Annual Rainfall Map, Botswana. In. Gaborone, Botswana: Botswana Tourism Organisation

Caetano, M.R., Oliveira, T., Paul, J.U., Vasconcelos, M.J., & Pereira, J.M.C. (1997). Mapping shrublands and forests with multispectral satellite images based on spectral unmixing of scene components. In, *Aerospace Remote Sensing'97* (pp. 4-14): International Society for Optics and Photonics

Casper, B.B., Schenk, H.J., & Jackson, R.B. (2003). Defining a plant's belowground zone of influence. *Ecology, 84,* 2313-2321

Caylor, K., Shugart, H., Dowty, P., & Smith, T. (2003). Tree spacing along the Kalahari transect in southern Africa. *Journal of Arid Environments, 54,* 281-296

Caylor, K.K., D'Odorico, P., & Rodriguez-Iturbe, I. (2006). On the ecohydrology of structurally heterogeneous semiarid landscapes. *Water Resources Research, 42,* W07424

Caylor, K.K., & Shugart, H.H. (2006). Pattern and process in savanna ecosystems. *Dryland Ecohydrology* (pp. 259-281): Springer

Chapin III, F.S., Chapin, M.C., Matson, P.A., & Vitousek, P. (2011). *Principles of terrestrial ecosystem ecology*: Springer

Chidumayo, E. (1990). Above-ground woody biomass structure and productivity in a Zambezian woodland. *Forest Ecology and Management, 36*, 33-46

Chidumayo, E. (1991). Woody biomass structure and utilisation for charcoal production in a Zambian miombo woodland. *Bioresource technology, 37*, 43-52

Chidumayo, E.N., & Kwibisa, L. (2003). Effects of deforestation on grass biomass and soil nutrient status in miombo woodland, Zambia. *Agriculture, ecosystems & environment, 96*, 97-105

Christensen, J.H., B. Hewitson, A. Busuioc, A. Chen, X. Gao, I. Held, R. Jones, R.K. Kolli, W.-T. Kwon, R. Laprise, V. Magaña Rueda, L. Mearns, C.G. Menéndez, J. Räisänen, A. Rinke, A. Sarr and P. Whetton (2007). Regional Climate Projections. In S. Solomon, D. Qin, M. Manning, Z. Chen, M. Marquis, K.B. Averyt, M. Tignor and H.L. Miller (eds.) (Ed.), *Climate Change 2007: The Physical Science Basis. Contribution of Working Group I to the Fourth Assessment Report of the Intergovernmental Panel on Climate Change* (pp. 847 - 940). Cambridge, United Kingdom and New York, NY, USA: Cambridge University Press

Colgan, M., Asner, G., Levick, S., Martin, R., & Chadwick, O. (2012). Topo-edaphic controls over woody plant biomass in South African savannas. *Biogeosciences Discussions, 9*

Connell, J.H. (1978). Diversity in tropical rain forests and coral reefs. In: Set

Couteron, P., & Lejeune, O. (2001). Periodic spotted patterns in semi-arid vegetation explained by a propagation-inhibition model. *Journal of Ecology, 89*, 616-628

Dayton, B. (1978). Standing crops of dominant Combretum species at three browsing levels in the Kruger National Park. *Koedoe-African Protected Area Conservation and Science, 21*, 67-76

Dennison, P.E., Halligan, K.Q., & Roberts, D.A. (2004). A comparison of error metrics and constraints for multiple endmember spectral mixture analysis and spectral angle mapper. *Remote sensing of environment, 93*, 359-367

Dougill, A.J., & Thomas, A.D. (2004). Kalahari sand soils: spatial heterogeneity, biological soil crusts and land degradation. *Land Degradation & Development, 15*, 233-242

Dougill, A.J., Thomas, D.S., & Heathwaite, A.L. (1999). Environmental change in the Kalahari: integrated land degradation studies for nonequilibrium dryland environments. *Annals of the Association of American Geographers, 89*, 420-442

DSM (2003). Digital Atlas of Botswana. In D.o.S.a. Mapping (Ed.). Gaborone, Botswana

DuToit (1966). *The geology of southern Africa*: Oliver and Boyd, London, Great Britain.

Eckmann, T.C., Roberts, D.A., & Still, C.J. (2008). Using multiple endmember spectral mixture analysis to retrieve subpixel fire properties from MODIS. *Remote sensing of environment, 112*, 3773-3783

Eldridge, D. (1998). Trampling of microphytic crusts on calcareous soils, and its impact on erosion under rain-impacted flow. *Catena, 33*, 221-239

Eldridge, D.J., Bowker, M.A., Maestre, F.T., Roger, E., Reynolds, J.F., & Whitford, W.G. (2011). Impacts of shrub encroachment on ecosystem structure and functioning: towards a global synthesis. *Ecology Letters, 14*, 709-722

ESRI (2000). Standard Image Data Set; World; ARC MAP software package. In E.S.R. Institute (Ed.): ESRI

FAO (1995). Digital Soil Map of the World. In F.a.A. Organisation (Ed.). Rome

Gessner, U., Conrad, C., Huttich, C., Keil, M., Schmidt, M., Schramm, M., & Dech, S. (2008). A Multi-Scale Approch for Retreiving Proportional Cover of Life Forms. In, *Geoscience and Remote Sensing Symposium, 2008. IGARSS 2008. IEEE International* (pp. III-700-III-703): IEEE

Gessner, U., Machwitz, M., Conrad, C., & Dech, S. (2013). Estimating the fractional cover of growth forms and bare surface in savannas. A multi-resolution approach based on regression tree ensembles. *Remote sensing of environment, 129*, 90-102

Giri, C., Zhu, Z., & Reed, B. (2005). A comparative analysis of the Global Land Cover 2000 and MODIS land cover data sets. *Remote sensing of environment, 94*, 123-132

Gobagoba, L., Meyer, T., Ringrose, S., Kampunzu, A.B. and Coetzee, S. (2005). Calcrete Mapping and Palaeo-Environments in the Quangwa Area, Northwest Botswana. In B. The Botswana Society Gaborone (Ed.), *Botswana Notes and Records*

Grace, J., José, J.S., Meir, P., Miranda, H.S., & Montes, R.A. (2006). Productivity and carbon fluxes of tropical savannas. *Journal of Biogeography, 33*, 387-400

Grime, J.P. (1973). Competitive exclusion in herbaceous vegetation. *Nature, UK, 242*, 344-347

Grist, J., Nicholson, S.E., & Mpolokang, A. (1997). On the use of NDVI for estimating rainfall fields in the Kalahari of Botswana. *Journal of Arid Environments, 35*, 195-214

Grossman, D., & Gandar, M. (1989). Land transformation in South African savanna regions. *South African Geographical Journal, 71*, 38-45

Guerschman, J.P., Hill, M.J., Renzullo, L.J., Barrett, D.J., Marks, A.S., & Botha, E.J. (2009). Estimating fractional cover of photosynthetic vegetation, non-photosynthetic vegetation and bare soil in the Australian tropical savanna region upscaling the EO-1 Hyperion and MODIS sensors. *Remote sensing of environment, 113*, 928-945

Higgins, S.I., Bond, W.J., & Trollope, W.S. (2000). Fire, resprouting and variability: a recipe for grass–tree coexistence in savanna. *Journal of Ecology, 88*, 213-229

Hijmans, R.J., Cameron, S.E., Parra, J.L., Jones, P.G., & Jarvis, A. (2005). Very high resolution interpolated climate surfaces for global land areas. *International journal of climatology, 25*, 1965-1978

Hill, M.J., Román, M.O., Schaaf, C.B., Hutley, L., Brannstrom, C., Etter, A., & Hanan, N.P. (2011). Characterizing vegetation cover in global savannas with an annual foliage clumping index derived from the MODIS BRDF product. *Remote sensing of environment, 115*, 2008-2024

Horn, H.S., Cody, M., & Diamond, J. (1975). Markovian properties of forest succession

Huete, A., Didan, K., Miura, T., Rodriguez, E.P., Gao, X., & Ferreira, L.G. (2002). Overview of the radiometric and biophysical performance of the MODIS vegetation indices. *Remote sensing of environment, 83*, 195-213

IPCC (Ed.) (2013). *Climate Change 2013: The Physical Science Basis. Contribution of Working Group I to the Fifth Assessment Report of the Intergovernmental Panel on Climate Change*

Cambridge University Press, Cambridge, United Kingdom and New York, NY, USA,

King, L. (1978). The geomorphology of central and southern Africa. *Biogeography and ecology of southern Africa* (pp. 1-17): Springer

Kirtman, B., S.B. Power, J.A. Adedoyin, G.J. Boer, R. Bojariu, I. Camilloni, F.J. Doblas-Reyes, A.M. Fiore, M. Kimoto, G.A. Meehl, M. Prather, A. Sarr, C. Schär, R. Sutton, G.J. van Oldenborgh, G. Vecchi and H.J. Wang, (Ed.) (2013). *Near-term Climate Change: Projections and Predictability.* Cambridge, United Kingdom and New York, NY, USA.: Cambridge University Press,

Koch, B. (2010). Status and future of laser scanning, synthetic aperture radar and hyperspectral remote sensing data for forest biomass assessment. *ISPRS Journal of Photogrammetry and Remote Sensing, 65*, 581-590

Kraaij, T., & Ward, D. (2006). Effects of rain, nitrogen, fire and grazing on tree recruitment and early survival in bush-encroached savanna, South Africa. *Plant Ecology, 186*, 235-246

Krebs, C.J. (1999). *Ecological methodology*: Benjamin/Cummings Menlo Park, California

Laio, F. (2006). A vertically extended stochastic model of soil moisture in the root zone. *Water Resources Research, 42*

Lal, R. (2000). Carbon sequestration in drylands. *Annals of Arid Zone (India), 39*, 1-10

Lange, R.T. (1969). The piosphere: sheep track and dung patterns. *Journal of Range Management*, 396-400

Lasdon, L.S., & Waren, A.D. (1986). *GRG2 Users Guide*. Cleveland, OH: Cleveland State University

Le Houérou, H., & Corra, M. (1980). Some browse plants of Ethiopia. *Browse in Africa. ILCA, Addis Ababa*, 109-114

Livingstone, D.M.T.a.R.i.S.A., Royal Geographic Society (1857). Missionary Travels and Research in Southern Africa. *Book*

Lomolino, M. (2000). A call for a new paradigm of island biogeography. *Global Ecology and Biogeography, 9*, 1-6

Lu, D., Batistella, M., & Moran, E. (2005). Satellite estimation of aboveground biomass and impacts of forest stand structure. *Photogrammetric Engineering and Remote Sensing, 71*, 967

Mainguet, M. (1994). *Desertification: natural Background and Human Miss-management*. Berlin: Springer Verlag

Marquet, P.A., Fernández, M., Navarrete, S.A., & Valdovinos, C. (2004). Diversity emerging: toward a deconstruction of biodiversity patterns. *Frontiers of biogeography: new directions in the geography of nature*, 191-209

McFadden, D. (1973). Conditional logit analysis of qualitative choice behavior

MEA (2005). *Millennium ecosystem assessment synthesis report*: Millennium Ecosystem Assessment

Mendelsohn, J., & El Obeid, S. (2004). *Okavango River: The flow of a lifeline*: Struik

Meyer, T. (1998). Ecological Mappings in the HOORC research area in the Okavango Delta, Botswana. In, *LOEL* (p. 181). Bernburg: Anhalt University of Applied Sciences

Meyer, T., D'Odorico, P., Okin, G.S., Shugart, H.H., Caylor, K.K., O'Donnell, F.C., Bhattachan, A., & Dintwe, K. (2013). An analysis of structure: biomass structure relationships for characteristic species of the western Kalahari, Botswana. *African Journal of Ecology*

Midgley, J., & Bond, W. (2001). A synthesis of the demography of African acacias. *Journal of Tropical Ecology, 17*, 871-886

Mishra, N.B., Crews, K.A., & Okin, G.S. (2014). Relating spatial patterns of fractional land cover to savanna vegetation morphology using multi-scale remote sensing in the Central Kalahari. *International Journal of Remote Sensing, 35*, 2082-2104

Mitchard, E., Saatchi, S., Woodhouse, I., Nangendo, G., Ribeiro, N., Williams, M., Ryan, C., Lewis, S., Feldpausch, T., & Meir, P. (2009). Using satellite radar backscatter to predict above-ground woody biomass: A consistent relationship across four different African landscapes. *Geophysical Research Letters, 36*

Mohamed, M., Babiker, I.S., Chen, Z., Ikeda, K., Ohta, K., & Kato, K. (2004). The role of climate variability in the inter-annual variation of terrestrial net primary production (NPP). *Science of the Total Environment, 332*, 123-137

Moleele, N., Ringrose, S., Matheson, W., & Vanderpost, C. (2002). More woody plants? The status of bush encroachment in Botswana's grazing areas. *Journal of Environmental Management, 64*, 3-11

Mouillot, F., & Field, C.B. (2005). Fire history and the global carbon budget: a 1× 1 fire history reconstruction for the 20th century. *Global Change Biology, 11*, 398-420

Muir, J. (2011). *Field measurement of fractional ground cover: a technical handbook supporting ground cover monitoring for Australia*: ABARES

Mutanga, O., & Rugege, D. (2006). Integrating remote sensing and spatial statistics to model herbaceous biomass distribution in a tropical savanna. *International Journal of Remote Sensing, 27*, 3499-3514

Noy-Meir, I. (1975). Stability of grazing systems: an application of predator-prey graphs. *The Journal of Ecology*, 459-481

O'Halloran, L.R., Shugart, H.H., Wang, L., Caylor, K.K., Ringrose, S., & Kgope, B. (2010). Nutrient limitations on aboveground grass production in four savanna types along the Kalahari Transect. *Journal of Arid Environments, 74*, 284-290

Okin, G.S. (2007). Relative spectral mixture analysis—A multitemporal index of total vegetation cover. *Remote sensing of environment, 106*, 467-479

Okin, G.S. (2010). The contribution of brown vegetation to vegetation dynamics. *Ecology, 91*, 743-755

Okin, G.S., Clarke, K.D., & Lewis, M.M. (2013). Comparison of methods for estimation of absolute vegetation and soil fractional cover using MODIS normalized BRDF-adjusted reflectance data. *Remote sensing of environment, 130*, 266-279

Okin, G.S., Roberts, D.A., Murray, B., & Okin, W.J. (2001). Practical limits on hyperspectral vegetation discrimination in arid and semiarid environments. *Remote sensing of environment, 77*, 212-225

Palgrave, K.C. (1977). *Trees of southern Africa*: C. Struik.

Palmer, A.R., & van Rooyen, A.F. (1998). Detecting vegetation change in the southern Kalahari using Landsat TM data. *Journal of Arid Environments, 39*, 143-153

Passarge, S. (1904). *Die Kalahari*: Reimer Berlin

Perkins, J., & Thomas, D. (1993). Spreading deserts or spatially confined environmental impacts? Land degradation and cattle ranching in the Kalahari desert of Botswana. *Land Degradation & Development, 4*, 179-194

Porporato, A., Laio, F., Ridolfi, L., Caylor, K.K., & Rodriguez-Iturbe, I. (2003). Soil moisture and plant stress dynamics along the Kalahari precipitation gradient. *Journal of Geophysical Research: Atmospheres (1984–2012), 108*

Qi, J., Chehbouni, A., Huete, A., Kerr, Y., & Sorooshian, S. (1994). A modified soil adjusted vegetation index. *Remote sensing of environment, 48*, 119-126

Ravi, S., D'Odorico, P., Breshears, D.D., Field, J.P., Goudie, A.S., Huxman, T.E., Li, J., Okin, G.S., Swap, R.J., & Thomas, A.D. (2011). Aeolian processes and the biosphere. *Reviews of Geophysics, 49*

Ringrose, S., Chipanshi, A.C., Matheson, W., Chanda, R., Motoma, L., Magole, I., & Jellema, A. (2002). Climate- and Human-Induced Woody Vegetation Changes in Botswana and Their Implications for Human Adaptation. *Environmental Management, 30*, 98-109

Ringrose, S., Matheson, W., & Vanderpost, C. (1998). Analysis of soil organic carbon and vegetation cover trends along the Botswana Kalahari Transect. *Journal of Arid Environments, 38*, 379-396

Ringrose, S., Matheson, W., Wolski, P., & Huntsman-Mapila, P. (2003). Vegetation cover trends along the Botswana Kalahari transect. *Journal of Arid Environments, 54*, 297-317

Ringrose, S., Vanderpost, C., & Matheson, W. (1996). The use of integrated remotely sensed and GIS data to determine causes of vegetation cover change in southern Botswana. *Applied Geography, 16*, 225-242

Roberts, D.A., Gardner, M., Church, R., Ustin, S., Scheer, G., & Green, R.O. (1998a). Mapping chaparral in the Santa Monica Mountains using multiple endmember spectral mixture models. *Remote Sensing Of Environment, 65*, 267-279

Roberts, D.A., Gardner, M., Church, R., Ustin, S., Scheer, G., & Green, R.O. (1998b). Mapping chaparral in the Santa Monica Mountains using multiple endmember spectral mixture models. *Remote sensing of environment, 65*, 267-279

Roberts, D.A., Gardner, M.E., Church, R., Ustin, S.L., & Green, R.O. (1997). Optimum strategies for mapping vegetation using multiple-endmember spectral mixture models. In, *Optical Science, Engineering and Instrumentation'97* (pp. 108-119): International Society for Optics and Photonics

Robinson, J.A., & Parsons, Q.N. (2006). State formation and governance in Botswana. *Journal of African Economies, 15*, 100-140

Sala, O., Lauenroth, W., & Golluscio, R. (1997). ф Plant functional types in temperate semi-arid regions

Sankaran, M., Hanan, N.P., Scholes, R.J., Ratnam, J., Augustine, D.J., Cade, B.S., Gignoux, J., Higgins, S.I., Le Roux, X., & Ludwig, F. (2005). Determinants of woody cover in African savannas. *Nature, 438*, 846-849

Sankaran, M., Ratnam, J., & Hanan, N. (2008). Woody cover in African savannas: the role of resources, fire and herbivory. *Global Ecology and Biogeography, 17*, 236-245

Sankaran, M., Ratnam, J., & Hanan, N.P. (2004). Tree–grass coexistence in savannas revisited–insights from an examination of assumptions and mechanisms invoked in existing models. *Ecology Letters, 7*, 480-490

Santos, J., Lacruz, M.P., Araujo, L., & Keil, M. (2002). Savanna and tropical rainforest biomass estimation and spatialization using JERS-1 data. *International Journal of Remote Sensing, 23*, 1217-1229

Sarmiento, G. (1984). *The ecology of neotropical savannas*: Harvard University Press

Scanlon, T.M., Albertson, J.D., Caylor, K.K., & Williams, C.A. (2002). Determining land surface fractional cover from NDVI and rainfall time series for a savanna ecosystem. *Remote sensing of environment, 82*, 376-388

Scanlon, T.M., Caylor, K.K., Levin, S.A., & Rodriguez-Iturbe, I. (2007). Positive feedbacks promote power-law clustering of Kalahari vegetation. *Nature, 449*, 209-212

Scanlon, T.M., Caylor, K.K., Manfreda, S., Levin, S.A., & Rodriguez-Iturbe, I. (2005). Dynamic response of grass cover to rainfall variability: implications for the function and persistence of savanna ecosystems. *Advances in Water Resources, 28*, 291-302

Schaaf, C.B., Gao, F., Strahler, A.H., Lucht, W., Li, X., Tsang, T., Strugnell, N.C., Zhang, X., Jin, Y., & Muller, J.-P. (2002). First operational BRDF, albedo nadir reflectance products from MODIS. *Remote sensing of environment, 83*, 135-148

Schenk, H.J. (2005). Vertical vegetation structure below ground: scaling from root to globe. *Progress in Botany* (pp. 341-373): Springer

Schlesinger, W.H., Reynolds, J., Cunningham, G.L., Huenneke, L., Jarrell, W., Virginia, R., & Whitford, W. (1990). Biological feedbacks in global desertification. *Science, 247*, 1043-1048

Scholes, R., & Archer, S. (1997). Tree-grass interactions in savannas 1. *Annual Review of Ecology and Systematics, 28*, 517-544

Scholes, R.J., Frost, P.G., & Tian, Y. (2004). Canopy structure in savannas along a moisture gradient on Kalahari sands. *Global Change Biology, 10*, 292-302

Scholes, R.J., & Walker, B.H. (1993). *An African savanna: synthesis of the Nylsvley study*: Cambridge University Press

Schultz, A., Launchbaugh, J., & Biswell, H. (1955). Relationship between grass density and brush seedling survival. *Ecology, 36*, 226-238

Scurlock, J., & Hall, D. (1998). The global carbon sink: a grassland perspective. *Global Change Biology, 4*, 229-233

Shimabukuro, Y.E., & Smith, J.A. (1991). The least-squares mixing models to generate fraction images derived from remote-sensing. *Ieee Transactions on Geoscience and Remote Sensing, 29*, 16-20

Shreve, C.M., Okin, G.S., & Painter, T.H. (2009). Indices for estimating fractional snow cover in the western Tibetan Plateau. *Journal of Glaciology, 55,* 737-745

Shugart, H.H., Macko, S.A., Lesolle, P., Szuba, T.A., Mukelabai, M.M., Dowty, P., & Swap, R.J. (2004). The SAFARI 2000 – Kalahari Transect Wet Season Campaign of year 2000. *Global Change Biology, 10,* 273-280

Skarpe, C. (1990). Shrub layer dynamics under different herbivore densities in an arid savanna, Botswana. *Journal of Applied Ecology*, 873-885

Sprugel, D. (1983). Correcting for bias in log-transformed allometric equations. *Ecology, 64,* 209-210

Stringer, L., & Reed, M. (2007). Land degradation assessment in southern Africa: integrating local and scientific knowledge bases. *Land Degradation & Development, 18,* 99-116

Taylor, J.A., & Lloyd, J. (1992). Sources and sinks of atmospheric CO2. *Australian Journal of Botany, 40,* 407-418

Ter-Mikaelian, M.T., & Korzukhin, M.D. (1997). Biomass equations for sixty-five North American tree species. *Forest Ecology and Management, 97,* 1-24

Thomas, A.D. (2012). Impact of grazing intensity on seasonal variations in soil organic carbon and soil CO2 efflux in two semiarid grasslands in southern Botswana. *Philosophical Transactions of the Royal Society B: Biological Sciences, 367*, 3076-3086

Thomas, D.S. (1991). *The Kalahari Environment*: Cambridge University Press

Tietema, T. (1993). Biomass determination of fuelwood trees and bushes of Botswana, Southern Africa. *Forest Ecology and Management, 60*, 257-269

Tilman, D. (1982). *Resource Competition and Community Structure.(MPB-17)*: Princeton University Press

Tilman, D. (1988). *Plant Strategies and the Dynamics and Structure of Plant Communities.(MPB-26)*: Princeton University Press

Tobin, J. (1958). Estimation of relationships for limited dependent variables. *Econometrica: Journal of the Econometric Society*, 24-36

Trollope, W. (1980). Controlling bush encroachment with fire in the savanna areas of South Africa. *Proceedings of the Annual Congresses of the Grassland Society of Southern Africa, 15*, 173-177

Trollope, W.S., & Trollope, L.A. (2004). Prescribed burning in African grasslands and savannas for wildlife management. *Arid Lands Newsletter, 55*

Van Auken, O. (2000). Shrub invasions of North American semiarid grasslands. *Annual Review of Ecology and Systematics*, 197-215

Van Regenmortel, G. (1995). Regionalization of Botswana rainfall during the 1980s using principal component analysis. *International journal of climatology, 15*, 313-323

Van Rooyen, N., Bezuidenhout, H., & De Kock, E. (2001). *Flowering plants of the Kalahari dunes*: Ekotrust

van Wilgen, B.W., Trollope, W.S., Biggs, H.C., Potgieter, A., & Brockett, B.H. (2003). Fire as a driver of ecosystem variability. *The Kruger Experience: Ecology and Management of Savanna Heterogeneity. Island Press. Washington, DC*, 149-170

Vohland, M., Stoffels, J., Hau, C., & Schuler, G. (2007). Remote sensing techniques for forest parameter assessment: multispectral classification and linear spectral mixture analysis. *Silva Fennica, 41*, 441

Walker, B.H., Ludwig, D., Holling, C.S., & Peterman, R.M. (1981). Stability of semi-arid savanna grazing systems. *The Journal of Ecology*, 473-498

Walter, H. (1954). Die Verbuschung, eine Erscheinung der subtropischen savannengebiete, und ihre ökologischen ursachen. *Vegetatio, 5-6*, 6-10

Walter, H., & Mueller-Dombois, D. (1971). *Ecology of tropical and subtropical vegetation*: Edinburgh, UK, Oliver & Boyd

Wang, L., D'Odorico, P., Manzoni, S., Porporato, A., & Macko, S. (2009). Soil carbon and nitrogen dynamics in southern African savannas: the effect of vegetation-induced patch-scale heterogeneities and large scale rainfall gradients. *Climatic Change, 94*, 63-76

Wang, L., D'Odorico, P., O'Halloran, L.R., Caylor, K., & Macko, S. (2010). Combined effects of soil moisture and nitrogen availability variations on grass productivity in African savannas. *Plant and soil, 328*, 95-108

Wang, L., D'odorico, P., Ringrose, S., Coetzee, S., & Macko, S. (2007). Biogeochemistry of Kalahari sands. *Journal of Arid Environments, 71*, 259-279

Ward, D. (2005). Do we understand the causes of bush encroachment in African savannas? *African Journal of Range and Forage Science, 22*, 101-105

Wellington, J.H. (1955). *Southern Africa: a geographical study*: University Press Cambridge

White, M.A., Asner, G.P., Nemani, R.R., Privette, J.L., & Running, S.W. (2000). Measuring fractional cover and leaf area index in arid ecosystems: digital camera, radiation transmittance, and laser altimetry methods. *Remote sensing of environment, 74*, 45-57

Wiegand, K., Ward, D., & Saltz, D. (2005). Multi-scale patterns and bush encroachment in an arid savanna with a shallow soil layer. *Journal of Vegetation Science, 16*, 311-320

Williams, C.A., Hanan, N.P., Neff, J.C., Scholes, R.J., Berry, J.A., Denning, A.S., & Baker, D.F. (2007). Africa and the global carbon cycle. *Carbon balance and management, 2*, 1-13